doi.org/10.26434/chemrxiv.11385906.v1

SuFEx-Enabled High-Throughput Medicinal Chemistry

Seiya Kitamura, Qinheng Zheng, Jordan L. Woehl, angelo solan, Emily Chen, Nicholas Dillon, Mitchell Hull, Miyako Kotaniguchi, Shinichi Kitamura, Victor Nizet, K. Barry Sharpless, Dennis Wolan

Submitted date: 17/12/2019 • Posted date: 20/12/2019

Citation information: Kitamura, Seiya; Zheng, Qinheng; Woehl, Jordan L.; solan, angelo; Chen, Emily; Dillon, Nicholas; et al. (2019): SuFEx-Enabled High-Throughput Medicinal Chemistry. ChemRxiv. Preprint. https://doi.org/10.26434/chemrxiv.11385906.v1

Optimization of small-molecule probes or drugs is a lengthy, challenging and resource-intensive process. Lack of automation and reliance on skilled medicinal chemists is cumbersome in both academic and industrial settings. Here, we demonstrate a high-throughput hit-to-lead process based on the biocompatible SuFEx click chemistry. A modest high-throughput screening hit against a bacterial cysteine protease SpeB was modified with a SuFExable iminosulfur oxydifluoride [RN=S(O)F2] motif, rapidly diversified into 460 analogs in overnight reactions, and the products directly screened to yield drug-like inhibitors with 300-fold higher potency. We showed that the improved molecule is drug-like and biologically active in a bacteria-host coculture. Since these reactions can be performed on a picomole scale to conserve reagents, we anticipate our methodology can accelerate the development of robust biological probes and drug candidates.

SuFEx-enabled high-throughput medicinal chemistry

Seiya Kitamura[1#], Qinheng Zheng[2#], Jordan L. Woehl[1], Angelo Solania[1], Emily Chen[3], Nicholas Dillon[5,7], Mitchell V. Hull[3], Miyako Kotaniguchi[8], Shinichi Kitamura[8], Victor Nizet[5,6,7], K. Barry Sharpless[2*] and Dennis W. Wolan[1,4*]

Department of Molecular Medicine[1], Department of Chemistry[2], California Institute for Biomedical Research[3], and Department of Integrative Structural and Computational Biology[4], The Scripps Research Institute, La Jolla, CA, 92037, USA. Department of Pediatrics[5], Collaborative to Halt Antibiotic-Resistant Microbes (CHARM)[6], Skaggs School of Pharmacy and Pharmaceutical Sciences[7], UC San Diego, La Jolla, CA 92093, USA. Laboratory of Advanced Food Process Engineering, Osaka Prefecture University, 1-2, Gakuen-cho, Nakaku, Sakai, Osaka 599-8570, Japan[8].

ABSTRACT:

Optimization of small-molecule probes or drugs is a lengthy, challenging and resource-intensive process. Lack of automation and reliance on skilled medicinal chemists is cumbersome in both academic and industrial settings. Here, we demonstrate a high-throughput hit-to-lead process based on the biocompatible SuFEx click chemistry. A modest high-throughput screening hit against a bacterial cysteine protease SpeB was modified with a SuFExable iminosulfur oxydifluoride [$RN{=}S(O)F_2$] motif, rapidly diversified into 460 analogs in overnight reactions, and the products directly screened to yield drug-like inhibitors with 300-fold higher potency. We showed that the improved molecule is drug-like and biologically active in a bacteria-host coculture. Since these reactions can be performed on a picomole scale to conserve reagents, we anticipate our methodology can accelerate the development of robust biological probes and drug candidates.

The introduction of high-throughput screening (HTS) robotics, liquid handler systems, and assay miniaturization have revolutionized screening of bioactive molecules. Relatively inexpensive HTS processes are now routinely used in cell-based and *in vitro* assays against biomedically relevant targets. Nevertheless, compound optimization is typically necessary to improve target specificity, potency, and stability. Lead optimization relies heavily on medicinal chemists, and extensive time and labor costs remain significant hurdles for probe and drug development.

Click chemistry has found broad applications in materials chemistry, chemical biology, and drug development since the concept was first introduced in 1999[1-2]. The sulfur(VI) fluoride exchange (SuFEx) represents the most recent set of ideal click chemistry transformations[3]. Specifically, aryl fluorosulfates ($ArOSO_2F$) and iminosulfur oxydifluorides ($RN{=}S(O)F_2$) are readily synthesized using two connective oxyfluoride gases, sulfuryl fluoride (SO_2F_2) and thionyl tetrafluoride ($O{=}SF_4$), respectively[4]. These two $S^{VI}{-}F$ motifs have been successfully used as connective linkers in polymer synthesis and for construction of various functional molecules[5-7]. Sulfonyl fluoride (RSO_2F) and aryl fluorosulfate moieties have been successfully introduced into bioactive molecules in chemical biology and drug discovery[8-11], especially as covalently binding warheads[12]. However, the potential of SuFEx to unite diverse modules using an $O{=}SF_4$ hub has not been explored in medicinal chemistry. While the copper(I)-catalyzed azide-alkyne cycloaddition (CuAAC) reaction has been used in proof-of-concept studies on lead

optimization, including the direct evaluation of biological potency[13-18], there are only a couple of drugs that contain the 1,2,3-triazole linkage, supposedly because of several drawbacks of the reaction (Figure 1). Unlike CuAAC, the sulfur(VI)-containing motifs resulting from SuFEx reactions are common in drugs; for example, more than 150 sulfonamide drugs are available on the market[19]. Here, we present a rapid and high-throughput hit-to-lead optimization process based on iminosulfur oxydifluoride SuFEx click chemistry that can be performed on picomole scale.

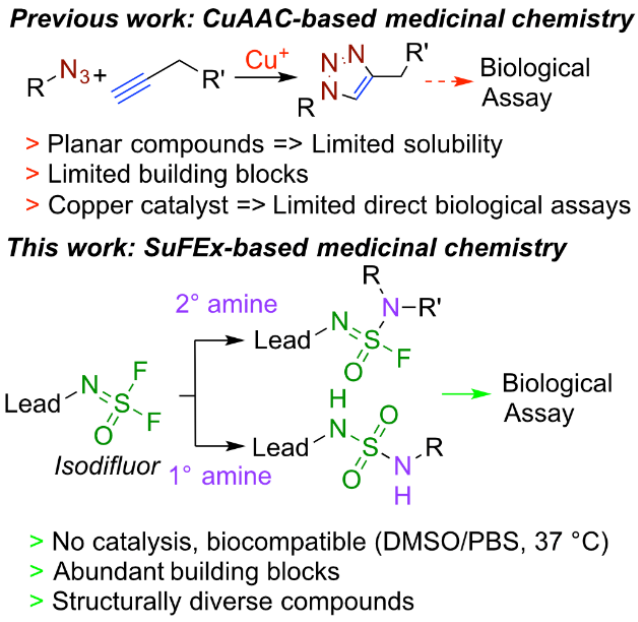

Figure 1. Comparison of CuAAC- and SuFEx-based medicinal chemistry campaigns. Lead molecules can be modified with an iminosulfur oxydifluoride (*isodifluor*) motif and reacted with a collection of primary and secondary amines to generate a diversified library.

We focused on the SuFEx reaction between iminosulfur oxydifluoride (RN=S(O)F_2, *isodifluor*) and primary or secondary amines to construct a focused library of lead compound analogs (Figure 1). This series of robust and near perfect reactions was recently described for bioconjugation and DNA-encoded library construction[20], and we posited that the biocompatible reaction conditions would enable us to measure the potency of products directly using *in vitro* enzyme assays to prioritize the molecules. Additionally, the rapid and diverse analog synthesis from the most available starting materials (*i.e.,* primary and secondary amines) and the non-planer 3-dimensional structures, multiple hydrogen-bond donors/acceptors, drug-like lipophilicity, and stability in biological conditions of the products are ideal for medicinal chemistry (Figure 1).

Our proof-of-concept started with a modest inhibitor (cmpd **1**, IC_{50} = 14 μM) of the cysteine protease SpeB, a virulence factor secreted from the bacterial pathogen *Streptococcus pyogenes*, previously identified in our HTS campaign (Figure 2a)[21-22]. Although peptidic SpeB inhibitors were reported, such as E64[23-24], potent small molecule inhibitors have not been developed against SpeB. In preliminary SAR studies, introduction of an (*S*)-benzyl moiety (cmpd **2**, Figure 2a) improved the potency to 2.1 μM. The SpeB:**1** co-complex x-ray structure[22]

and initial SAR campaign (Table S1) suggested that additional surface pockets on SpeB were accessible for compound optimization via extension of **2** from the meta positions of both benzyl rings. An isodifluor diversification handle was therefore introduced at the meta position of either benzyl moieties of **2** to generate **3** and **4** (Figure 2b). These molecules with an isodifluor hub were subsequently reacted with a panel of 230 amines to generate 460 analogs overnight using DMSO:PBS = 1:1 as a solvent and incubate at 37 °C (Figure 2c)**.** The representative reactions monitored using LC-CAD-MS^2 are shown in the Supporting Data and Table S3. It should be noted that the reactions between isodifluor-containing molecules with the amines showed an improved yield when PBS (pH 7.4) was added to the solvent (Table S2).

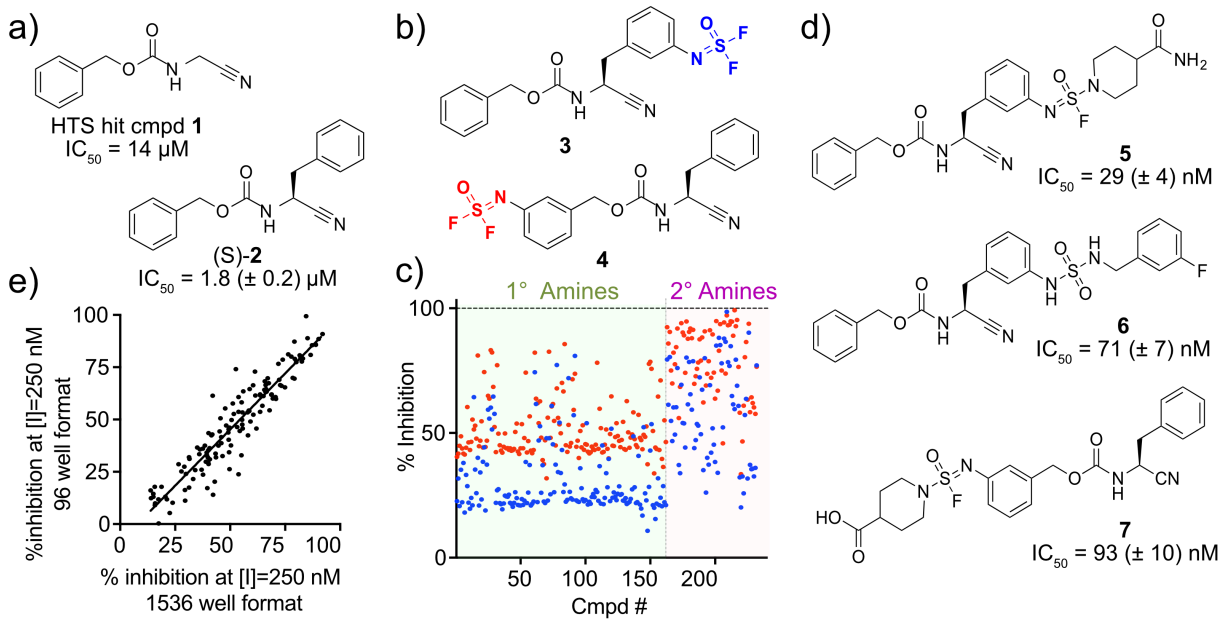

Figure 2. Focused library construction and screening. (a) Structures of HTS hit SpeB inhibitor **1** and its analog (*S*)-**2**. (b) Molecules with isodifluor diversification handle, and (c) scatter plot. Inhibition % at 250 nM (compound **3,** ●) or 2 μM (compound **4,** ●) are plotted. (d) Representative improved inhibitors and SpeB inhibition potency. (e) Correlation between picomole-scale and nanomole-scale syntheses.

The reaction products were directly screened for SpeB inhibition with an established kinetic fluorogenic substrate assay[22-23]. Scatter plots of the screening results are shown in Figure 2c. All 460 amine structures and the corresponding SpeB inhibition are provided in Tables S4 & S5. Additionally, the panel of amines alone (absence of **3** or **4** in reaction), the reaction condition, and the fluoride ion by-product (Figure 1) were assessed for inhibition of SpeB hydrolysis, with no appreciable effect on proteolysis or the assay observed (Figures S1 & S2). Molecules selected based on potency, lipophilicity, and molecular weight were manually re-synthesized and purified on milligram scale. We observed a correlation between potency estimated in the initial screen and those of re-synthesized compounds (Figure S3). Structures of representative molecules with improved IC_{50} values are shown in Figure 2d.

With significantly improved SpeB inhibitors in hand, we next assessed if miniaturization of the SuFEx reaction was feasible using an Echo Acoustic liquid handler. A strong correlation in inhibitory potency was observed between the picomole-scale (1536-well, 2 µL, 200 µM of isodifluor compound, 400 pmol) and nanomole-scale (96-well, 50 µL, 10 nmol) syntheses, demonstrating the successful miniaturization of the library construction (Figures 2e & S4). Importantly, unlike previously reported nanoscale medicinal chemistry attempts[25], our sub-nanoscale SuFEx-based library synthesis does not require specialized equipment, such as dry-boxed liquid handlers and highly sensitive mass spectrometry for the biological assay. Our SuFEx-based format can be readily adapted in screening facilities with standard HTS robotics and liquid handler systems.

We next characterized an improved compound **5** with biochemical and biophysical methods to substantiate the improved potency. Enzyme kinetics showed that **5** is a reversible, competitive inhibitor with K_i = 18 ± 1 nM (Figures S5 & S6). The improved binding affinity was further validated by surface plasmon resonance and differential scanning fluorometry (Figures S7 & S8). We determined the x-ray crystal structure of SpeB in complex with **5** to elucidate the origin of improved inhibition (Figures 3 & S9, Table S6). Interestingly, **5** binds SpeB in a U-shaped conformation with an intramolecular CH-π interaction[26-27] between the benzyl moiety and a hydrogen on the piperidyl group that likely contributes the binding confirmation (Figure S10). Compound **5** binds within the SpeB active site whereby the carbonyl oxygen is oriented toward the SpeB oxyanion hole created by the main-chain nitrogen atoms of residues Cys192 and Val193 (Figure 3).

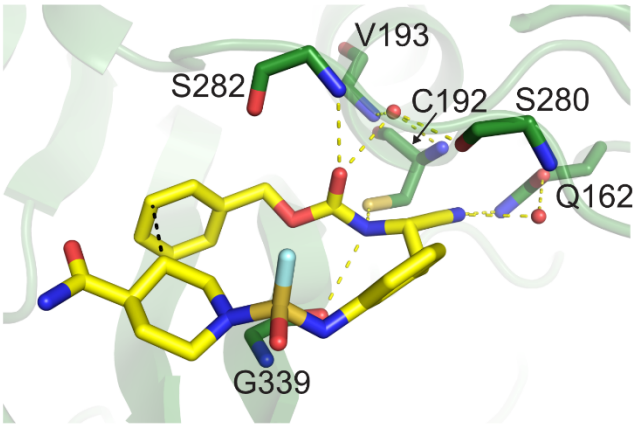

Figure 3. X-ray structure of SpeB-compound **5** structure (PDB ID 6UQD). Cmpd **5** (yellow carbon) bound to the SpeB (green carbon) are shown as sticks (red oxygen, blue nitrogen, mustard sulfur, teal fluorine).

Based on biological stability and solubility in PBS (Table S8), compound **7** was selected for further biological characterization. As shown in Figure 4a, **7** is stable against human liver microsomes *in vitro,* soluble in PBS, selective for SpeB (over other cysteine proteases), non-cytotoxic, and adheres to Lipinski's rules. We tested the effect of inhibitor **7** in an established neutrophil killing assay, wherein SpeB activity provides relative resistance to *S. pyogenes* against human neutrophils[28-29]. Wild-type (WT) *S. pyogenes* (M1 serotype strain 5448) and a corresponding isogenic mutant strain lacking SpeB (ΔSpeB) were preincubated with **7** prior to introduction of freshly isolated neutrophils from human blood. The presence of **7** decreased the viability of WT *S. pyogenes* in

a concentration-dependent manner, while no similar drug effect of **7** occurred in the ΔSpeB mutant strain (Figure 4b).

In conclusion, we provide a proof-of-concept of high-throughput process to improve potency of an HTS hit molecule to generate a drug-like, biologically active molecule using biocompatible SuFEx click chemistry. This study highlights the utility of SuFEx chemistry for rapidly generating diversified molecules for hit-to-lead applications and shows the potential of the combination of click chemistry, miniaturized synthesis, and direct evaluation of biological potency. Efforts to improve and expand the method are underway to develop an HT medicinal chemistry platform applicable for routine use[30]. Molecules described here represent the first potent and selective small molecule SpeB inhibitors and can be used to address biological functions of this protease in cellular and animal models and establish as a potential target for the development of treatments to combat streptococcal infections.

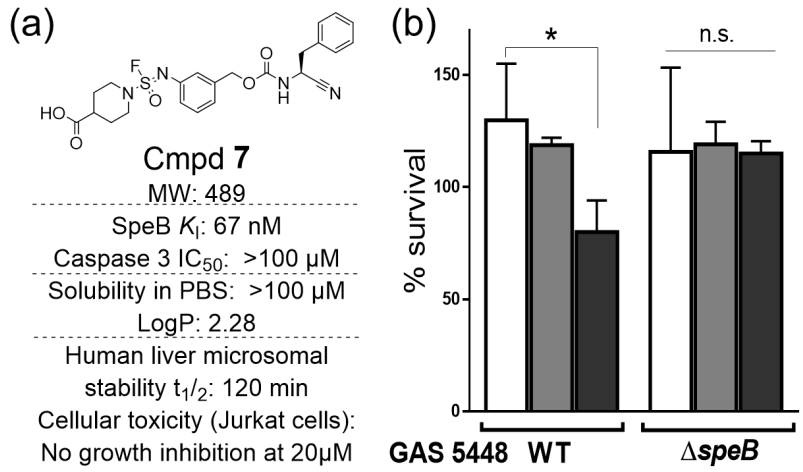

Figure 4 Improved SpeB inhibitor **7** is drug-like and biologically active in bacteria-neutrophil co-culture. (a) Drug-likeness of cmpd **7**. Solubility in PBS[31-32], caspase activity[33], microsomal stability and cellular toxicity were measured as described[34], LogP was predicted with ChemDraw Ultra 17.1. (b) cmpd **7** prevents *S. pyogenes* WT GAS5448 from neutrophil killing by the inhibition of SpeB; however, no effect is observed on the □SpeB strain. Vehicle (□), Cmpd **7** (20 μM (■) or 40 μM (■)). Statistical analysis was performed using one-way ANOVA with Dunnett's multiple comparisons test, *≤ 0.05.

Supporting Information

Additional texts, figures, and tables are provided.

AUTHOR INFORMATION

[#]Authors contributed equally.

Corresponding Authors

Correspondence: sharples@scripps.edu, wolan@scripps.edu

Author Contributions

SK, QZ, KBS, and DWW conceived the project. SK designed the experiments. SK designed, synthesized, and characterized molecules. QZ and SK performed SOF_4 reaction. SK, AS, and JW performed the *in vitro* kinetics studies and analysis. SK, EC, and MVH performed the high-throughput synthesis and assay. SK and DWW performed the crystallography and structure analysis. AS performed the toxicity screen. ND and VN performed neutrophil assays. SK and MK performed LC-CAD analysis. The manuscript was written through contributions of all authors. All authors have given approval to the final version of the manuscript.

Funding Sources

The authors gratefully acknowledge financial support from The Scripps Research Institute (to D.W.W.) and NIH grant R01 AI077780 (to V.N.), R01 GM117145 (to K.B.S.), the Ellen Browning Scripps Foundation (to Q.Z.).

Notes

The authors declare no competing financial interests.

ACKNOWLEDGMENT

We thank I. Wilson, R. Stanfield, M. Elsliger, and X. Dai for computational assistance, H. Rosen and A. Ward for access to instrumentation, and the staff of the Stanford Synchrotron Radiation Lightsource.

References

1. Sharpless, K. B.; Kolb, H. C., *217th ACS National Meeting, Anaheim, CA, March 21 – 25*. 1999.
2. Kolb, H. C.; Finn, M. G.; Sharpless, K. B., Click chemistry: diverse chemical function from a few good reactions. *Angew. Chem. Int. Ed.* **2001,** *40* (11), 2004-2021.
3. Dong, J.; Krasnova, L.; Finn, M. G.; Sharpless, K. B., Sulfur(VI) fluoride exchange (SuFEx): another good reaction for click chemistry. *Angew. Chem. Int. Ed.* **2014,** *53* (36), 9430-9448.
4. Li, S.; Wu, P.; Moses, J. E.; Sharpless, K. B., Multidimensional SuFEx click chemistry: sequential sulfur(VI) fluoride exchange connections of diverse modules launched from an SOF_4 hub. *Angew. Chem. Int. Ed.* **2017,** *56* (11), 2903-2908.
5. Wang, H.; Zhou, F.; Ren, G.; Zheng, Q.; Chen, H.; Gao, B.; Klivansky, L.; Liu, Y.; Wu, B.; Xu, Q.; Lu, J.; Sharpless, K. B.; Wu, P., SuFEx-based polysulfonate formation from ethenesulfonyl fluoride–amine adducts. *Angew. Chem. Int. Ed.* **2017,** *56* (37), 11203-11208.
6. Dong, J.; Sharpless, K. B.; Kwisnek, L.; Oakdale, J. S.; Fokin, V. V., SuFEx-based synthesis of polysulfates. *Angew. Chem. Int. Ed.* **2014,** *53* (36), 9466-9470.
7. Gao, B.; Zhang, L.; Zheng, Q.; Zhou, F.; Klivansky, L. M.; Lu, J.; Liu, Y.; Dong, J.; Wu, P.; Sharpless, K. B., Bifluoride-catalysed sulfur(VI) fluoride exchange reaction for the synthesis of polysulfates and polysulfonates. *Nat. Chem.* **2017,** *9*, 1083.
8. Liu, Z.; Li, J.; Li, S.; Li, G.; Sharpless, K. B.; Wu, P., SuFEx click chemistry enabled late-stage drug functionalization. *J. Am. Chem. Soc.* **2018,** *140* (8), 2919-2925.
9. Baranczak, A.; Liu, Y.; Connelly, S.; Du, W.-G. H.; Greiner, E. R.; Genereux, J. C.; Wiseman, R. L.; Eisele, Y. S.; Bradbury, N. C.; Dong, J.; Noodleman, L.; Sharpless, K. B.; Wilson, I. A.; Encalada, S. E.; Kelly, J. W., A fluorogenic aryl fluorosulfate for intraorganellar transthyretin imaging in living cells and in *Caenorhabditis elegans*. *J. Am. Chem. Soc.* **2015,** *137* (23), 7404-7414.

10. Chen, W.; Dong, J.; Li, S.; Liu, Y.; Wang, Y.; Yoon, L.; Wu, P.; Sharpless, K. B.; Kelly, J. W., Synthesis of sulfotyrosine-containing peptides by incorporating fluorosulfated tyrosine using an Fmoc-based solid-phase strategy. *Angew. Chem. Int. Ed.* **2016,** *128* (5), 1867-1870.
11. Mortenson, D. E.; Brighty, G. J.; Plate, L.; Bare, G.; Chen, W.; Li, S.; Wang, H.; Cravatt, B. F.; Forli, S.; Powers, E. T.; Sharpless, K. B.; Wilson, I. A.; Kelly, J. W., "Inverse drug discovery" strategy to identify proteins that are targeted by latent electrophiles as exemplified by aryl fluorosulfates. *J. Am. Chem. Soc.* **2018,** *140* (1), 200-210.
12. Zheng, Q.; Woehl, J. L.; Kitamura, S.; Santos-Martins, D.; Smedley, C. J.; Li, G.; Forli, S.; Moses, J. E.; Wolan, D. W.; Sharpless, K. B., SuFEx-enabled, agnostic discovery of covalent inhibitors of human neutrophil elastase. *Proc. Natl. Acad. Sci. USA* **2019**, *116* (38), 18808-18814.
13. Srinivasan, R.; Li, J.; Ng, S. L.; Kalesh, K. A.; Yao, S. Q., Methods of using click chemistry in the discovery of enzyme inhibitors. *Nat. Protoc.* **2007,** *2* (11), 2655-2664.
14. Grimster, N. P.; Stump, B.; Fotsing, J. R.; Weide, T.; Talley, T. T.; Yamauchi, J. G.; Nemecz, A.; Kim, C.; Ho, K. Y.; Sharpless, K. B.; Taylor, P.; Fokin, V. V., Generation of candidate ligands for nicotinic acetylcholine receptors via in situ click chemistry with a soluble acetylcholine binding protein template. *J. Am. Chem. Soc.* **2012,** *134* (15), 6732-6740.
15. Hirose, T.; Sunazuka, T.; Sugawara, A.; Endo, A.; Iguchi, K.; Yamamoto, T.; Ui, H.; Shiomi, K.; Watanabe, T.; Sharpless, K. B.; Omura, S., Chitinase inhibitors: extraction of the active framework from natural argifin and use of *in situ* click chemistry. *J. Antibiot. (Tokyo).* **2009,** *62* (5), 277-282.
16. Manetsch, R.; Krasiński, A.; Radić, Z.; Raushel, J.; Taylor, P.; Sharpless, K. B.; Kolb, H. C., *In situ* click chemistry: Enzyme inhibitors made to their own specifications. *J. Am. Chem. Soc.* **2004,** *126* (40), 12809-12818.
17. Mamidyala, S. K.; Finn, M. G., *In situ* click chemistry: probing the binding landscapes of biological molecules. *Chem. Soc. Rev.* **2010,** *39* (4), 1252-1261.
18. Rillahan, C. D.; Schwartz, E.; McBride, R.; Fokin, V. V.; Paulson, J. C., Click and pick: identification of sialoside analogues for siglec-based cell targeting. *Angew. Chem. Int. Ed.* **2012,** *51* (44), 11014-11018.
19. Zhao, C.; Rakesh, K. P.; Ravidar, L.; Fang, W.-Y.; Qin, H.-L., Pharmaceutical and medicinal significance of sulfur (VI)-containing motifs for drug discovery: a critical review. *Eur. J. Med. Chem.* **2019,** *162*, 679-734.
20. Liu, F.; Wang, H.; Li, S.; Bare, G. A. L.; Chen, X.; Wang, C.; Moses, J. E.; Wu, P.; Sharpless, K. B., Biocompatible SuFEx click chemistry: thionyl tetrafluoride (SOF_4)-derived connective hubs for bioconjugation to DNA and proteins. *Angew. Chem. Int. Ed.* **2019,** *48* (24), 6974-8033.
21. Chuang, W.-J.; Lin, Y.-S.; Wu, J.-J.; Liu, C.-C.; Lin, M. T., Chapter 483 - Streptopain. In *Handbook of proteolytic enzymes (3rd edition)*, Rawlings, N. D.; Salvesen, G., Eds. Academic Press: 2013; 2142-2150.
22. Wang, A. Y.; González-Páez, G. E.; Wolan, D. W., Identification and co-complex structure of a new *S. pyogenes* SpeB small molecule inhibitor. *Biochemistry* **2015,** *54* (28), 4365-4373.
23. González-Páez, G. E.; Wolan, D. W., Ultrahigh and high resolution structures and mutational analysis of monomeric *Streptococcus pyogenes* SpeB reveal a fnctional role for the glycine-rich C-terminal loop. *J. Biol. Chem.* **2012,** *287* (29), 24412-24426.
24. Connolly, K. L.; Braden, A. K.; Holder, R. C.; Reid, S. D., Srv mediated dispersal of Streptococcal biofilms through SpeB is observed in CovRS+ strains. *PLOS ONE* **2011,** *6* (12), e28640.
25. Gesmundo, N. J.; Sauvagnat, B.; Curran, P. J.; Richards, M. P.; Andrews, C. L.; Dandliker, P. J.; Cernak, T., Nanoscale synthesis and affinity ranking. *Nature* **2018,** *557* (7704), 228-232.
26. Kumar, M.; Balaji, P. V., C-H···π interactions in proteins: prevalence, pattern of occurrence, residue propensities, location, and contribution to protein stability. *J. Mol. Model.* **2014,** *20* (2), 2136.

27. Brandl, M.; Weiss, M. S.; Jabs, A.; Sühnel, J.; Hilgenfeld, R., C-H···π-interactions in proteins. *J. Mol. Biol.* **2001,** *307* (1), 357-377.
28. Buchanan, J. T.; Simpson, A. J.; Aziz, R. K.; Liu, G. Y.; Kristian, S. A.; Kotb, M.; Feramisco, J.; Nizet, V., DNase expression allows the pathogen group A Streptococcus to escape killing in neutrophil extracellular traps. *Curr. Biol.* **2006,** *16* (4), 396-400.
29. Walker, M. J.; Hollands, A.; Sanderson-Smith, M. L.; Cole, J. N.; Kirk, J. K.; Henningham, A.; McArthur, J. D.; Dinkla, K.; Aziz, R. K.; Kansal, R. G.; Simpson, A. J.; Buchanan, J. T.; Chhatwal, G. S.; Kotb, M.; Nizet, V., DNase Sda1 provides selection pressure for a switch to invasive group A streptococcal infection. *Nat. Med.* **2007,** *13* (8), 981-985.
30. Erb, M. A.; Wolan, D.; Kitamura, S.; Chatterjee, A. Pharmacological inhibitors of the ENL YEATS domain TSRI-014PR00, 2019.
31. Morisseau, C.; Goodrow, M. H.; Newman, J. W.; Wheelock, C. E.; Dowdy, D. L.; Hammock, B. D., Structural refinement of inhibitors of urea-based soluble epoxide hydrolases. *Biochem. Pharmacol.* **2002,** *63* (9), 1599-1608.
32. Kitamura, S.; Hvorecny, K. L.; Niu, J.; Hammock, B. D.; Madden, D. R.; Morisseau, C., Rational design of potent and selective inhibitors of an epoxide hydrolase virulence factor from *Pseudomonas aeruginosa*. *J. Med. Chem.* **2016,** *59* (10), 4790-4799.
33. Solania, A.; González-Páez, G. E.; Wolan, D. W., Selective and rapid cell-permeable inhibitor of human caspase-3. *ACS Chem. Biol.* **2019**, *14* (11), 2463-2470.
34. Kitamura, S.; Owensby, A.; Wall, D.; Wolan, D. W., Lipoprotein signal peptidase inhibitors with antibiotic properties identified through design of a robust *In vitro* HT platform. *Cell Chem. Biol.* **2017,** *25* (3), 301-308.e12.

Supplemental Information:

SuFEx-enabled high-throughput medicinal chemistry

Seiya Kitamura[1#], Qinheng Zheng[2#], Jordan L. Woehl[1], Angelo Solania[1], Emily Chen[3], Nicholas Dillon[5,7], Mitchell V. Hull[3], Miyako Kotaniguchi[8], Shinichi Kitamura[8], Victor Nizet[5,6,7], K. Barry Sharpless[2*] and Dennis W. Wolan[1,4*]

Department of Molecular Medicine[1], Department of Chemistry[2], California Institute for Biomedical Research[3], and Department of Integrative Structural and Computational Biology[4], The Scripps Research Institute, La Jolla, CA, 92037, USA. Department of Pediatrics[5], Collaborative to Halt Antibiotic-Resistant Microbes (CHARM)[6], Skaggs School of Pharmacy and Pharmaceutical Sciences[7], UC San Diego, La Jolla, CA 92093, USA. Laboratory of Advanced Food Process Engineering, Osaka Prefecture University, 1-2, Gakuen-cho, Nakaku, Sakai, Osaka 599-8570, Japan[8].

[#]Authors contributed equally.

*Correspondence: wolan@scripps.edu, sharples@scripps.edu

Table of contents

S2-S11 Detailed synthetic methods and compound characterization

Methods:

- Measurement of SpeB inhibition
- Library construction
- NanoDSF
- Neutrophil killing assays
- X-ray crystallography
- Analytical LC method to determine the purity of synthetic compounds
- Analytical method to monitor SuFEx reactions

Tables

S12-S13 **Table S1.** Preliminary structure-activity relationships of compound **1**.
S14 **Table S2.** PBS improves the yield of SuFEx reaction.
S15 **Table S3.** Scope of SuFEx reactions in the HT library synthesis.
S16 **Table S4.** Secondary amine library information and their potency in the screening.
S20 **Table S5.** Primary amine library information and their potency in the screening.
S30 **Table S6.** SpeB in complex with compound **5** x-ray data processing and structure refinement statistics.
S31 **Table S7.** Structure-activity relationships of selected analogs.
S32 **Table S8.** Key parameters of selected inhibitors.

Figures

S33 **Figure S1.** Inhibitory potency of amines on SpeB enzyme activity.
S33 **Figure S2.** Effects of fluoride ion on SpeB enzyme activity and inhibitor potency.
S34 **Figure S3.** Correlation of pIC_{50} estimated by the measurement of inhibitory potency of reaction mixture vs Manual measurement of pIC_{50} of pure compounds.
S34 **Figure S4.** Additional correlation of pIC_{50} between picomole-scale synthesis vs 96 well plate synthesis.
S35 **Figure S5.** K_I determination of compounds **5** and **7** against SpeB.
S35 **Figure S6.** Compounds **5** & **7** are reversible inhibitors.
S37 **Figure S7.** Differential scanning fluorimetry melting curves.
S38 **Figure S8.** Surface plasmon resonance analysis of cmpd **5** against rSpeB.
S38 **Figure S9.** X-ray structure of compound **5**-SpeB complex.
S39 **Figure S10.** Intramolecular CH-π interaction between piperidine and benzyl moiety of compound **5** bound to SpeB.
S40 **Supplementary References**

Supplementary Data

S41-S108 NMR spectra, LC-CAD trace of the SuFEx reaction

Detailed synthetic methods and compound characterization

General

All reagents and solvents were purchased from commercial suppliers and were used without further purification. ^{1}H and ^{13}C NMR spectra were collected using a Bruker 600, 500, or 400 MHz spectrometer with chemical shifts reported relative to residual deuterated solvent peaks or a tetramethylsilane internal standard. $CFCl_3$ was used as an internal standard for ^{19}F-NMR. Accurate masses were measured using an ESI-TOF (HRMS, Agilent MSD) or MSQ Plus mass spectrometer (LRMS, Thermo Scientific). Reactions were monitored on TLC plates (silica gel 60, F254 coating, EMD Millipore, 1057150001), and spots were either monitored under UV light (254 mm) or stained with phosphomolybdic acid. The same TLC system was used to test purity, and all final products showed a single spot on TLC with both $KMnO_4$ and UV absorbance. The purity of the compounds that were tested in the assay was >95% based on ^{1}H NMR and reverse phase HPLC-UV on monitoring absorption at 240 nm (detailed in the section 'analytical LC method to determine the purity of synthetic compounds'). It should be noted that SpeB is susceptible to divalent cations such as Cu^{2+}, Zn^{2+}; thus, care was taken to ensure that the final products did not contain contaminations of these metals.

METHODS

Synthesis

Representative procedure for Cbz synthesis (Method A)

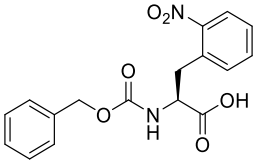

To an ACN/aqueous $NaHCO_3$ solution (1:1) of (S)-2-amino-3-(2-nitrophenyl)propanoic acid (1 g, 4.76 mmol) was added N-(Benzyloxycarbonyloxy)succinimide (1.2 g, 4.82 mmol, 1.01 eq.) and stirred overnight. To this solution was added ethyl acetate and 1M HCl, and the aqueous phase was extracted with ethyl acetate. The organic layer was combined, washed with brine, dried over $MgSO_4$, filtered and concentrated in vacuo to give a fairly pure target molecule an off-white solid (1.6 g, quant.). The compound was used into the next step without further purification. ((*S*)-2-(((benzyloxy)carbonyl)amino)-3-(2-nitrophenyl)propanoic acid). ^{1}H NMR (600 MHz, DMSO-d_6) δ 8.03 – 7.92 (m, 1H), 7.68 (d, *J* = 8.8 Hz, 1H), 7.63 (td, *J* = 7.5, 1.4 Hz, 1H), 7.51 (t, *J* = 7.5 Hz, 2H), 7.36 – 7.32 (m, 2H), 7.32 – 7.27 (m, 1H), 7.25 – 7.19 (m, 2H), 4.94 (s, 2H), 4.36 (ddd, *J* = 10.7, 8.9, 4.5 Hz, 1H), 3.48 (dd, *J* = 13.9, 4.5 Hz, 1H), 3.01 (dd, *J* = 14.0, 10.7 Hz, 1H). ^{13}C NMR (151 MHz, DMSO) δ 172.8, 155.9, 149.2, 137.0, 133.1, 133.0, 132.3, 128.3, 128.2, 127.7, 127.4, 124.6, 65.3, 53.9, 33.7. (+) calcd for $(M+H)^+$ 345.1. Found 345.2. (^{t}R= 10.4 min).

Representative procedure for the conversion from carboxylic acid into amide (Method B)

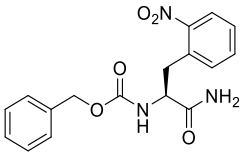

To a dioxane solution of (*S*)-2-(((benzyloxy)carbonyl)amino)-3-(2-nitrophenyl)propanoic acid (2 g, 5.83 mmol) was added pyridine (484 µL, 475 mg, 6 mmol, 1.02 eq.) followed by Di-*tert*-butyl dicarbonate (2.6 g, 11.9 mmol, 2.0 eq.) and ammonium bicarbonate (1.15 g, 14.6 mmol, 2.5 eq.), and stirred overnight at RT. To this solution was added water, and the precipitate was collected by filtration. Recrystallization from acetone gave fairly pure target molecule as an off-white solid (1.2 g, 3.5 mmol, 60 %). ^{1}H NMR (600 MHz, DMSO-d_6) δ 7.96 (dd, *J* = 8.4, 1.4 Hz, 1H), 7.62 (td, *J* = 7.6, 1.4 Hz, 1H), 7.52 – 7.47 (m, 3H), 7.38 – 7.27 (m, 4H), 7.22 (d, *J* = 7.4 Hz, 2H), 7.14 (s, 1H), 4.99 – 4.88 (m, 2H), 4.41 – 4.32 (m, 1H), 3.38 (dt, *J* = 14.5, 3.7 Hz, 1H), 3.01 (ddd, *J* = 13.9, 10.2, 2.5 Hz, 1H). ^{13}C NMR (151 MHz, DMSO) δ 172.7, 155.8,

149.3, 137.0, 133.0, 132.6, 132.5, 128.3, 128.0, 127.7, 127.4, 124.5, 65.3, 54.3, 34.2. (+) calcd for $(M+H)^+$ 344.1. Found 344.2. (^{t}R= 10.0 min).

Representative procedure for the conversion of amide into nitrile (Method C)

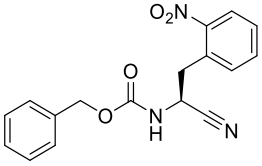

To a DMF solution of benzyl (*S*)-(1-amino-3-(2-nitrophenyl)-1-oxopropan-2-yl)carbamate (1.2 g, 3.5 mmol) was added cyanuric chloride (1.2 g, 6.5 mmol, 1.86 eq.) at 0°C and stirred overnight at RT. To this solution was added ethyl acetate and water, and the aqueous phase was extracted with ethyl acetate. The organic layer was combined, washed with brine, dried over $MgSO_4$, filtered and concentrated in vacuo. Recrystalization from acetone gave a pure target molecule as an off-white solid (1.6 g, quant.). ^{1}H NMR (400 MHz, DMSO-d_6) δ 8.37 (d, *J* = 8.2 Hz, 1H), 8.05 (d, *J* = 8.1 Hz, 1H), 7.76 – 7.68 (m, 1H), 7.62 – 7.50 (m, 2H), 7.41 – 7.22 (m, 5H), 5.04 (s, 2H), 4.94 (dd, *J* = 15.6, 7.9 Hz, 1H), 3.46 (dd, *J* = 13.7, 6.7 Hz, 1H), 3.32 (m (overlap with water signal), 1H).^{13}C NMR (101 MHz, DMSO-d_6) δ 155.3, 149.1, 136.4, 133.7, 133.2, 130.0, 129.1, 128.4, 128.0, 127.9, 125.0, 118.8, 66.2, 42.7, 34.8. LRMS (+) calcd for $(M+H)^+$ 326.1. Found 326.3. Purity (HPLC-UV): >99% (^{t}R= 11.3 min).

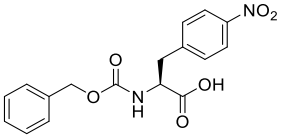

Method A (2 g, quant.). ^{1}H NMR (600 MHz, Chloroform-*d*) δ 8.12 (d, *J* = 8.2 Hz, 2H), 7.38 – 7.29 (m, 7H), 5.33 – 5.17 (m, 1H), 5.15 – 5.03 (m, 2H), 4.73 (dd, *J* = 13.8, 6.9 Hz, 1H), 3.36 (dd, *J* = 13.9, 5.6 Hz, 1H), 3.17 (dd, *J* = 14.0, 6.7 Hz, 1H). ^{13}C NMR (151 MHz, $CDCl_3$) δ 173.8, 155.6, 147.2, 143.4, 135.8, 130.3, 128.6, 128.5, 128.2, 123.8, 67.4, 54.2, 37.8. LRMS (+) calcd for $(M+H)^+$ 345.1. Found 345.3. (^{t}R= 10.6 min).

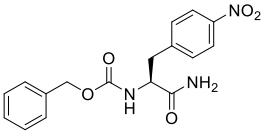

Method B (1.56 g, 4.55 mmol, 78%). ^{1}H NMR (600 MHz, DMSO-d_6) δ 8.17 – 8.12 (m, 2H), 7.59 – 7.50 (m, 4H), 7.34 – 7.25 (m, 3H), 7.25 – 7.19 (m, 2H), 7.17 – 7.11 (m, 1H), 4.95 (d, *J* = 12.7 Hz, 1H), 4.91 (d, *J* = 12.7 Hz, 1H), 4.26 (ddd, *J* = 10.8, 8.8, 4.2 Hz, 1H), 3.15 (dd, *J* = 13.6, 4.2 Hz, 1H), 2.89 (dd, *J* = 13.6, 10.8 Hz, 1H). ^{13}C NMR (151 MHz, DMSO) δ 172.8, 155.9, 146.8, 146.2, 137.0, 130.5, 128.2, 127.7, 127.4, 123.2, 65.2, 55.5, 37.4. LRMS (+) calcd for $(M+NH_4)^+$ 344.1. Found 344.2. (^{t}R= 10.0 min).

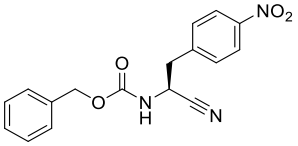

Method C, white solid (81 mg, 0.25 mmol, 5%).^{1}H NMR (600 MHz, DMSO-d_6) δ 8.29 (d, *J* = 8.3 Hz, 1H), 8.21 – 8.14 (m, 2H), 7.64 – 7.54 (m, 2H), 7.35 – 7.28 (m, 3H), 7.29 – 7.25 (m, 2H), 5.03 (s, 2H), 4.90 (dd, *J* = 15.6, 8.2 Hz, 1H), 3.30 – 3.24 (m, 1H), 3.22 – 3.18 (m, 1H). ^{13}C NMR (151 MHz, DMSO) δ 155.3, 149.9, 146.7, 143.6, 136.4, 130.8, 128.3, 128.0, 127.8, 123.4, 119.1, 66.1, 43.1, 40.0. LRMS (+) calcd for $(M+NH_4)^+$ 343.1. Found 343.4. Purity (HPLC-UV): >99% (^{t}R= 11.3 min).

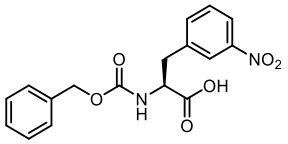

Method A (1.46 g, 4.24 mmol, 92%). ^{1}H NMR (600 MHz, DMSO-d_6) δ 8.18-8.16 (m, 1H), 8.12 – 8.08 (m, 1H), 7.78 – 7.74 (m, 2H), 7.58 (t, J = 7.9 Hz, 1H), 7.33 – 7.27 (m, 3H), 7.25 – 7.19 (m, 2H), 4.99 – 4.92 (m, 2H), 4.29 (ddd, J = 10.8, 8.6, 4.4 Hz, 1H), 3.25 (dd, J = 13.9, 4.4 Hz, 1H), 2.98 (dd, J = 13.8, 10.8 Hz, 1H). ^{13}C NMR (151 MHz, DMSO-d_6) δ 172.9, 156.0, 147.6, 140.3, 137.0, 136.1, 129.7, 128.3, 127.8, 127.4, 124.0, 121.6, 65.3, 55.0, 35.9. LRMS (+) calcd for $(M+H)^+$ 345.1. Found 345.3. (^{t}R= 10.6 min).

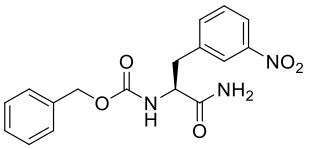

Method B (136 mg, 400 µmol, 40%). ^{1}H NMR (600 MHz, DMSO-d_6) δ 8.23 (t, J = 2.0 Hz, 1H), 8.09 (ddd, J = 8.2, 2.5, 1.0 Hz, 1H), 7.75 (dt, J = 7.8, 1.3 Hz, 1H), 7.58 (t, J = 7.9 Hz, 1H), 7.54 – 7.42 (m, 1H), 7.33 – 7.24 (m, 3H), 7.23 – 7.18 (m, 2H), 7.15 – 7.08 (m, 1H), 4.97 – 4.86 (m, 2H), 4.28 – 4.19 (m, 1H), 3.14 (dd, J = 13.6, 4.0 Hz, 1H), 2.88 (dd, J = 13.6, 10.9 Hz, 1H). ^{13}C NMR (151 MHz, DMSO-d_6) δ 172.9, 155.9, 147.6, 140.7, 137.0, 136.2, 129.5, 128.2, 127.7, 127.3, 123.9, 121.4, 65.2, 55.7, 37.1. LRMS (+) calcd for $(M+H)^+$ 344.1. Found 344.2. (^{t}R= 10.1 min).

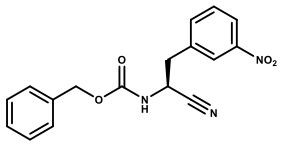

Method C (43 mg, 130 mmol, 40%). ^{1}H NMR (600 MHz, DMSO-d_6) δ 8.30 (d, J = 8.1 Hz, 1H), 8.26 (t, J = 2.0 Hz, 1H), 8.14 (ddd, J = 8.2, 2.4, 1.0 Hz, 1H), 7.78 (dt, J = 7.7, 1.3 Hz, 1H), 7.62 (t, J = 7.9 Hz, 1H), 7.38 – 7.29 (m, 3H), 7.28 – 7.23 (m, 2H), 5.02 (s, 2H), 4.96 – 4.84 (m, 1H), 3.34 – 3.24 (m, 2H), 3.25 – 3.11 (m, 1H). ^{13}C NMR (151 MHz, DMSO-d_6) δ 155.3, 147.7, 137.8, 136.4, 129.8, 128.3, 128.0, 127.7, 124.3, 122.2, 119.2, 66.0, 43.3, 36.7. LRMS (+) calcd for $(M+NH_4)^+$ 343.1. Found 343.3. Purity (HPLC-UV): >99% (^{t}R= 11.4 min).

Representative procedure for reduction of nitro moiety to amine using $SnCl_2$ (Method D)

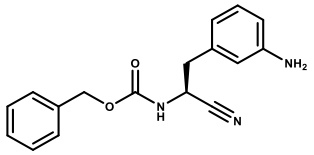

To an ethanol solution of benzyl (*S*)-(1-cyano-2-(3-nitrophenyl)ethyl)carbamate (400 mg, 1.23 mmol) was added $SnCl_2$ (585 mg, 3.1 mmol, 2.5 eq.) and refluxed for 2 hours. Solvent was evaporated in vacuo and to the residue was added ethyl acetate and washed twice with 1N $NaOH_{aq}$., dried over $NaSO_4$, filtered and concentrated in vacuo. Column chromatography (Hexane: ethyl acetate=2:1) gave a pure target molecule as an off-white solid (170 mg, 0.58 mmol, 47 %). ^{1}H NMR (600 MHz, DMSO-d_6) δ 8.24 (d, J = 8.0 Hz, 1H), 7.40 – 7.35 (m, 2H), 7.35 – 7.29 (m, 3H), 6.95 (t, J = 7.7 Hz, 1H), 6.49 – 6.40 (m, 3H), 5.10 – 4.99 (m, 4H), 4.64 (dd, J =16.2, 8.0 Hz, 1H), 2.90 (d, J = 8.1 Hz, 2H). ^{13}C NMR (151 MHz, DMSO-d_6) δ 155.3, 148.7, 136.5, 135.9, 128.9, 128.4, 128.0, 127.9, 119.4, 116.5, 114.6, 112.8, 66.1, 44.0, 37.8. LRMS (+) calcd for $(M+H)^+$ 296.2. Found 296.3. Purity (HPLC-UV): >99% (^{t}R= 9.4 min).

Representative procedure for the conversion of aniline into iminosulfur oxydifluorides (Method E)

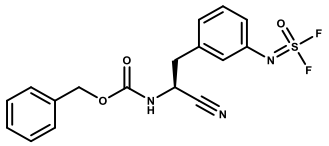

The method for the preparation of iminosulfur oxydifluorides is adapted from Li et al.[1] In a 25-mL round bottom flask, benzyl (*S*)-(2-(3-aminophenyl)-1-cyanoethyl)carbamate trifluoroacetate salt (135.8 mg, 0.3317 mmol) and triethylamine (139 µL, 1.00 mmol, 3.0 equiv) were dissolved in anhydrous acetonitrile (3.3 mL). Sealed with a rubber septum, the flask was evacuated and backfilled with thionyl tetrafluoride gas (~25 mL). Mild exotherm was observed at the start of the reaction in company with fume generation. The reaction was monitored by TLC and found complete in 30 min. Volatiles were removed by a rotary evaporator. The crude was purified by flash column chromatography (hexanes to 30% ethyl acetate in hexanes) to give the target iminosulfur oxydifluoride as a white crystalline (118.2 mg, 0.3116 mmol, 94% yield). ^{1}H NMR (600 MHz, Chloroform-*d*) δ 7.41 – 7.30 (m, 6H), 7.14 (d, *J* = 7.7 Hz, 1H), 7.10 (ddd, *J* = 8.1, 2.2, 1.0 Hz, 1H), 7.03 (s, 1H), 5.15 – 5.08 (m, 3H), 4.92 – 4.85 (m, 1H), 3.14 – 3.04 (m, 2H). ^{13}C NMR (151 MHz, Chloroform-*d*) δ 155.0, 136.9 (t, J_{CF} = 3.0 Hz), 135.8, 135.5, 130.5, 128.8, 128.7, 128.5, 127.3, 124.9 (t, J_{CF} = 3.0 Hz), 123.3 (t, J_{CF} = 3.0 Hz), 117.8, 68.0, 43.7, 38.9. ^{19}F NMR (377 MHz, $CDCl_3$) δ 47.0. LRMS (+) calcd for $(M+H)^+$ 380.1. Found 380.2. Purity (HPLC-UV): >99% (^{t}R= 12.2 min).

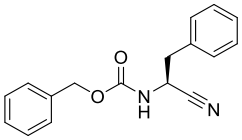

Method C (3.5 g, 12.5 mmol, 89%). ^{1}H NMR (600 MHz, DMSO-d_6) δ 8.27 (d, *J* = 8.1 Hz, 1H), 7.43 – 7.21 (m, 10H), 5.05 (s, 2H), 4.78-4.74 (m, 1H), 3.15 – 2.97 (m, 2H). ^{13}C NMR (151 MHz, DMSO-d_6) δ 155.4, 136.5, 135.5, 129.4, 128.40, 128.39 128.0, 127.8, 127.1, 119.4, 66.0, 43.8, 37.4. (+) calcd for $(M+NH_4)^+$ 298.2. Found 298.3. Purity (HPLC-UV): >99% (^{t}R= 11.5 min).

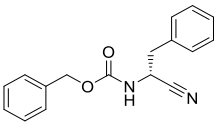

Method C (11 mg, 39 µmol, 12 %). ^{1}H & ^{13}C NMR was identical to the L-isomer. (+) calcd for $(M+NH_4)^+$ 298.2. Found 298.4. Purity (HPLC-UV): >99% (^{t}R= 11.5 min).

Procedure for Cbz deprotection

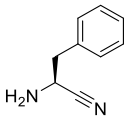

To a dioxane solution of benzyl (*S*)-(1-cyano-2-phenylethyl)carbamate (3.5 g, 12.5 mmol) was added 10% Pd/C (1 g) and the reaction flask was purged with hydrogen gas and stirred overnight at RT. The reaction mixture was filtered through celite and concentrated in vacuo. Column chromatography (ethyl acetate 100%) gave a target molecule as a reddish oil and used for the next step without further purification (1.6 g, 11 mmol, 88%). ^{1}H NMR (600 MHz, DMSO-d_6) δ 7.35 – 7.23 (m, 7H), 3.95 (dd, *J* = 8.5, 6.5 Hz, 1H), 2.95 (dd, *J* = 13.4, 6.5 Hz, 1H), 2.88 (dd, *J* = 13.5, 8.5 Hz, 1H). ^{13}C NMR (151 MHz, DMSO-d_6) δ 136.7, 129.4, 128.3, 126.8, 122.7, 44.9, 41.0. (+) calcd for $(M+CH_4CN)^+$ 188.1. Found 188.3.

Synthesis of (*S*)-1-benzyl-3-(1-cyano-2-phenylethyl) urea

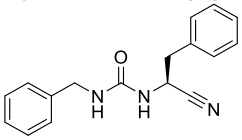

To a THF solution of (*S*)-2-amino-3-phenylpropanenitrile (146 mg, 1 mmol) was added DIPEA (200 µL, 1.2 mmol) and benzyl isocyanate (146 mg, 1.1 mmol, 1.1 eq.) and stirred overnight. Solvent was removed

and ethyl acetate was added to the residue, then washed with 1N HCl_{aq} and brine. Column chromatography gave a target molecule as a brown solid (94 mg, 337 μmol, 34%). ^{1}H NMR (600 MHz, DMSO-d_6) δ 7.37 – 7.25 (m, 7H), 7.25 – 7.17 (m, 3H), 6.75 (d, *J* = 8.3 Hz, 1H), 6.71 (d, *J* = 6.0 Hz, 1H), 4.83 (dd, *J* = 15.6, 7.8 Hz, 1H), 4.20 (d, *J* = 6.0 Hz, 2H), 3.07 (d, *J* = 7.7 Hz, 2H). ^{13}C NMR (151 MHz, DMSO-d_6) δ 156.7, 140.3, 135.8, 129.4, 128.4, 128.2, 127.1, 127.0, 126.7, 120.1, 42.9, 42.9, 37.8. LRMS (+) calcd for $(M+H)^+$ 280.1. Found 280.3. Purity (HPLC-UV): >99% (^{t}R= 10.6 min).

Representative procedure for the carbamate compound from benzyl alcohol (Method F)

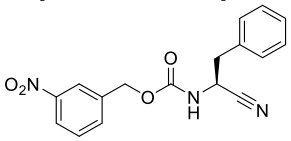

To a dry ACN solution of (3-nitrophenyl)methanol (3.26 g, 21.3 mmol) was added dry DIPEA (5.7 mL, 32.8 mmol, 1.5 eq.) followed by N,N′-Disuccinimidyl carbonate (5.6 g, 21.8 mmol, 1.03 eq.) and stirred overnight at RT. To this solution was added ethyl acetate and water, and the aqueous phase was extracted with ethyl acetate. The organic layer was combined, washed with brine, dried over $NaSO_4$, filtered and concentrated in vacuo. Column chromatography (hexane:ethyl acetate=3:1->1:1) gave a fairly pure 2,5-dioxopyrrolidin-1-yl (3-nitrobenzyl) carbonate (1.1 g, 3.7 mmol, 18%). The compound was used for the next step without further purification. ^{1}H NMR (600 MHz, DMSO-d_6) δ 8.40 (t, *J* = 2.0 Hz, 1H), 8.25 (ddd, *J* = 8.2, 2.4, 1.0 Hz, 1H), 7.97 (ddd, *J* = 7.6, 1.6, 1.0 Hz, 1H), 7.72 (t, *J* = 7.9 Hz, 1H), 5.19 (s, 2H), 2.63 (s, 4H). ^{13}C NMR (151 MHz, DMSO) δ 171.9, 147.7, 136.7, 135.7, 130.0, 123.7, 123.7, 76.5, 25.4. To a DMF solution of (*S*)-2-amino-3-phenylpropanenitrile (601 mg, 4.1 mmol, 1.1 eq.) was added DIPEA (3 mL, 17.3 mmol, 4.6 eq.) followed by 2,5-dioxopyrrolidin-1-yl (3-nitrobenzyl) carbonate (1.1 g, 3.7 mmol, 1 eq.) and stirred at RT overnight. To the reaction mixture was added ethyl acetate, then washed with 1N HCl_{aq} and brine. Recrystallization from DCM gave a target molecule as a brown solid (1.15 g, 3.5 mmol, 96% from 2,5-dioxopyrrolidin-1-yl (3-nitrobenzyl) carbonate). ^{1}H NMR (600 MHz, DMSO-d_6) δ 8.40 (d, *J* = 7.8 Hz, 1H), 8.22 – 8.18 (m, 2H), 7.80 – 7.72 (m, 1H), 7.68 (t, *J* = 7.8 Hz, 1H), 7.34 – 7.17 (m, 5H), 5.19 (d, *J* = 2.8 Hz, 2H), 4.77 (dd, *J* = 16.2, 8.0 Hz, 1H), 3.11 – 3.09 (m, 2H). ^{13}C NMR (151 MHz, DMSO) δ 155.1, 147.8, 138.9, 135.5, 134.2, 130.0, 129.4, 128.4, 127.1, 122.8, 122.1, 119.3, 64.8, 43.8, 37.4. LRMS (+) calcd for $(M+NH_4)^+$ 343.1. Found 343.2. Purity (HPLC-UV): 98% (^{t}R= 11.4 min).

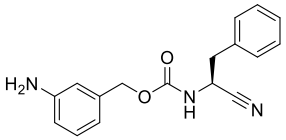

Method D (230 mg, 0.78 mmol, 22%). ^{1}H NMR (600 MHz, DMSO-d_6) δ 8.21 (d, *J* = 8.0 Hz, 1H), 7.34 – 7.30 (m, 4H), 7.28 – 7.26 (m, 1H), 6.98 (t, *J* = 7.6 Hz, 1H), 6.50 (d, *J* = 7.6 Hz, 2H), 6.43 (d, *J* = 7.4 Hz, 1H), 5.09 (s, 2H), 4.90 (d, *J* = 12.1 Hz, 1H), 4.85 (d, *J* = 12.1 Hz, 1H), 4.73 (dd, *J* = 15.6, 8.0 Hz, 1H), 3.15 – 2.96 (m, 2H). ^{13}C NMR (151 MHz, DMSO) δ 155.4, 148.7, 136.9, 135.5, 129.4, 128.9, 128.4, 127.1, 119.4, 115.3, 113.6, 113.3, 66.5, 43.9, 37.4. LRMS (+) calcd for $(M+H)^+$ 296.1. Found 296.3. Purity (HPLC-UV): 96% (^{t}R= 9.4 min).

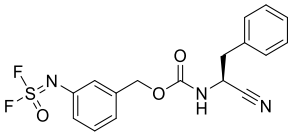

In a 25-mL round bottom flask, 3-aminobenzyl (*S*)-(1-cyano-2-phenylethyl)carbamate trifluoroacetate salt (180.0 mg, 0.4397 mmol) and triethylamine (183 μL, 1.32 mmol, 3.0 equiv) were dissolved in anhydrous acetonitrile (4.4 mL). Sealed with a rubber septum, the flask was evacuated and backfilled with thionyl tetrafluoride gas (~25 mL). Mild exotherm was observed at the start of the reaction in company with fume generation. The reaction was monitored by TLC and found complete in 30 min. Volatiles were removed by a rotary evaporator. The crude was purified by flash column chromatography (hexanes to 30% ethyl

acetate in hexanes) to give the target iminosulfur oxydifluoride as a white crystalline (136.7 mg, 0.3602 mmol, 82% yield). ^{1}H NMR (600 MHz, Acetonitrile-d_3) δ 7.41 (dd, J = 8.5, 7.7 Hz, 1H), 7.36 – 7.31 (m, 2H), 7.29 (td, J = 7.1, 1.2 Hz, 3H), 7.22 (d, J = 7.5 Hz, 1H), 7.17 – 7.12 (m, 2H), 6.53 (s, 1H), 5.07 (s, 2H), 4.83 – 4.67 (m, 1H), 3.13 (dd, J = 7.8, 6.3 Hz, 2H). ^{13}C NMR (151 MHz, CD_3CN) δ 156.3, 139.9, 137.0 (t, J_{CF} = 3.0 Hz), 136.3, 131.1, 130.4, 129.6, 128.5, 126.6, 124.0 (t, J_{CF} = 3.0 Hz), 123.7 (t, J_{CF} = 3.0 Hz), 119.7, 66.8, 45.1, 38.9. ^{19}F NMR (376 MHz, CD_3CN) δ 45.4. LRMS (+) calcd for $(M+H)^+$ 380.1. Found 380.2. Purity (HPLC-UV): 99% (^{t}R= 12.2 min).

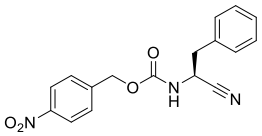

Method F (41 mg, 126 µmol, 16 %). ^{1}H NMR (600 MHz, DMSO-d_6) δ 8.43 (s, 1H), 8.23 (d, J = 8.7 Hz, 2H), 7.57 – 7.51 (m, 2H), 7.32 (d, J = 6.3 Hz, 4H), 7.27 (tt, J = 7.1, 2.3 Hz, 1H), 5.20 (s, 2H), 4.82 – 4.72 (m, 1H), 3.10 (dd, J = 11.7, 8.0 Hz, 2H). ^{13}C NMR (151 MHz, DMSO-d_6) δ 155.0, 146.9, 144.3, 135.4, 129.3, 128.3, 128.1, 127.0, 123.5, 119.2, 64.7, 43.7, 37.3. (+) calcd for $(M+NH_4)^+$ 343.1. Found 343.2. Purity (HPLC-UV): >99% (^{t}R= 11.4 min).

Representative procedure for the isofluor and amine reaction (Method G)

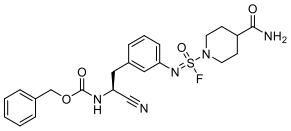

To an ACN solution of benzyl (S)-(1-cyano-2-(3-((difluoro(oxo)-λ^6-sulfaneylidene)amino)phenyl)ethyl) carbamate (10 mg, 26 µmol) was added 4-Piperidinecarboxamide (13 mg, 101 µmol, 5 eq.) in PBS and stirred overnight at 37°C. This solution was filtered through 0.22 µm filter and purified on preparative HPLC to give a pure benzyl ((1S)-2-(3-(((4-carbamoylpiperidin-1-yl)fluoro(oxo)-λ^6-sulfaneylidene) amino)phenyl)-1-cyanoethyl)carbamate (compound **5**, 6.5 mg, 13 µmol, 50%). ^{1}H NMR (600 MHz, DMSO-d_6) δ 8.25 (d, J = 8.1 Hz, 1H), 7.36 – 7.28 (m, 6H), 7.25 (t, J = 7.7 Hz, 1H), 7.05 – 7.00 (m, 2H), 6.97 (ddd, J = 7.9, 2.2, 1.0 Hz, 1H), 6.91 – 6.86 (m, 1H), 5.04 (d, J = 2.5 Hz, 2H), 4.74 (q, J = 7.5 Hz, 1H), 3.99 (d, J = 12.8 Hz, 1H), 3.95 – 3.88 (m, 1H), 3.18 – 3.10 (m, 2H), 3.08 – 3.00 (m, 2H), 2.39 – 2.30 (m, 1H), 1.90 – 1.81 (m, 2H), 1.64 (ddt, J = 11.4, 3.9, 1.8 Hz, 2H). ^{13}C NMR (151 MHz, DMSO-d_6) δ 175.2, 155.2, 139.8, 136.9, 136.4, 129.3, 128.3, 127.9, 127.7, 124.6, 124.1, 121.5, 119.2, 65.9, 46.8, 46.1, 43.6, 37.0, 27.24, 27.19. ^{19}F NMR (376 MHz, DMSO-d_6) δ 52.75. (+) calcd for $(M+Na)^+$ 510.1582. Found 510.1593. Purity (HPLC-UV): >99% (^{t}R= 10.6 min).

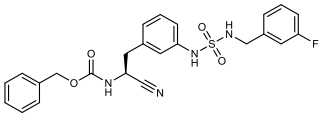

Method G (compound **6**, 5.3 mg, 11 µmol, 42%). ^{1}H NMR (600 MHz, DMSO-d_6) δ 9.80 (s, 1H), 8.28 (d, J = 8.0 Hz, 1H), 8.05 (t, J = 6.3 Hz, 1H), 7.41 – 7.34 (m, 2H), 7.34 – 7.25 (m, 4H), 7.21 (t, J = 7.8 Hz, 1H), 7.09 (t, J = 1.9 Hz, 1H), 7.07 – 6.98 (m, 4H), 6.96 (dt, J = 7.8, 1.3 Hz, 1H), 5.05 (d, J = 5.2 Hz, 2H), 4.73 (q, J = 8.0 Hz, 1H), 4.02 (d, J = 6.3 Hz, 2H), 3.02 (d, J = 8.0 Hz, 2H). ^{13}C NMR (151 MHz, DMSO) δ 162.0 (d, J_{CF} = -243 Hz), 155.4, 141.0 (d, J_{CF} = 7.2 Hz), 138.9, 136.4, 136.3, 130.0 (d, J_{CF} = 8.2 Hz), 129.0, 128.4, 128.0, 127.9, 123.44 (d, J_{CF} = 2.7 Hz), 123.39, 119.3, 118.9, 117.1, 114.1 (d, J_{CF} = 21.9 Hz), 113.7 (d, J_{CF} = 20.8 Hz), 66.1, 45.1, 45.0, 43.9, 37.5. ^{19}F NMR (376 MHz, DMSO-d_6) δ -113.38. (+) calcd for $(M+H)^+$ 483.1. Found 483.2. Purity (HPLC-UV): >99% (^{t}R= 11.4 min).

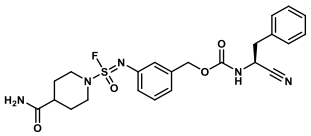

Method G (10 mg, 20 µmol, 79%). (+) calcd for $(M+H)^+$ 488.2. Found 488.3. Purity (HPLC-UV): 99% (^{t}R= 10.7 min). ^{1}H NMR (600 MHz, DMSO-d_6) δ 8.28 (d, *J* = 8.0 Hz, 1H), 7.36 (s, 1H), 7.34 – 7.27 (m, 5H), 7.29 – 7.23 (m, 1H), 7.04 – 6.99 (m, 3H), 6.90 (s, 1H), 5.05 – 4.98 (m, 2H), 4.74 (q, *J* = 8.0 Hz, 1H), 4.03 – 3.97 (m, 1H), 4.00 – 3.90 (m, 1H), 3.16 (q, *J* = 12.2 Hz, 2H), 3.12 – 3.03 (m, 2H), 2.38 – 2.33 (m, 1H), 1.90 – 1.84 (m, 2H), 1.69 – 1.59 (m, 2H). ^{13}C NMR (151 MHz, DMSO) δ 175.3, 155.3, 140.0, 137.9, 135.5, 129.5, 129.4, 128.4, 127.1, 123.0, 122.5, 122.4, 119.3, 65.7, 46.9, 46.2, 43.9, 37.3, 27.3. ^{19}F NMR (376 MHz, DMSO) δ 52.68. LRMS (+) calcd for $(M+H)^+$ 488.2. Found 488.4. Purity (HPLC-UV): 99% (^{t}R= 10.7 min).

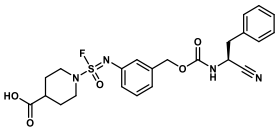

Method G (compound **7**, 6.8 mg, 14 µmol, 54%). ^{1}H NMR (600 MHz, DMSO-d_6) δ 12.46 (s, 1H), 8.29 (d, *J* = 8.0 Hz, 1H), 7.34 – 7.27 (m, 5H), 7.29 – 7.23 (m, 1H), 7.04 – 6.98 (m, 3H), 5.06 – 4.97 (m, 2H), 4.74 (q, *J* = 8.0 Hz, 1H), 3.97 – 3.91 (m, 1H), 3.89 – 3.84 (m, 1H), 3.27 – 3.20 (m, 2H), 3.12 – 3.03 (m, 2H), 2.57 – 2.50 (m, 1H, partially overlap with DMSO signal), 2.02 – 1.95 (m, 2H), 1.70 – 1.61 (m, 2H). ^{13}C NMR (151 MHz, DMSO-d_6) δ 174.9, 155.2, 139.9, 137.8, 135.4, 129.4, 129.3, 128.3, 127.0, 122.9, 122.4, 122.3, 119.2, 65.5, 46.6, 46.0, 43.8, 37.2, 26.8. ^{19}F NMR (376 MHz, DMSO-d_6) δ 52.55. (+) calcd for $(M+H)^+$ 489.1602. Found 489.1607. Purity (HPLC-UV): >99% (^{t}R= 11.5 min).

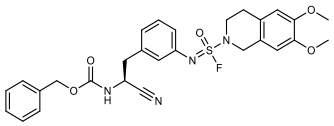

Method G (13.5 mg, 24 µmol, 94%). ^{1}H NMR (600 MHz, DMSO-d_6) δ 8.26 (d, *J* = 8.1 Hz, 1H), 7.37 – 7.34 (m, 2H), 7.33 – 7.29 (m, 2H), 7.32 – 7.24 (m, 2H), 7.07 – 7.03 (m, 2H), 7.02 – 6.98 (m, 1H), 6.86 (s, 1H), 6.79 (s, 1H), 5.04 (s, 2H), 4.75 (dd, *J* = 16.2, 8.0 Hz, 1H), 4.71 – 4.61 (m, 2H), 3.85 – 3.75 (m, 2H), 3.73 (s, 3H), 3.72 (s, 3H), 3.10 – 3.01 (m, 2H), 2.88 (t, *J* = 6.0 Hz, 2H). ^{13}C NMR (151 MHz, DMSO-d_6) ^{13}C NMR (151 MHz, DMSO-d_6) δ 155.3, 147.7, 147.4, 139.8, 136.3, 129.3, 128.3, 127.9, 127.7, 124.7, 124.5, 124.2, 122.5, 121.6, 119.2, 111.8, 109.5, 65.9, 55.43, 55.39, 47.7, 44.8, 43.6, 37.0, 26.8. (+) calcd for $(M+H)^+$ 553.2. Found 553.3. Purity (HPLC-UV): >99% (^{t}R= 12.4 min).

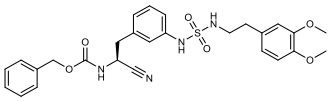

Method G (12.5 mg, 23 µmol, 88%). ^{1}H NMR (600 MHz, DMSO-d_6) δ 9.73 (s, 1H), 8.26 (d, *J* = 8.0 Hz, 1H), 7.54 (t, *J* = 5.8 Hz, 1H), 7.41 – 7.27 (m, 5H), 7.21 (t, *J* = 7.8 Hz, 1H), 7.10 (t, *J* = 1.9 Hz, 1H), 7.04 (ddd, *J* = 8.1, 2.3, 1.0 Hz, 1H), 6.94 (dt, *J* = 7.7, 1.3 Hz, 1H), 6.80 (d, *J* = 8.2 Hz, 1H), 6.70 (d, *J* = 2.0 Hz, 1H), 6.61 (dd, *J* = 8.2, 2.0 Hz, 1H), 5.03 (q, *J* = 12.3 Hz, 2H), 4.74 (dd, *J* = 15.6, 8.0 Hz, 1H), 3.69 (s, 6H), 3.07 – 2.93 (m, 4H), 2.58 (dd, *J* = 8.8, 6.6 Hz, 2H). ^{13}C NMR (151 MHz, DMSO-d_6) δ 155.3, 148.6, 147.2, 139.1, 136.4, 136.3, 131.3, 129.0, 128.4, 128.0, 127.8, 123.2, 120.4, 119.3, 118.5, 116.8, 112.4, 111.8, 66.1, 55.5, 55.4, 43.84, 43.81, 37.5, 34.6. (+) calcd for $(M+H)^+$ 539.2. Found 539.4. Purity (HPLC-UV): >99% (^{t}R= 11.1 min).

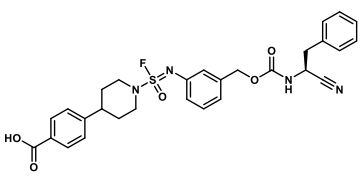

Method G (11.3 mg, 20 µmol, 77%). ^{1}H NMR (600 MHz, DMSO-d_6) δ 8.29 (d, *J* = 8.0 Hz, 1H), 7.92 – 7.88 (m, 2H), 7.44 – 7.39 (m, 2H), 7.35 – 7.28 (m, 5H), 7.26 (ddd, *J* = 6.3, 5.3, 2.5 Hz, 1H), 7.07 – 7.01 (m, 3H), 5.07 – 4.98 (m, 2H), 4.74 (dd, *J* = 15.6, 8.0 Hz, 1H), 4.19 – 4.12 (m, 1H), 4.10 – 4.03 (m, 1H), 3.29 – 3.20 (overlap with HDO signal, m, 2H), 3.08 (dd, *J* = 7.9, 3.7 Hz, 2H), 2.90 (s, 1H), 1.95 (dd, *J* =

11.3, 2.5 Hz, 2H), 1.85 – 1.73 (m, 2H). ^{13}C NMR (151 MHz, DMSO) δ 167.2, 155.3, 150.0, 140.0, 138.0, 135.5, 129.6, 129.5, 129.4, 129.0, 128.4, 127.1, 127.0, 123.0, 122.5, 122.4, 119.3, 65.7, 48.0, 47.0, 43.9, 37.4, 31.4, 31.3. ^{19}F NMR (377 MHz, DMSO-d_6) δ 52.31. (+) calcd for $(M+H)^+$ 565.2. Found 565.4. Purity (HPLC-UV): 98% (^{t}R= 11.9 min).

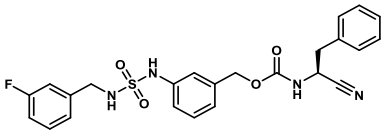

Method G (12 mg, 25 μmol, 96%). ^{1}H NMR (600 MHz, DMSO-d_6) δ 9.84 (s, 1H), 8.27 (d, J = 8.0 Hz, 1H), 8.07 (t, J = 6.3 Hz, 1H), 7.35 – 7.23 (m, 7H), 7.12 – 7.09 (m, 2H), 7.08 – 6.98 (m, 3H), 6.94 (dt, J = 7.7, 1.2 Hz, 1H), 4.99 (d, J = 12.0 Hz, 1H), 4.96 (d, J = 12.0 Hz, 1H), 4.74 (dd, J = 16.2, 8.0 Hz, 1H), 4.05 (d, J = 6.3 Hz, 2H), 3.07 (dd, J = 8.0, 4.3 Hz, 2H). ^{13}C NMR (151 MHz, DMSO) δ 162.0 (d, J_{CF} = -243 Hz), 155.3, 141.0 (d, J_{CF} = 7.6 Hz), 138.8, 137.2, 135.5, 130.0 (d, J_{CF} = 8.3 Hz), 129.4, 129.0, 128.4, 127.2, 123.5 (d, J_{CF} = 2.7 Hz), 121.9, 119.3, 117.8, 117.7, 114.1 (d, J_{CF} = 21.3 Hz), 113.7 (d, J_{CF} = 21.0 Hz), 66.0, 45.0, 43.9, 37.4. ^{19}F NMR (376 MHz, DMSO-d_6) δ -113.39. (+) calcd for $(M+H)^+$ 483.1497. Found 483.1505. Purity (HPLC-UV): >99% (^{t}R= 11.4 min).

Methods for measurement of SpeB and papain inhibition

Recombinant SpeB was expressed in *E. coli* as described previously[2, 3]. The inhibitory potency against SpeB and papain were measured as described previously using Ac-AIK-AMC as a substrate[2, 3].

Methods for library construction

In 96 well plate, to a DMSO solution of isodifluor (20 μL, 200 μM, final conc. 50 μM) was added amine library in DMSO (20 μL, 1 mM, final conc. 250 μM) and PBS buffer (pH 7.4, 40 μL) and the reaction was shaken at 37 °C overnight. The library solution was diluted 50-fold into the buffer (1 %DMSO final concentration) and a 2-fold serial dilution was prepared for the measurement of IC_{50}. For the 1536-well plate format, 1 μL of PBS (pH 7.4) was added followed by difluoride solution in DMSO (1 μL, 400 μM, final concentration for the reaction: 200 μM). The amine library in DMSO was subsequently dispensed using Echo 555 Liquid Handler (100 nL, 20 mM, final concentration for the reaction: 1 mM). The plate was centrifuged, sealed, and incubated at 37 °C with a humidifier overnight. Inhibitory potency was measured in a similar manner as the 96-well format, with the total volume of 6 μL. Both for 96 well format and 1536 well format, amine library alone in PBS+DMSO (without difluoride) was tested and showed that the amines did not interfere with the assay or SpeB activity at the condition used (Supplementary Fig. 1).

NanoDSF

Effects of molecules on thermal stability of protein was measured by differential scanning fluorimetry (DSF) using the Prometheus NT.48 instrument (NanoTemper Technologies). Recombinant SpeB protein in assay buffer ($[SpeB]_{final}$ = 0.25 mg/mL ~16 μM) with different concentrations of molecule (DMSO 2% final conc.) was loaded onto nano-DSF grade standard capillaries. Thermal unfolding of the protein was analyzed in a thermal ramp from 20 to 95 °C with a heating rate of 1 °C/min. EC_{50} values were determined by isothermal analysis as described previously[4].

Neutrophil killing assays

Group A Streptococcus (GAS)(*Streptococcus pyogenes*) strain GAS 5448 or a *SpeB* deletion mutant of the 5448 strain[5] was cultured in Todd-Hewitt broth (Neogen 7161D) medium for both a prior overnight and same day mid-logarithmic culture. The latter was used to inoculate 400 μL of the incubation media which contained 198 μL of Rosewell-Park Memorial Institute (Gibco 11835-030) medium amended with 10% Lauria-Broth (Criterion C6323), 20% (100 μL) fresh human serum, 12.5% (50 μL) bacterial cell culture supernatant from the mid-logarithmic cultures, and 2 μL DMSO (vehicle control), 1 μL DMSO with 1 μL of 10mM compound **7** (20 μM final conc.), or 2 μL of 10 mM compound **7** (40 μM final conc.) at $2x10^6$ colony forming units (CFU) (~OD_{600}= 0.008) via the addition of 50 μL of a working bacterial culture. The culture was then incubated for 30 min at 37 °C with 5% CO_2. After the 30 min incubation 10 μL of

culture were removed for CFU enumeration. The remaining culture had 100 µL of freshly isolated human neutrophils, prepared as previously described[6], added at a multiplicity of infection (MOI) of 1 (~$2x10^6$), and were incubated an additional 30 min at 37 °C with 5% CO_2. Cultures were then serial diluted in molecular biology grade water (Corning 46-000-C1) to lyse the neutrophils and spot plated onto Lauria-Agar and incubated at 37°C overnight for enumeration of CFU.

Crystallization and x-ray data collection

SpeB-inhibitor complex was crystallized as described previously[2]. Briefly, compound **5** was added in 2-fold molar excess to SpeB (10 mg/mL) and incubated for 30 min at 25 °C prior to crystallization experiments. Crystals were grown by sitting drop-vapor diffusion by mixing equal volumes (2 µL) of the complex and reservoir solution consisting of 0.1-0.15 M Na Nitrate, 22-27% PEG 3350. X-ray data was collected on a single, flash-cooled crystal at 100 K to 2.02 Å on beamline 12.2 at the Stanford Synchrotron Radiation Lightsource (SSRL) (Menlo Park, CA) in a cryoprotectant consisting of mother liquor and 20% glycerol. Data was processed with HKL2000[7] in monoclinic space group $P2_1$ (Supplementary Table 6).

Structure solution and refinement

All structure solutions were determined by MR with Phaser[8] using the previously published structure of SpeB (PDB ID: 4RKX) as the initial search model. All structures were manually built with Coot[9] and iteratively refined using Phenix[10] with cycles of conventional positional refinement with isotropic B-factor refinement. TLS B-factor refinement was carried out in the last round of refinement. Water molecules were automatically positioned by Phenix using a 2.5σ cutoff in f_o-f_c maps and manually inspected. The naïve electron density maps clearly identified that compound **5** was covalently attached to SpeB Cys192 (Supplementary Fig. 5). The final R_{cryst} and R_{free} values are 21.4% and 25.7%. The SpeB:**5** co-complex was analyzed and validated with the PDB Validation Server prior to PDB deposition. Analysis of backbone dihedral angles indicated that all residues are located in the most favorable and additionally allowed regions in the Ramachandran plot. Coordinates and structure factors have been deposited in the Protein Data Bank, www.wwpdb.org with accession entry 6UQD. Structure refinement statistics are shown in Supplementary Table 6.

Analytical LC method to determine the purity of synthetic compounds

Purity determination of synthetic compounds was performed on a Thermo Scientific Accela HPLC system using Accela 1250 pump as described previously[11]. The UV absorption between 190 nm and 400 nm was monitored, and the purity was determined by the peak area at 240 nm. The HPLC gradient method consisted of an aqueous phase (Milli-Q water with 0.1% formic acid) and an organic phase (acetonitrile with 0.1% formic acid) with a 0.5 mL/min flow. The first step consisted of 90% aqueous and 10% organic phases for 1 min, followed by a 15-min gradient to 100% organic phase. A subsequent 3-min step of 100% organic phase was followed by a 3-min gradient to 90% aqueous and 10% organic phases.

Analytical method to monitor SuFEx reactions

An UltiMate 3000 series HPLC system equipped with quaternary pumps, an online degasser, a corona charged aerosol detector (CAD, Thermo Fisher Scientific K.K., Yokohama, Japan), and an LTQ XL linear ion trap mass spectrometer (Thermo Fisher Scientific, Inc., Waltham, MA, USA) was used for the RP-HPLC/CAD/MS to monitor reactions for library construction. Mobile phase A was Milli-Q water with 0.1% formic acid and B was acetonitrile: water =90:10 with 0.1% formic acid. The solvent gradient program was as follows: 0–10 min A/B (v/v %) 70/30 to 10/90; 10–12 min A/B (v/v %) 10/90. Flow rate was 1.2 mL/min. Molecules were separated with Accucore C18 RP HPLC column (150 mm, 4.6 mm, particle size 2.6 µm, Thermo Scientific) at 45 °C. The CAD was used with an acquisition range of 500 pA, and an N_2 gas pressure of 241.3 kPa. ESI-MS was used to with positive ion mode; N_2 sheath gas flow rate: 5 units; capillary temperature: 250 °C; source voltage: 5 kV; capillary voltage: 30 V; tube lens voltage: 80 V. The data-dependent mode was set up with two scan events: one to collect the full mass spectrum of all the ions in the sample (MS range *m/z*: 300–2000), and the other to collect the tandem MS (MS^2) spectra of the most intense ions at each time point from the MS spectrum in the scan event. The dynamic exclusion setting was as follows: the repeat count for each ion was set to three, with a report duration of 10 s, an

exclusion list size of 30, and exclusion duration of 30 s. The collision-induced dissociation was conducted with an isolation width of 4 Da and normalized collision energy of 35.

Table S1. Preliminary structure-activity relationships of compound **1**.

#	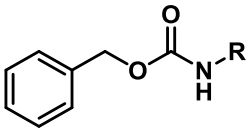 R	IC_{50}[a] (μM)
Compound **1**	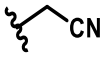	14
Z-GLYCINE amide	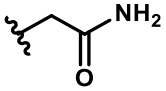	>400
Sk061-47-A	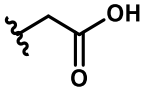	>400
Wang 2	H	>400
Wang 6	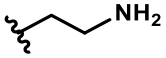	>400
sk061-81 L (=S)	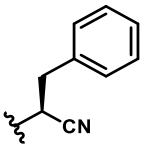	1.8
Sk061-85D (=R)	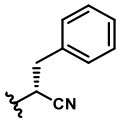	>100
sk099-3o	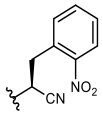	0.38
sk064-21-2 NO_2	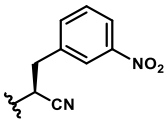	0.19
sk099-3p	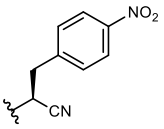	4.0

[a]IC_{50} values were determined using a fluorescence assay against SpeB. [b][rSpeB] = 20 nM. Reported IC_{50} values are the average of triplicates with at least two datum points above and at least two below the IC_{50}. The fluorescent-based assay as performed here has a standard error between 10% and 20%, suggesting that differences of two-fold or greater are significant.

Table S1. Continued. Preliminary structure-activity relationships of compound **1**.

#		IC_{50}[a] (μM)
sk061-120-1	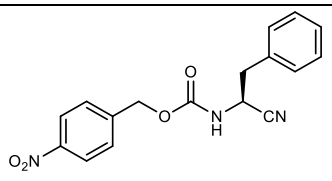	8.1
Sk064-91	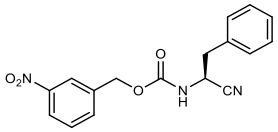	2.7
Sk064-46	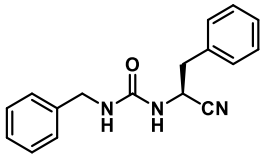	~79
sk064-93	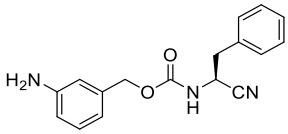	1.6
Sk064-88	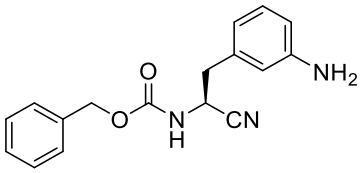	0.91
Sk064-96-1875	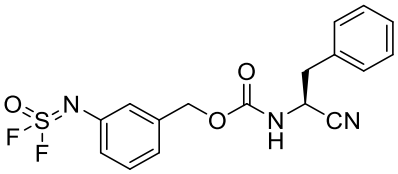	2.7
Sk064-96-1866	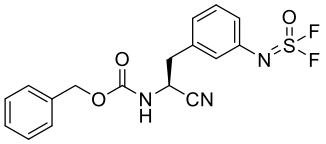	1.6

[a]IC_{50} values were determined using a fluorescence assay against SpeB. Mean ± SD values from at least two independent experiments performed in duplicate are shown. [b][rSpeB] = 20 nM. Reported IC_{50} values are the average of triplicates with at least two datum points above and at least two below the IC_{50}. The fluorescent-based assay as performed here has a standard error between 10% and 20%, suggesting that differences of two-fold or greater are significant.

Table S2. PBS improves the yield of SuFEx reaction.

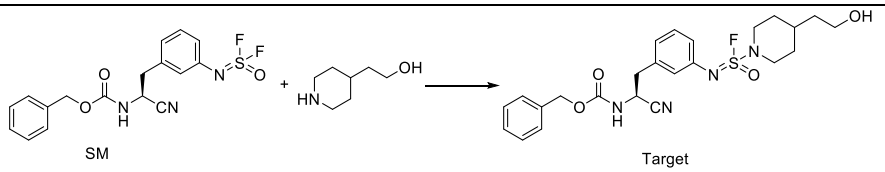

Entry#	Solvent	Base/buffer	Temp	Time	Target	SM
1	DMSO	DIPEA 5 eq.	RT	12 h	41%	59 %
2	ACN	DIPEA 5 eq.	RT	12 h	32 %	68 %
3	DMSO	PBS pH7.4	37°C	12 h	100 %	0 %

Conversion and starting material (SM) % were determined by LC-UV-MS detecting at wavelength at 254 nm (chromatogram below). 1 mM starting material with 5 mM amine was reacted in the condition.

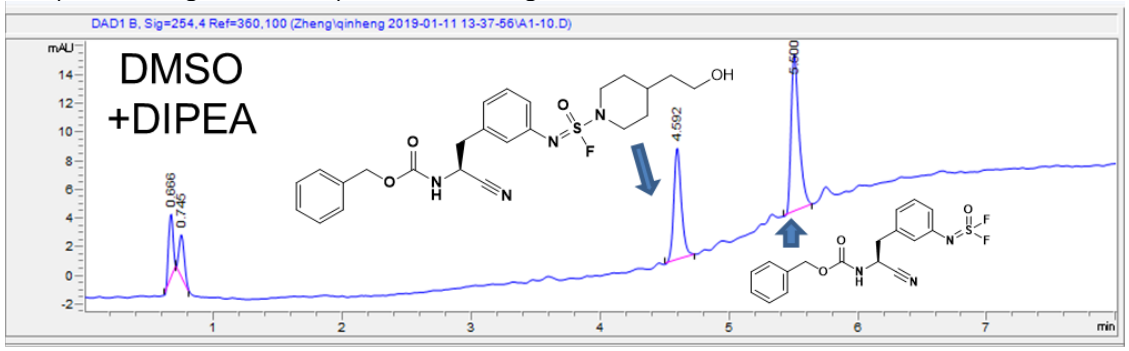

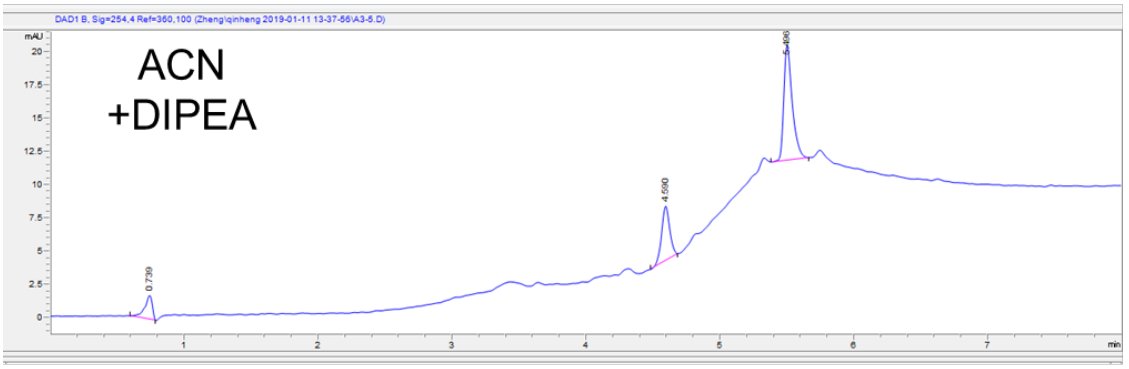

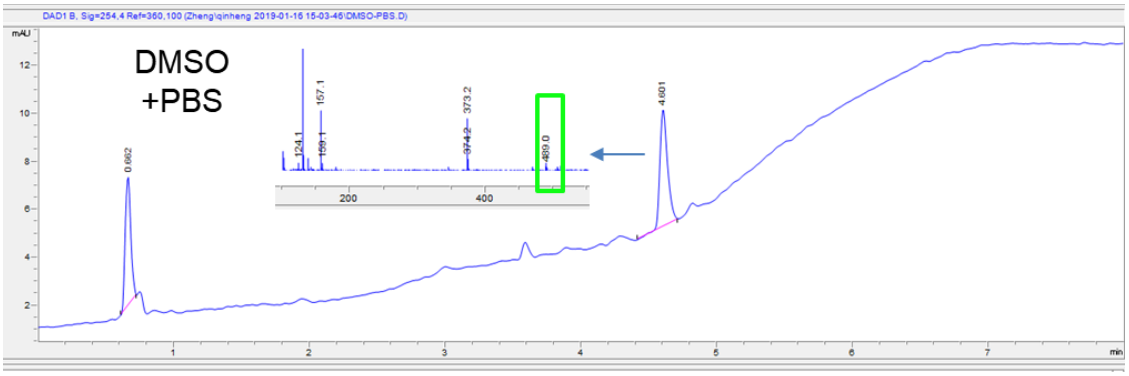

Table S3. Scope of SuFEx reactions in the HT library synthesis. Reaction between compound **4** and representative amines was monitored using LC-CAD-MS^n. The chromatograms are shown in supporting data.

amine	Target %	NH_2 %	Target conc*	NH_2 conc*
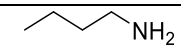	71	24	76	26
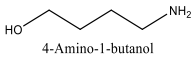 4-Amino-1-butanol	73	18	82	18
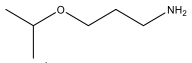	77	12	108	15
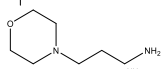	73	14	73	14
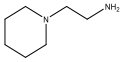	64	28	57	28
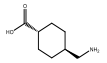	64	20	76	27
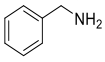	79	18	99	21
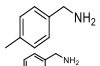	80	15	105	19
	40	39	37	48
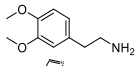	77	14	96	19
	73	19	71	18
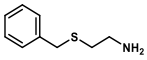	49	30	101	15
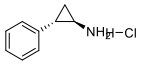 trans-2-Phenylcyclopropylamine hydrochloride	67	12	95	18
	40	56	35	61
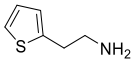	37	31	45	49
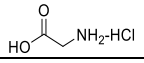	49	30	52	36
	58	6	134	8
	64	18	133	24
	63	25	98	28
	60	21	106	27
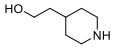	72	17	132	21
	46	42	65	44
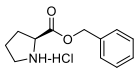	31	28	51	43
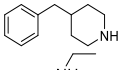	36	30	41	24
	4	85	3	83
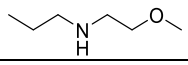	0	81	0	75

*Concentration was estimated based on a standard curve of representative molecules shown in Supporting data LC-CAD.

Table S4. Secondary amine library information and their potency in the screening.

CAS	Structure	MW	**3**		**4**	
			% inhibition at 250 nM	IC_{50} (nM)	% inhibition at 2 μM	IC_{50} (nM)
5382-16-1	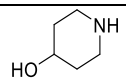	101	78	46	66	136
16652-71-4	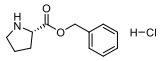	241.7	69	152	49	318
36520-39-5		93.56	76	43	55	180
6921-28-4	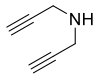	93.13	48	185	29	724
111-95-5	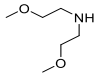	133	48	284	28	857
(1R,2S,5R,6S)-9-azabicyclo[4.2.1]nonane-2,5-diol	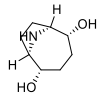	157	71	154	43	451
626-56-2	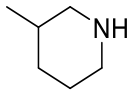	99.18	51	243	31	600
109-01-3	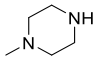	100.16	54	160	40	346
18621-18-6	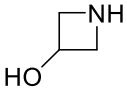	109.56	72	60	59	135
16369-21-4	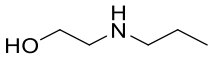	103.17	45	441	15	1600
101-83-7	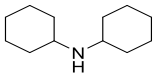	181	39	423	24	1050
60399-02-2	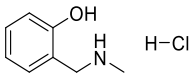	173.64	78	133	59	256
7755-92-2	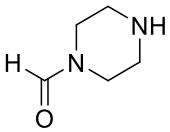	114.15	68	217	56	296
109-01-3	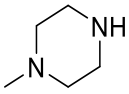	100	58	218	41	341
111-42-2	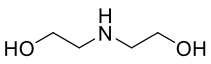	105	54	317	33	772
172603-05-3	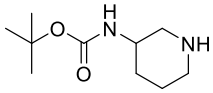	200	87	68	68	128
6511-88-2	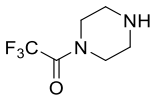	181	64	158	49	298
99724-19-3	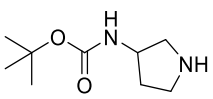	186	83	79	62	149

745048-12-8	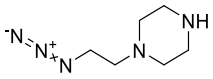	155	73	136	64	156
	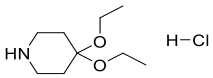	173	71	179	50	274
	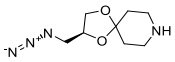	198.11	82	74	60	114
35161-71-8	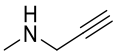	69.11	45	316	30	876
		87	61	90	42	299
		99	55	248	34	616
		45	56	113	40	666
		73	40	451	15	1290
		71	82	72	46	346
51-35-4	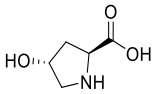	131.13	50	600	30	1030
609-36-9	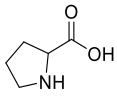	115.13	49	355	29	811
344-25-2	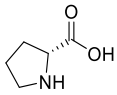	115	50	410	38	565
110-85-0		86	67	108	54	216
768-66-1		141.25	58	354	40	812
2812-46-6	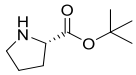	171.24	61	235	40	437
51207-66-0	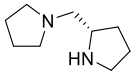	154.25	62	298	31	830
1484-84-0	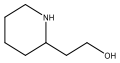	129.2	46	425	21	1220
177-11-7	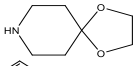	143.18	89	58	64	226
169447-86-3	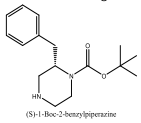 (S)-1-Boc-2-benzylpiperazine	276.38	50	664	19	971
2328.12.3	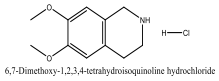 6,7-Dimethoxy-1,2,3,4-tetrahydroisoquinoline hydrochloride	229.7	85	15	56	88
622-26-4	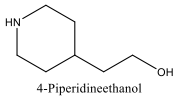 4-Piperidineethanol	129.2	89	56	73	130
1683-49-4	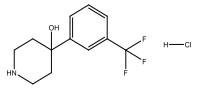 4-[3-(Trifluoromethyl)phenyl]-4-piperidinol hydrochloride	282	74	76	40	559
31252-42-3	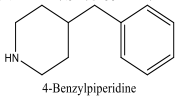 4-Benzylpiperidine	175	52	207	21	2360

39546-32-2	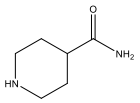 4-Piperidinecarboxamide	128	90	35	72	114
57988-58-6	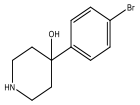 4-(4-Bromophenyl)-4-piperidinol	256	79	38	35	484
196204-01-0	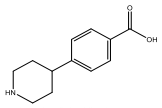 4-(4'-Carboxyphenyl)piperidine (CAS 196204-01-0)	205	85	11	53	105
1153950-54-9	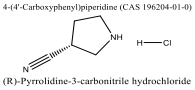 (R)-Pyrrolidine-3-carbonitrile hydrochloride	132.59	79	64	67	150
1153950-49-2	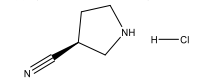 (S)-Pyrrolidine-3-carbonitrile hydrochloride	132.59	80	70	65	202
136725-53-6	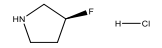 (S)-(+)-3-Fluoropyrrolidine hydrochloride Caution: Stereochemical terms discarded: +	126	87	49	65	171
6000-50-6	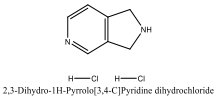 2,3-Dihydro-1H-Pyrrolo[3,4-C]Pyridine dihydrochloride	193	75	152	66	156
132958-72-6	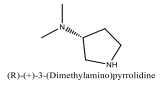 (R)-(+)-3-(Dimethylamino)pyrrolidine Caution: Stereochemical terms discarded: +	114	69	167	53	280
132883-44-4	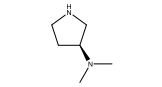 (S)-(?)-3-(Dimethylamino)pyrrolidine	114	69	173	54	439
63468-63-3	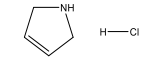 2,5-Dihydro-1H-pyrrole hydrochloride	105.57	82	81	56	227
147740-02-1	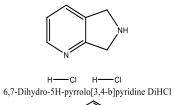 6,7-Dihydro-5H-pyrrolo[3,4-b]pyridine DiHCl	193.1	79	124	66	121
	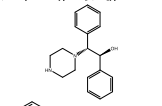	282	42	133	41	563
	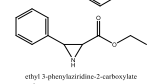 ethyl 3-phenylaziridine-2-carboxylate	191	47	472	23	1440
	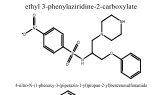	420	43	1050	18	3380
	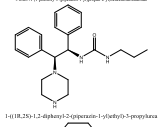	367	55	643	42	2270
1121-92-2	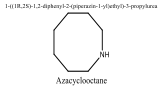 Azacyclooctane	113.2	51	190	27	574
11-49-9	 HOMOPIPERIDINE	99.17	66	153	36	433
505-19-1	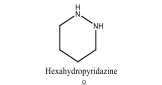 Hexahydropyridazine	86.14	31	547	16	1110
1126-09-6	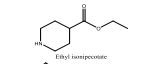 Ethyl isonipecotate	157	92	28	66	128
1135-40-6	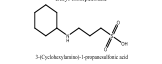	221	38	453	16	1360

29915-38-6	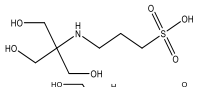	243	36	423	14	1130
7365-44-8	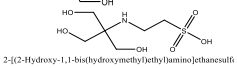 2-[(2-Hydroxy-1,1-bis(hydroxymethyl)ethyl)amino]ethanesulfo	229	38	453	16	1390
68399-81-5	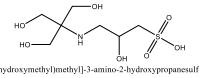 N-[Tris(hydroxymethyl)methyl]-3-amino-2-hydroxypropanesulf	259.28	39	534	17	1390
7365-82-4	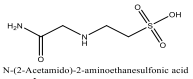 N-(2-Acetamido)-2-aminoethanesulfonic acid	182	41	495	16	1530
165528-81-4	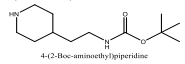 4-(2-Boc-aminoethyl)piperidine	228	83	63	46	205
498-94-2		129	66	120	97	90

IC_{50} was estimated by measuring inhibition at 2, 1, 0.5, and 0.25 μM.

Table S5. Primary amine library information and their potency in the screening.

CAS	Structure	MW	**3** 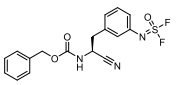 Inhibition % at 250 nM	**4** 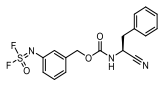 % inhibition at 2 μM
2978-58-7	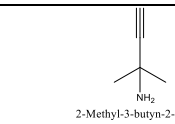 2-Methyl-3-butyn-2-amine	83	23	41
929-06-6	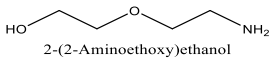 2-(2-Aminoethoxy)ethanol	105.14	32	42
2906-12-09	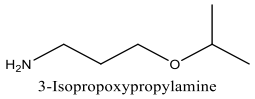 3-Isopropoxypropylamine	117.19	21	45
13325-10-5	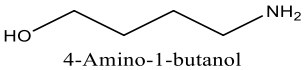 4-Amino-1-butanol	89	35	49
1003-03-8	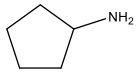 Cyclopentylamine	85.15	22	44
109-76-2	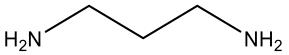 1,3-Diaminopropane	74.12	38	42
109-73-9	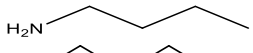	73	18	41
156-87-6	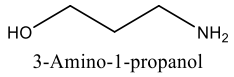 3-Amino-1-propanol	75	33	44
6291-84-5	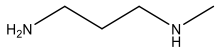 3-(Methylamino)propylamine	88	29	60
2867-59-6	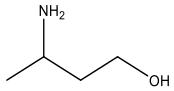 3-Amino-butan-1-ol	89	22	46
115-70-8	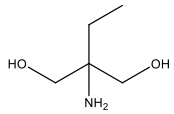 2-Amino-2-ethyl-1,3-propanediol	119	20	43
87120-72-7	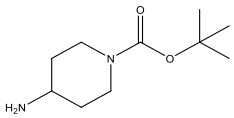 4-Amino-1-Boc-piperidine	200	24	47
60142-96-3	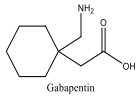 Gabapentin	171	21	55
120-20-7	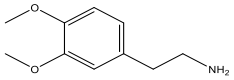	181	64	51
3731-52-0	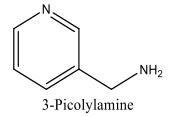 3-Picolylamine	108	35	53
3300-51-4	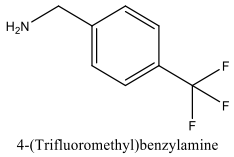 4-(Trifluoromethyl)benzylamine	175	26	48

26177-43-5	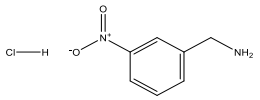	189	40	81
1118-89-4	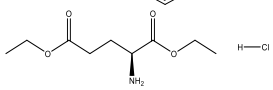 L-Glutamic acid diethyl ester hydrochloride	240	21	45
123-00-2	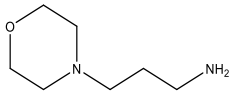 3-Morpholinopropylamine	144	34	47
156917-23-6	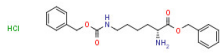	407	23	55
57260-73-8	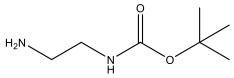 N-Boc-ethylenediamine	160	38	44
439117-39-2	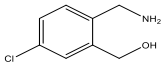 [2-(AMINOMETHYL)-5-CHLOROPHENYL]METHANOL	172	44	74
2491-18-1	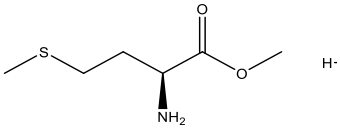 L-Methionine methyl ester hydrochlorid	200	19	44
56-92-8	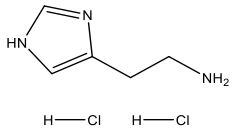 Histamine dihydrochloride	184	37	47
696-60-6	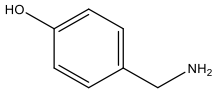 4-Hydroxybenzylamine	123	59	65
100-46-9	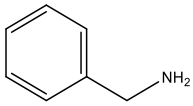 Benzylamine	107	56	64
63649-14-9	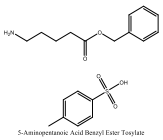	379	60	83
22572-33-4	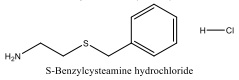 S-Benzylcysteamine hydrochloride	204	51	82
2039-66-9	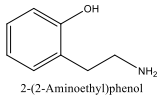 2-(2-Aminoethyl)phenol	137.18	65	69
35303-76-5	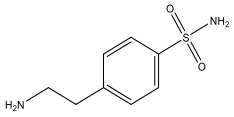 4-(2-Aminoethyl)benzenesulfonamide	200	58	52
16652-64-5	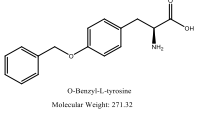 O-Benzyl-L-tyrosine Molecular Weight: 271.32	271	22	42

	Molecular Weight: 231.68			
3417-91-2	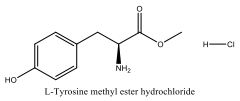 L-Tyrosine methyl ester hydrochloride	232	27	77
	Molecular Weight: 131.18			
60-32-2	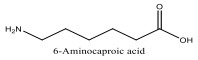 6-Aminocaproic acid	131	27	50
	Molecular Weight: 190.20			
57213-48-6	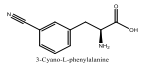 3-Cyano-L-phenylalanine	190	22	45
	Molecular Weight: 154.14			
5466-22-8	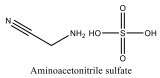 Aminoacetonitrile sulfate	154	21	43
	Molecular Weight: 210.19			
19883-74-0	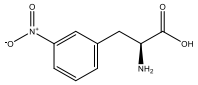 L-3-Nitrophenylalanine	210	19	42
	Caution: Stereochemical terms discarded: 1			
	Molecular Weight: 115.22			
4083-572	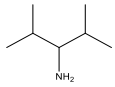 2,4-Dimethylpentan-3-amine	115	22	45
	Molecular Weight: 146.19			
	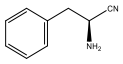	146	25	50
	Molecular Weight: 233.19			
14464-68-7	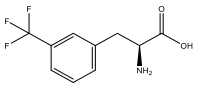 3-(Trifluoromethyl)-L-phenylalanine	233	25	44
	Molecular Weight: 199.63			
80126-51-8	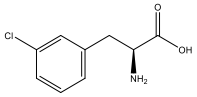 3-Chloro-L-phenylalanine	199	24	44
	Molecular Weight: 183.18			
19883-77-3	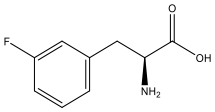 m-Fluoro-L-phenylalanine	183	25	43
	Molecular Weight: 199.63			
103616-89-3	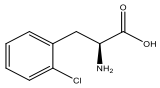 2-Chloro-L-phenylalanine	199	22	44
	Molecular Weight: 117.15			
72-18-4	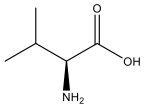 L-Valine	117	22	43
	Molecular Weight: 229.70			
3182-93-2	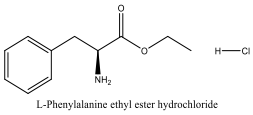 L-Phenylalanine ethyl ester hydrochloride	230	20	43
28211-04-3	Poly epsilon L-lysine HCl	385	22	44
6850-28-8	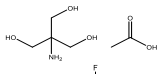	181	26	50
3048-01-09	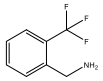	175	24	54
	Molecular Weight: 59.11			
107-10-8	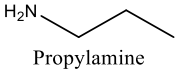 Propylamine	59	21	43

5978-75-6	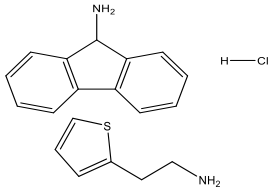	217.7	23	48
30433-91-1		127	37	57
75-64-9		73	22	42
108607-02-9	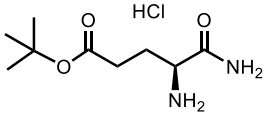	239	23	43
100-82-3	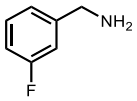	125	74	82
20781-21-9	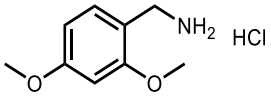	204	62	64
132388-58-0	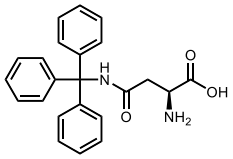	374	22	62
2393-23-9	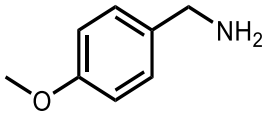	137	47	54
140-75-0	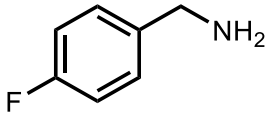	125	53	63
593-51-1	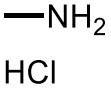	68	37	39
20859-02-3	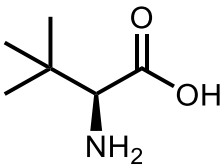	131	23	38
04-12-5198	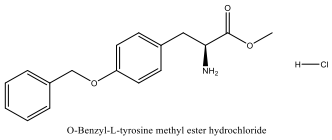	322	22	47
1798-50-1	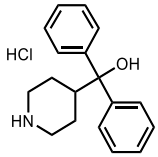	304	48	32
32462-30-9	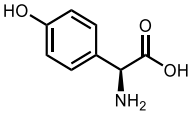	167	23	56
	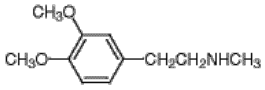	195	48	83
18542-42-2	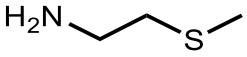	91	25	48

459-19-8	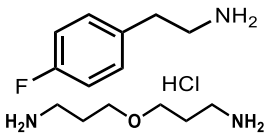	176	61	61
		132	45	62
150517-77-4	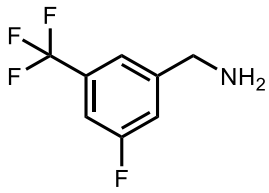	193	26	55
15996-76-6	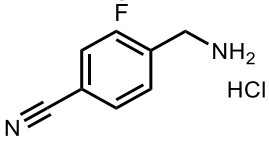	169	37	45
104-86-9	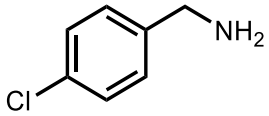	162	77	68
7663-77-6	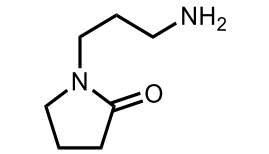	142	34	56
156-41-2	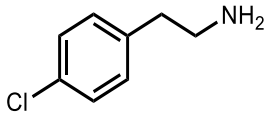	156	54	53
3886-70-2	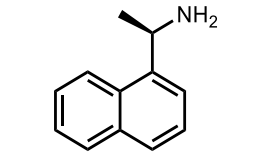	171	34	50
696-40-2	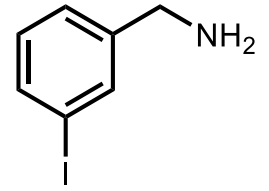	233	43	70
2432-99-7	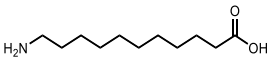	201	26	67
70-78-0	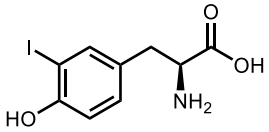	307	29	86
492-41-1	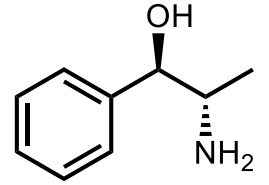	151	22	45
4747-21-1	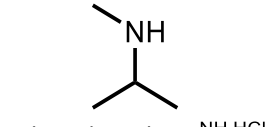	73	23	42
2017-67-6	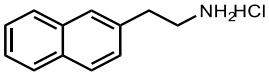	208	72	53

78-81-9	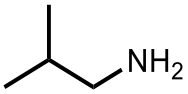	73	26	45
2935-35-5	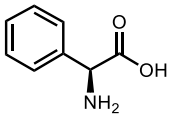	151	24	46
	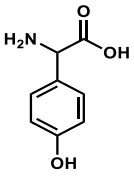	167	23	72
4104-45-4	racemic 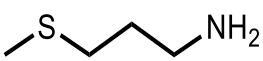	105	57	59
1986-47-6	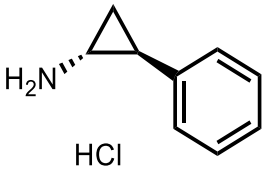	170	81	74
04-12-5147	HCl 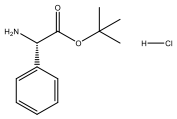	244	23	44
150-30-1	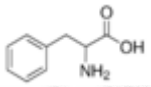	165	23	47
	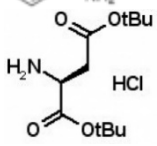	282	22	40
13288-57-8	HCl 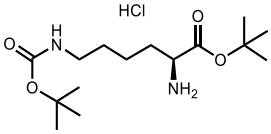	339	36	51
	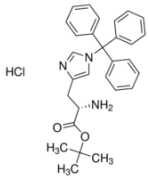	490	28	44
16874-09-2	HCl 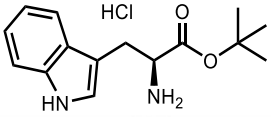	297	23	53
	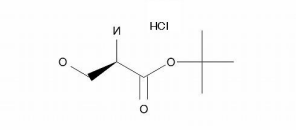	198	23	43
349-46-2	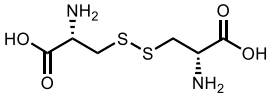	240	23	46
04-12-5047	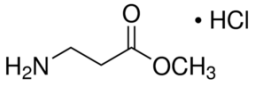	103	54	45
6893-26-1	D-glutamic acid	147	21	42

	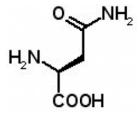	132	22	42
73-32-5	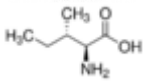	131	22	42
27894-50-4	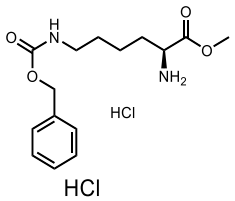	331	24	45
51537-21-4	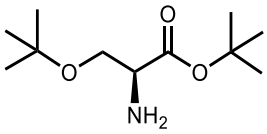	253	26	44
18905-73-2	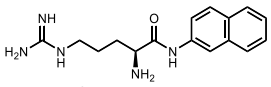	336	24	43
14907-27-8	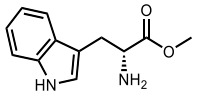	255	27	45
04-13-5043	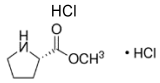	166	26	78
	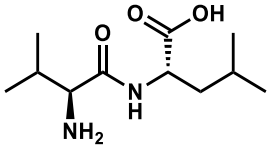 L-Valyl-L-Leucine	230	23	44
	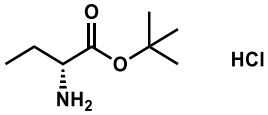	154	37	60
200353-65-7	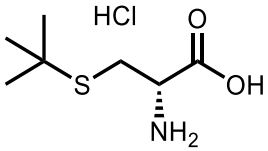	214	22	52
04-12-5044	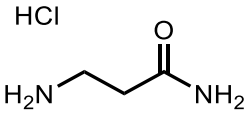	125	45	42
145306-65-6	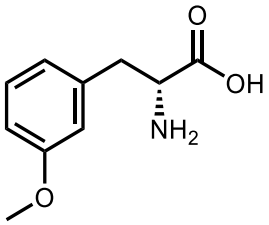	195	21	42
21394-81-0	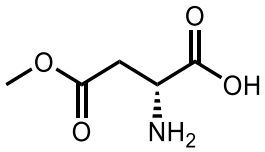	184	24	45

13188-89-1	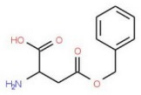	223	34	51
75/04/07		45	28	44
141-43-5	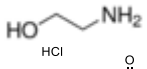	61	40	40
52142-01-5	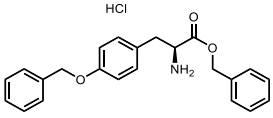	398	23	50
	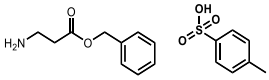	351	52	65
69320-89-4	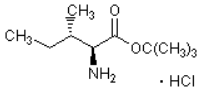	224	24	45
15100-75-1	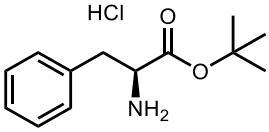	258	26	45
04-12-5075	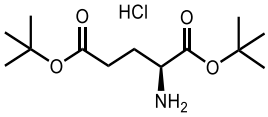	296	24	48
1738-76-7	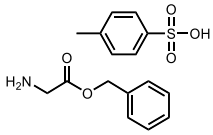	337	23	54
32677-01-3	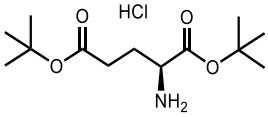	296	26	49
13033-84-6-	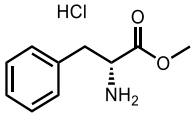	216	29	47
14173-41-2	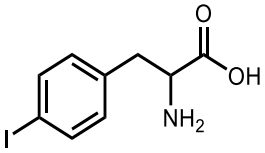	291	25	44
2791-84-6	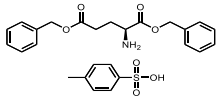	500	25	47
63594-37-6	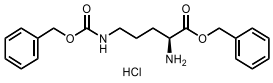	393	23	54
5854-78-4	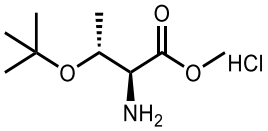	231	23	44
23239-35-2	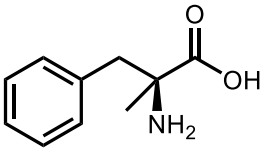	179	24	43

632-12-2	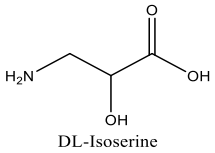 DL-Isoserine	105	22	63
7389-87-9	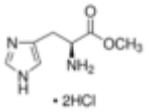	242	22	50
04-12-5004	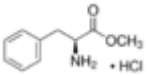	216	22	44
13188-89-1	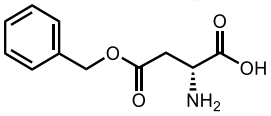	223	24	48
5856-62-2	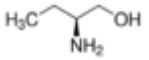	89	27	49
13472-00-9	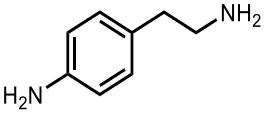	136	49	58
5856-63-3	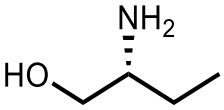	89	28	48
1492-24-6	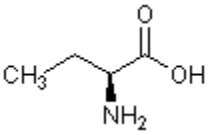	103	22	45
	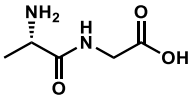 L-alanylglycine	146	22	44
2432-74-8	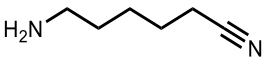	112	41	57
56-12-2	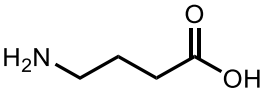	103	21	48
929-17-9	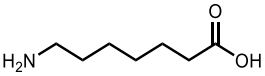	145	20	47
1187-42-4	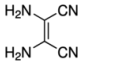	108	17	44
4-amino-1-butanol	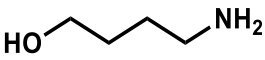	89	52	49
96-20-8	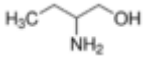	89	26	48
50910-54-8	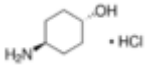	152	23	53
	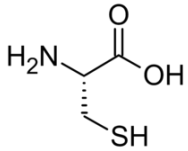	121	11	37
	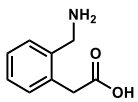	165	28	78

79286-79-6	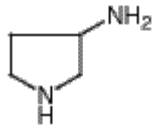	86	43	79
	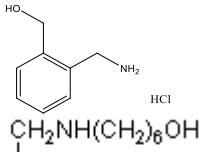	174	54	76
133437-08-8	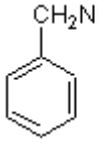	207	21	51
24123-14-6	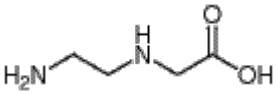	118	20	34
5098-14-6	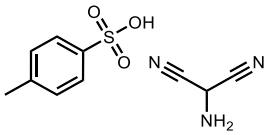	253	15	44
2079-89-2	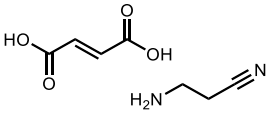	128	22	44
1002-57-9	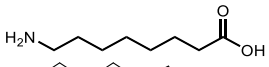	159	32	65
	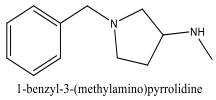	190	21	43
693-57-2	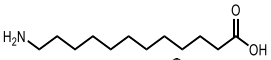	215	24	71
17702-88-4	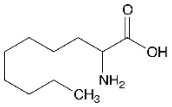	187	21	40
23159-07-1	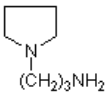	128	29	36
1197-18-8	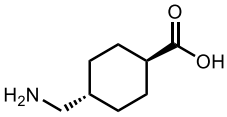	157	22	55
163061-73-2	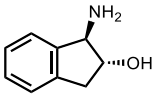	149	21	46
107-95-9	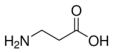	89	21	55
5036-48-6	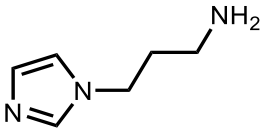	125	41	50
108-91-8	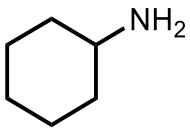	99	28	55
768-94-5	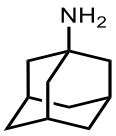	151	29	49

Table S6. SpeB in complex with compound **5** x-ray data processing and structure refinement statistics.

	Compound **5**
PDB ID	6UQD
Wavelength (Å)	0.97946
Space group	$P2_1$
Unit Cell Parameters (a,b,c) (Å)	45.62,115.52,50.27
(α,β,γ) (º)	90.0,112.6,90.0
Data Processing	
Resolution range (Å) (outer shell)	43.07-2.02 (2.05-2.02)
Unique reflections	29,212 (1,464)
Completeness (%)	94.5 (93.1)
Redundancy	2.6 (2.5)
R_{meas} (%)[a]	23.6 (78.6)
R_{merge} (%)[b]	18.2 (54.4)
$R_{p.i.m.}$ (%)[c]	13.6 (45.6)
Average I/σ(I)	7.2 (2.1)
Wilson B (Å^2)	10.6
Refinement	
Resolution range (Å)	43.07-2.02 (2.09-2.02)
No. reflections (test set)[d]	29,181 (1,384)
R_{cryst} (%)[e]	21.4 (27.3)
R_{free} (%)	25.7 (34.1)
Protein atoms / waters / ligands	3867 / 385 / 68
CV coordinate error (Å)[f]	0.25
Rmsd bonds (Å) / angles (º)	0.021 / 0.55
B-values protein/waters/ligands (Å^2)	13.6 / 23.8 / 32.1
Ramachandran Statistics (%)	
Most favored	98.8
Additional allowed	1.2
Generously allowed	0.0

[a]$R_{meas} = \{\Sigma_{hkl}[N/(N-1)]1/2\Sigma_i|I_{i(hkl)} - \langle I_{(hkl)}\rangle|\}/\Sigma_{hkl}\Sigma_i\ I_{i(hkl)}$, where $I_{i(hkl)}$ are the observed intensities, $\langle I_{(hkl)}\rangle$ are the average intensities and N is the multiplicity of reflection hkl. [b]$R_{merge} = \Sigma_{hkl}\Sigma_i|I_{i(hkl)} - \langle I_{(hkl)}\rangle|/\ \Sigma_{hkl}\Sigma_i I_{i(hkl)}$ where $I_{i(hkl)}$ is the i^{th} measurement of reflection h and $\langle I_{(hkl)}\rangle$ is the average measurement value. [c]$R_{p.i.m.}$ (precision-indicating R_{merge}) $= \Sigma_{hkl}[1/(N_{hkl} - 1)]^{1/2}\Sigma_i|I_{i(hkl)} - \langle I_{(hkl)}\rangle|/\Sigma_{hkl}\Sigma_i I_{i(hkl)}$. [d]Reflections with I > 0 were used for refinement (Weiss & Hilgenfeld, 1997; Weiss, 2001; Karplus & Diederichs, 2015). [e]$R_{cryst} = \Sigma_h||F_{obs}|-|F_{calc}||/\Sigma|F_{obs}|$, where F_{obs} and F_{calc} are the calculated and observed structure factor amplitudes, respectively. R_{free} is R_{cryst} with 5.0% test set structure factors. [f]Cross-validated (CV) Luzzati coordinate errors.

Table S7. Structure-activity relationships of selected analogs.

#	Structure	SpeB IC_{50} (nM)	cLogP[b]	LiPE[c]	MW	Solubility[d] (μM)
1	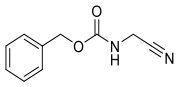	14,000[a]	0.94	3.9	190	>100
Sk064-119-2	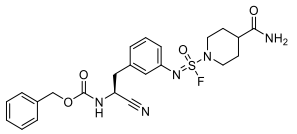	29	1.36	6.0	488	25-50
sk064-149-D	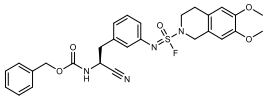	53	4.32	2.96	553	ND
sk064-150-G	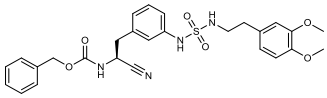	71	3.61	3.54	539	25-50
sk064-150-H	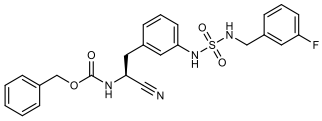	71	3.77	3.15	483	25-50
sk064-142-1	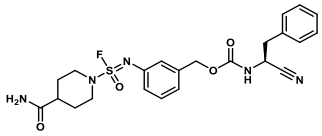	93	1.36	5.67	488	12.5-25
sk064-142-2	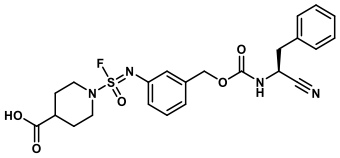	93	2.28	4.77	489	>100
sk064-142-3	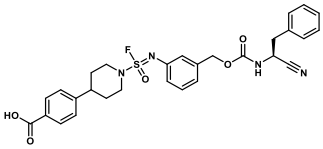	110	4.95	2.03	565	ND
sk064-143-3	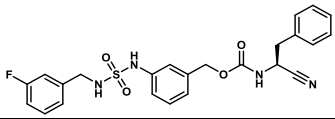	380	3.77	2.50	483	6.25-12.5

IC_{50} values were determined using a fluorescence assay against SpeB. [rSpeB] = 20 nM. Reported IC_{50} values are the average of triplicates with at least two datum points above and at least two below the IC_{50}. The fluorescent-based assay as performed here has a standard error between 10% and 20%, suggesting that differences of two-fold or greater are significant. [a]From Wang et al.[b]Predicted value using Chembiodraw Ultra 17.1.[c]LiPE = pIC_{50} – cLogP. [d]Solubility was measured using a method described previously[12, 13]. [e]Microsomal stability and cellular toxicity was measured using a method as described previously[11].

Table S8. Key parameters of selected inhibitors.

#	**1** (Hit)	**5** (119-2)	**6** (sk064-150H)	**7** (sk064-142-2)
	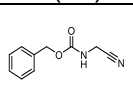	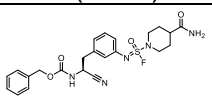	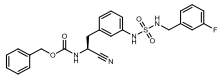	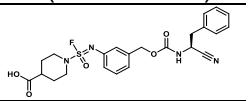
MW	190	488	483	489
SpeB IC_{50} (nM)	14,000[a]	29 ± 4 K_I=18 ± 1	71 ± 7	93 ± 10 K_I= 67 ± 3
cLogP	0.94	1.36	3.77	2.28
Papain IC_{50} (μM)[a]	77[a]	31	-	10
Caspase 3 IC_{50} (μM)	-	>100	-	>100
Solubility (μM)	>100	25-50	25-50	>100
Human liver microsomal stability $t_{1/2}$ (min)[e]	-	13.1	8.9	118
% remaining after 40 min incubation	-	12%	2%	79%
% remaining after 40 min incubation without cofactor	-	94%	105%	79%
Cellular toxicity (Jurkat cells) [e]	-	40% growth inhibition at 20 μM	Not cytotoxic at 20 μM	Not cytotoxic at 20 μM

[a]From Wang et al. [b]Predicted value using Chembiodraw Ultra 17.1. [d]Solubility was measured using a method described previously[12, 13]. [e]Microsomal stability and cellular toxicity was measured using a method as described previously[11].

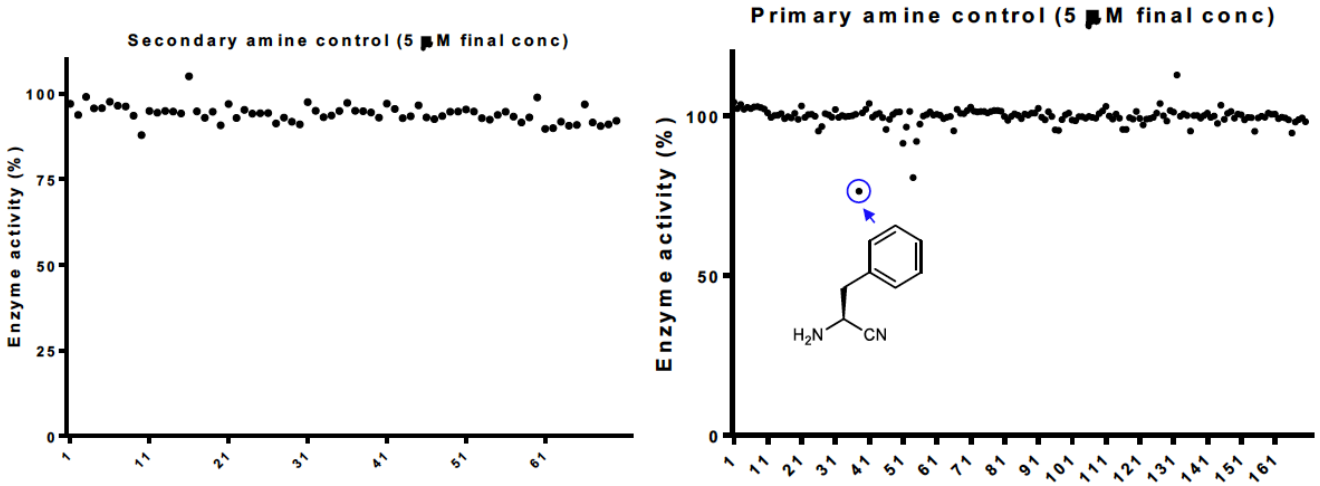

Figure S1. Inhibitory potency of amines on SpeB enzyme activity. Most amines did not show inhibition at final concentration at 5 μM. The highest inhibition was observed with an amine which is a building block of compound **2** (structure shown in the figure).

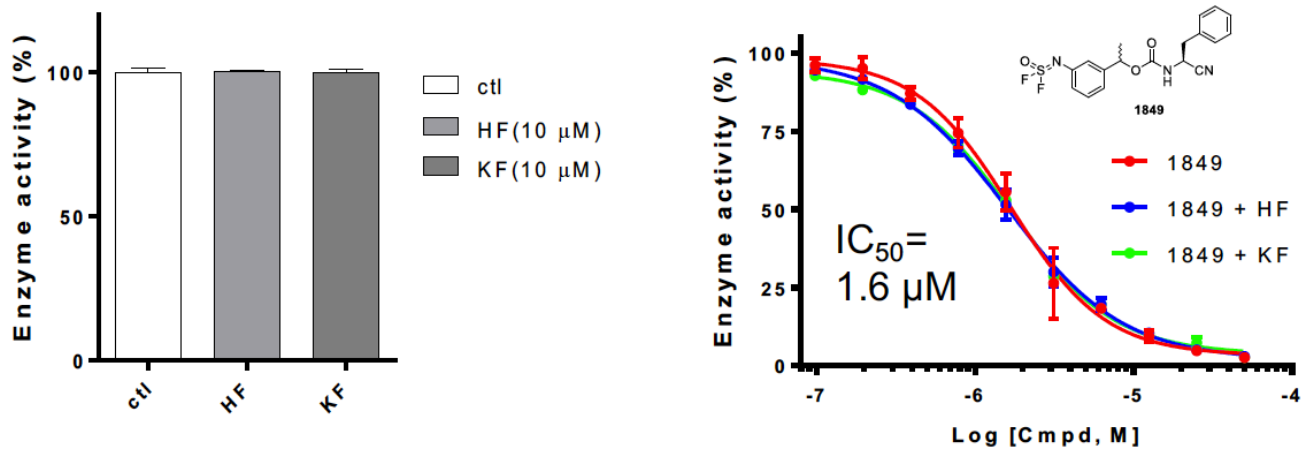

Figure S2. Effects of fluoride ion on SpeB enzyme activity and inhibitor potency. (a) Enzyme activity does not change in the presence of fluoride ion (10 μM). (b) Inhibitor potency does not change in the presence of fluoride ion (10 μM).

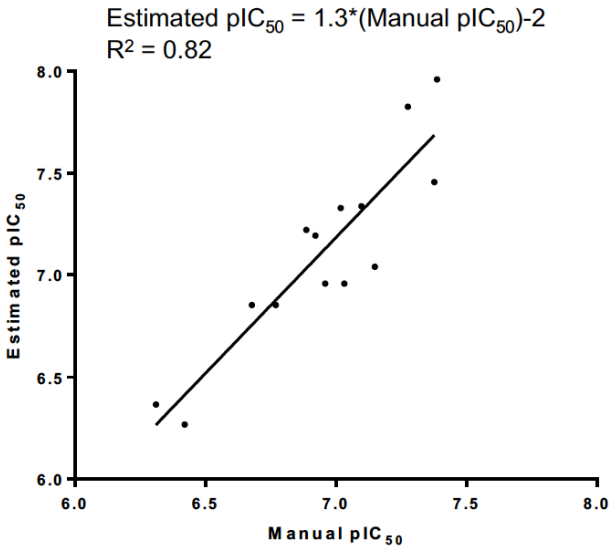

Figure S3. Correlation of pIC_{50} estimated by the measurement of inhibitory potency of reaction mixture vs. manual measurement of pIC_{50} of pure compounds.

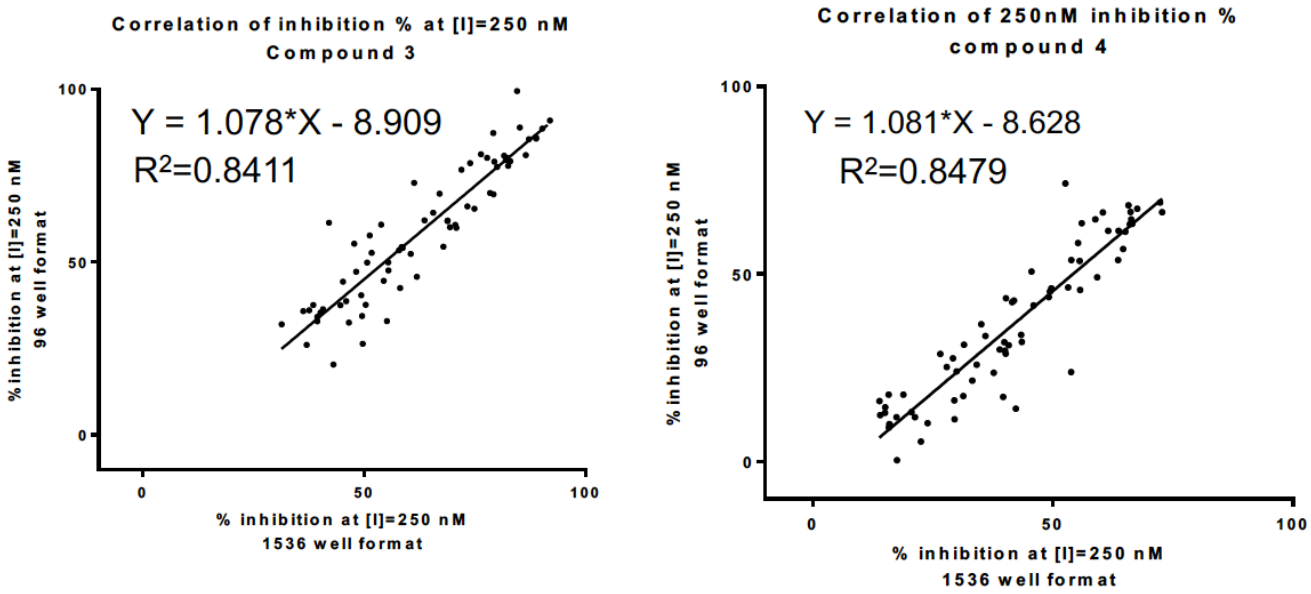

Figure S4. Additional correlation of pIC_{50} between picomole scale synthesis vs. 96 well plate synthesis.

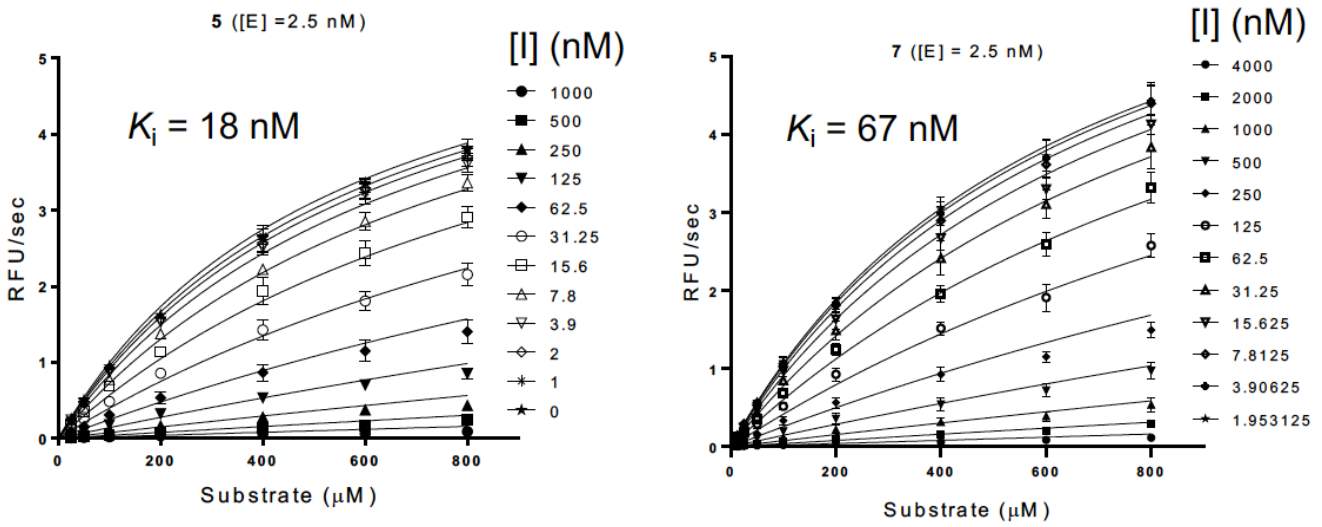

Figure S5. K_I determination of compounds **5** and **7** against SpeB. Enzyme activity was measured as described in the method section. Mean ± SD values of three independent experiments are shown. [Recombinant SpeB] = 2.5 nM. Nonlinear fitting to competitive inhibition model gave K_i = 18 ± 1 nM with R^2 = 0.99 (cmpd **5**) or K_i = 67 ± 3 nM with R^2 = 0.99 (cmpd **7**).

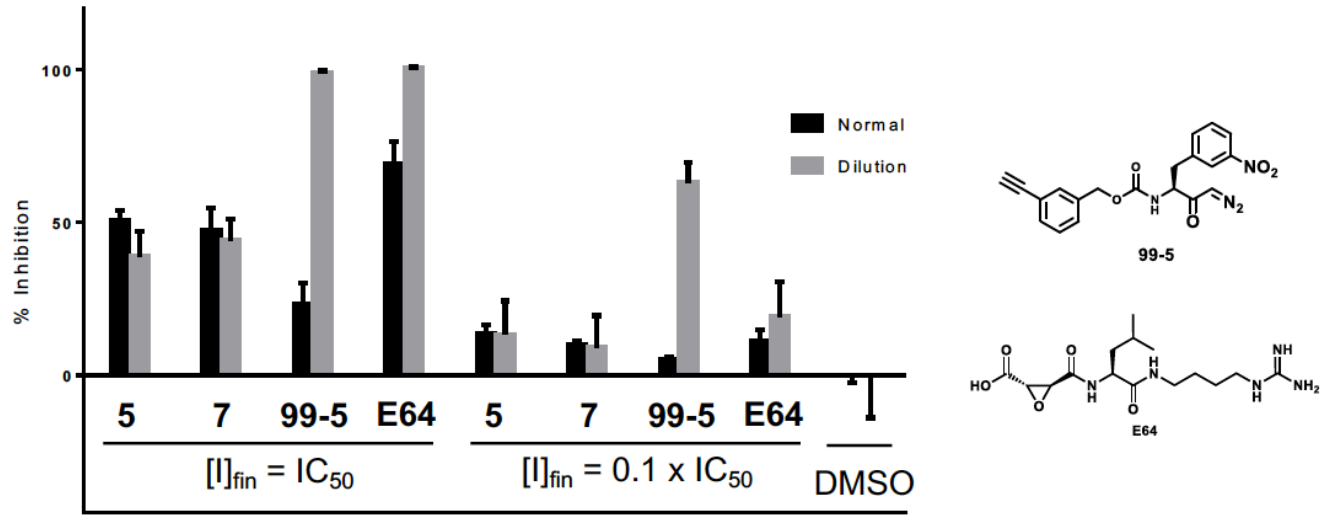

Figure S6. Compounds **5** & **7** are reversible inhibitors. Reversibility of the inhibitor binding was assessed using dilution assay as described previously (Copeland, Evaluation of Enzyme Inhibitors in Drug Discovery 2005). Cmpds **99-5** (SpeB-specific covalent inhibitor, publication in preparation) and E64 (general covalent cysteine protease inhibitor) were used as positive controls. Inhibitors ([I] = IC_{50} x200 or x20) and SpeB ([E] = 4 μM) were incubated for 20 min, then diluted 100-fold into buffer. The enzyme activity of the diluted sample was measured ($[I]_{fin}$ = IC_{50} x1 or x0.1) and the enzyme inhibition was compared between the dilution condition and normal enzyme assay condition. Mean ± SD (n=4) values are shown. $[I]_{fin}$ for each compounds are: 40 or 4 nM (**5**), 90 or 9 nM (**7**), 1,000 or 100 nM (**99-5**), 100 or 10 nM (E64), respectively. Compound **99-5** has IC_{50} at 1.6 μM against SpeB with 10 min incubation. Raw data are shown in the next figure.

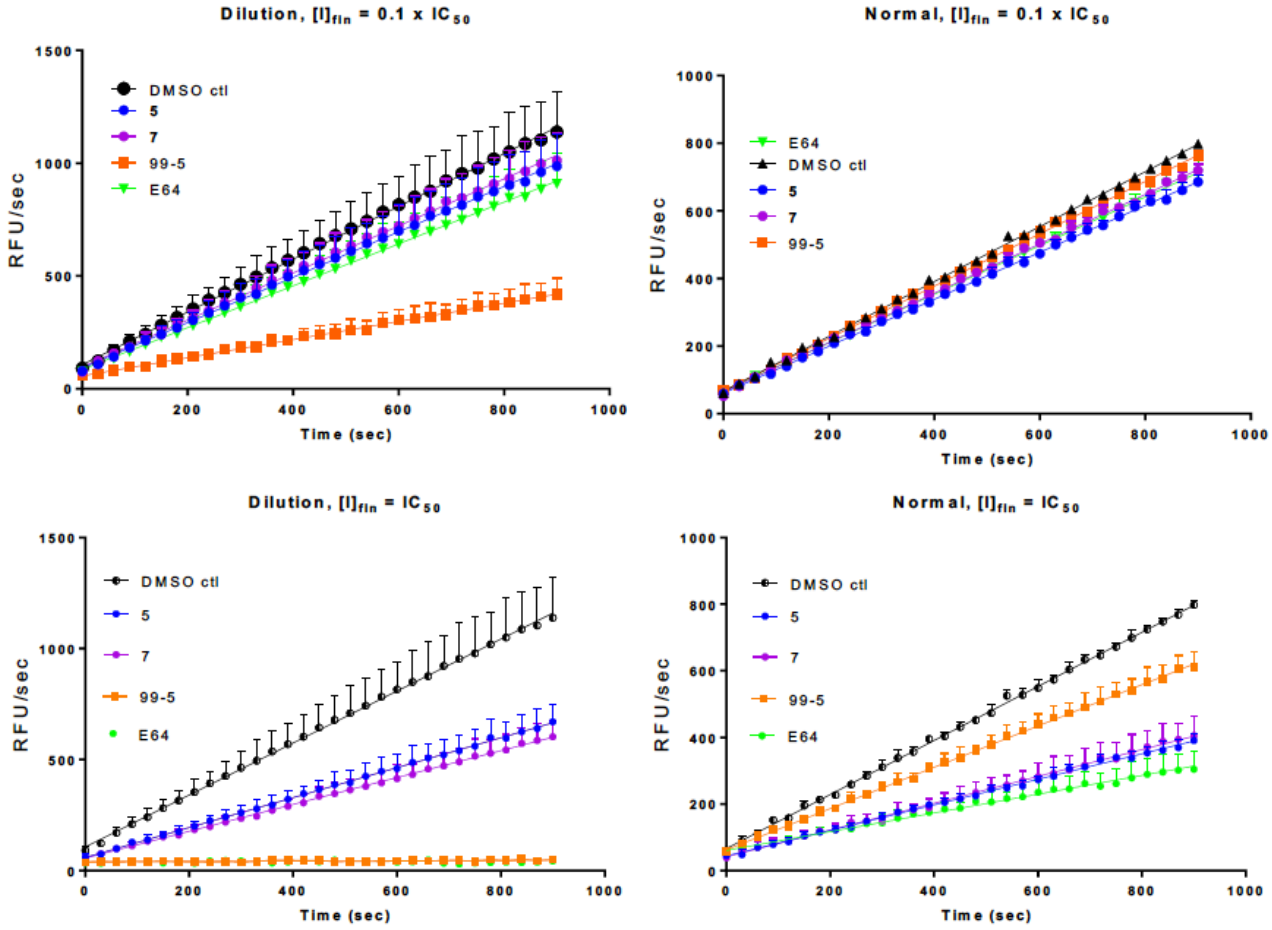

Figure S6. (continued) Compounds **5** & **7** are reversible inhibitors.

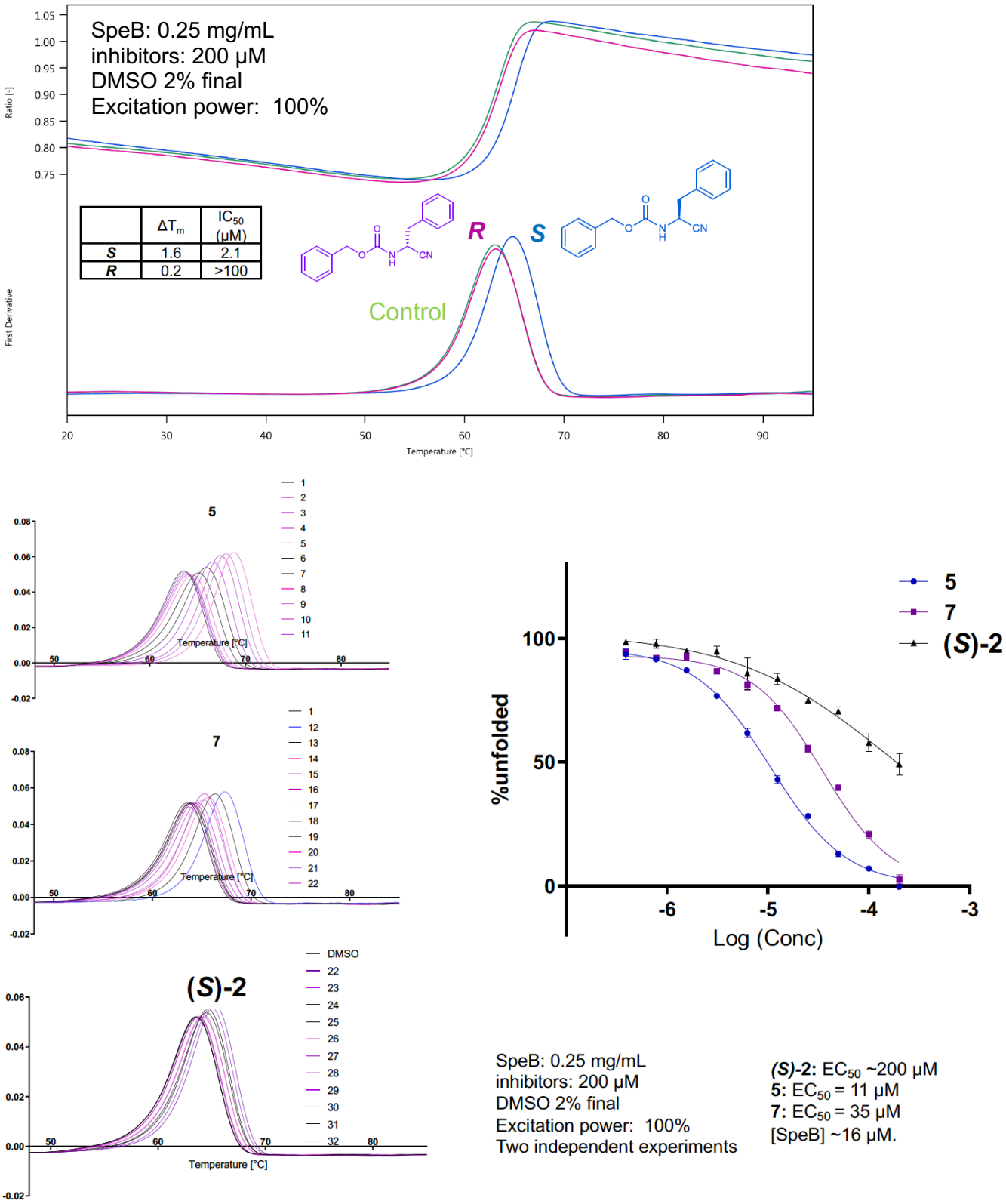

Figure S7. Differential scanning fluorimetry melting curves.

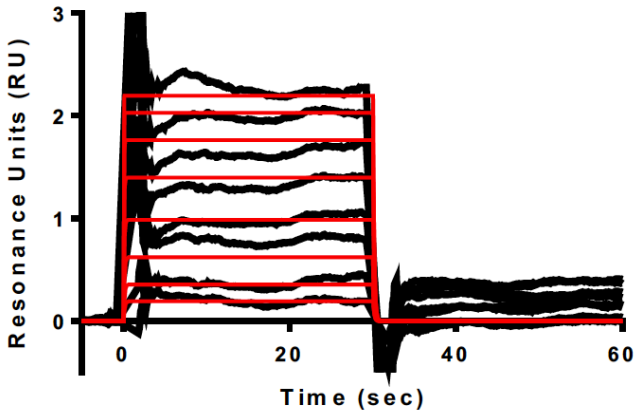

Flow: 30 µL/min
PBS (7.4) + 5% DMSO
rSpeB was immobilized on CM5 chip

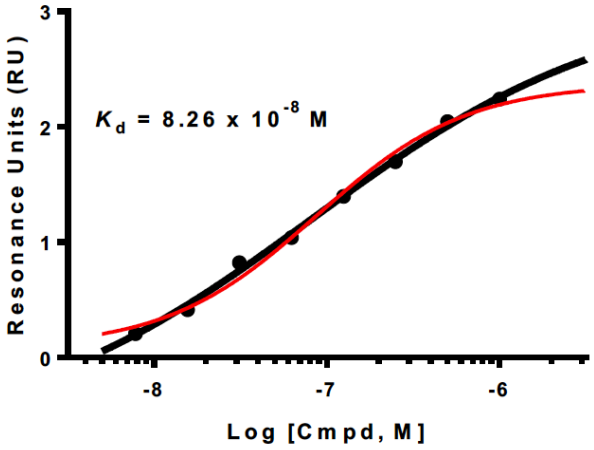

A K_d value was calculated from a steady-state fit

Figure S8. Surface plasmon resonance analysis of cmpd **5** against rSpeB.

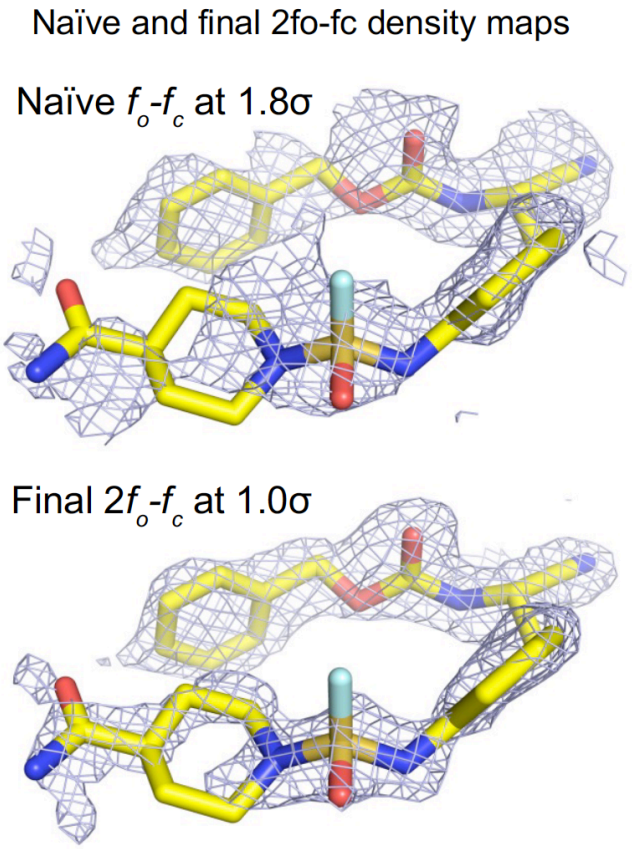

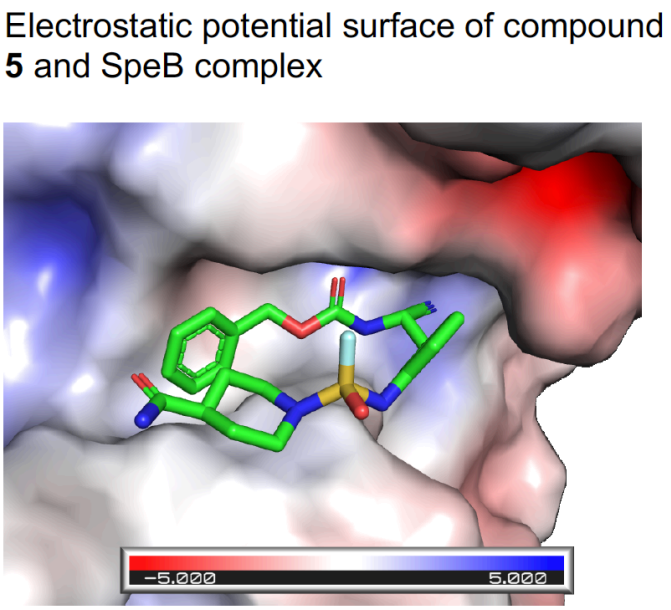

Figure S9. X-ray structure of compound **5**-SpeB complex.

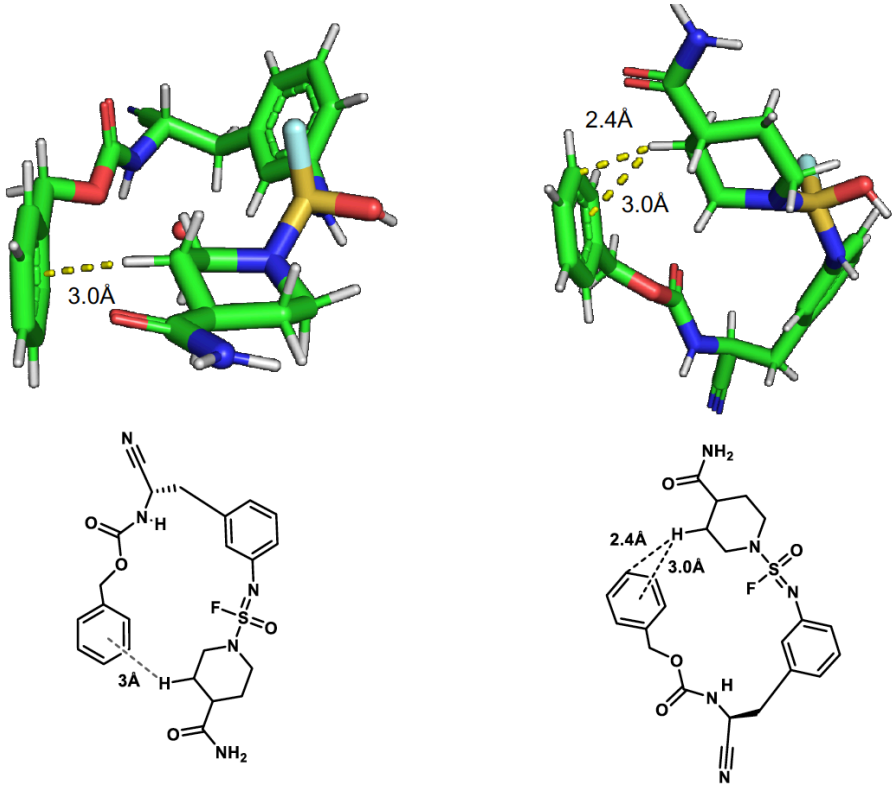

Figure S10. Intramolecular CH-π interaction between piperidine and benzyl moiety of compound **5** bound to SpeB.

References

1. Li, S.; Wu, P.; Moses, J. E.; Sharpless, K. B., Multidimensional SuFEx click chemistry: Sequential sulfur(VI) fluoride exchange connections of diverse modules launched from an SOF_4 hub. *Angew. Chem. Int. Ed.* **2017,** *56* (11), 2903-2908.
2. Wang, A. Y.; González-Páez, G. E.; Wolan, D. W., Identification and co-complex structure of a new S. pyogenes SpeB small molecule inhibitor. *Biochemistry* **2015,** *54* (28), 4365-4373.
3. González-Páez, G. E.; Wolan, D. W., Ultrahigh and high resolution structures and mutational analysis of monomeric *Streptococcus pyogenes* SpeB rveal a fnctional role for the glycine-rich C-terminal loop. *J. Biol. Chem.* **2012,** *287* (29), 24412-24426.
4. Bai, N.; Roder, H.; Dickson, A.; Karanicolas, J., Isothermal analysis of thermofluor data can readily provide quantitative binding affinities. *Sci. Rep.* **2019,** *9* (1), 2650.
5. Aziz, R. K.; Pabst, M. J.; Jeng, A.; Kansal, R.; Low, D. E.; Nizet, V.; Kotb, M., Invasive M1T1 group A *Streptococcus* undergoes a phase-shift *in vivo* to prevent proteolytic degradation of multiple virulence factors by SpeB. *Mol. Microbiol.* **2004,** *51* (1), 123-134.
6. Ulloa, E. R.; Dillon, N.; Tsunemoto, H.; Pogliano, J.; Sakoulas, G.; Nizet, V., Avibactam sensitizes carbapenem-resistant NDM-1–producing *Klebsiella pneumoniae* to innate immune clearance. *J. Infect. Dis.* **2019,** *220* (3), 484-493.
7. Otwinowski, Z.; Minor, W., *et al.,* Processing of X-ray diffraction data collected in oscillation mode. In *Methods Enzymol.*, Academic Press: 1997; Vol. 276, pp 307-326.
8. McCoy, A. J.; Grosse-Kunstleve, R. W.; Adams, P. D.; Winn, M. D.; Storoni, L. C.; Read, R. J., Phaser crystallographic software. *J. Appl. Crystallogr.* **2007,** *40* (4), 658-674.
9. Emsley, P.; Lohkamp, B.; Scott, W. G.; Cowtan, K., Features and development of Coot. *Acta Crystallogr.* **2010,** *D66* (4), 486-501.
10. Adams, P. D.; Afonine, P. V.; Bunkoczi, G.; Chen, V. B.; Davis, I. W.; Echols, N.; Headd, J. J.; Hung, L.-W.; Kapral, G. J.; Grosse-Kunstleve, R. W.; McCoy, A. J.; Moriarty, N. W.; Oeffner, R.; Read, R. J.; Richardson, D. C.; Richardson, J. S.; Terwilliger, T. C.; Zwart, P. H., PHENIX: a comprehensive Python-based system for macromolecular structure solution. *Acta Crystallogr.* **2010,** *D66* (2), 213-221.
11. Kitamura, S.; Owensby, A.; Wall, D.; Wolan, D. W., Lipoprotein signal peptidase inhibitors with antibiotic properties identified through design of a robust *in vitro* HT platform. *Cell Chem. Biol.* **2017,** *25* (3), 301-308.e12.
12. Morisseau, C.; Goodrow, M. H.; Newman, J. W.; Wheelock, C. E.; Dowdy, D. L.; Hammock, B. D., Structural refinement of inhibitors of urea-based soluble epoxide hydrolases. *Biochem. Pharmacol.* **2002,** *63* (9), 1599-1608.
13. Kitamura, S.; Hvorecny, K. L.; Niu, J.; Hammock, B. D.; Madden, D. R.; Morisseau, C., Rational design of potent and selective inhibitors of an epoxide hydrolase virulence factor from *Pseudomonas aeruginosa*. *J. Med. Chem.* **2016,** *59* (10), 4790-4799.

skita60020191022-1.2.fid —

NMR spectra of compound **5**

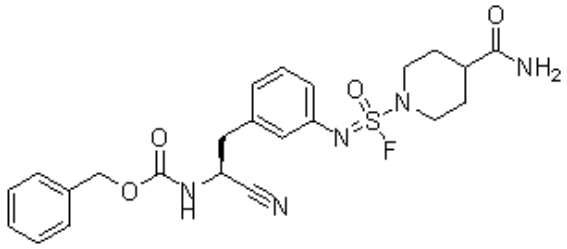

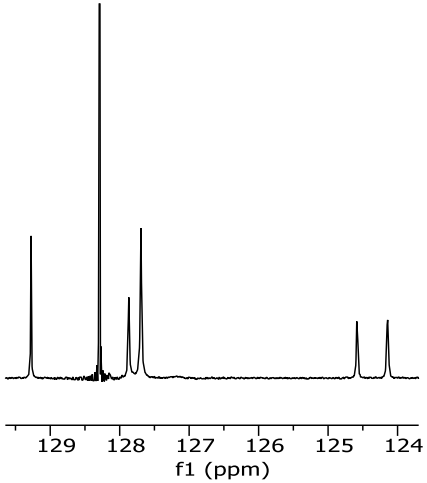

NMR spectra of compound **5**

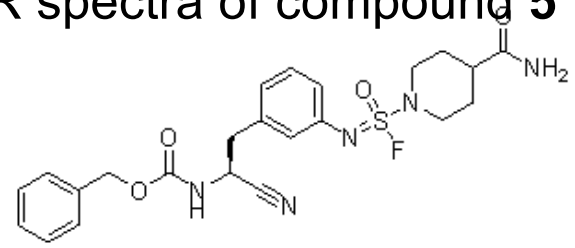

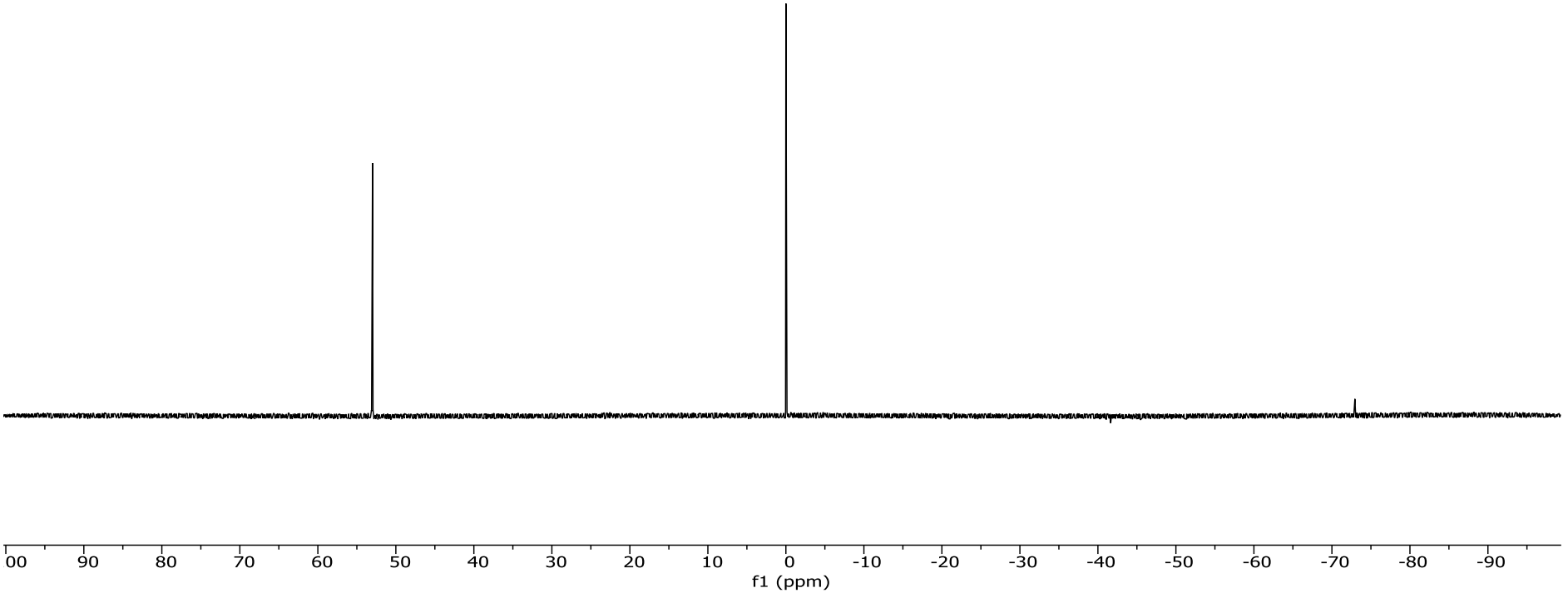

NMR spectra of compound **6**

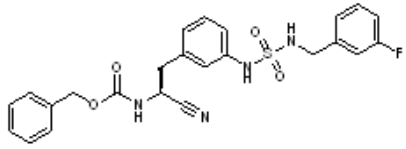

NMR spectra of compound **6**

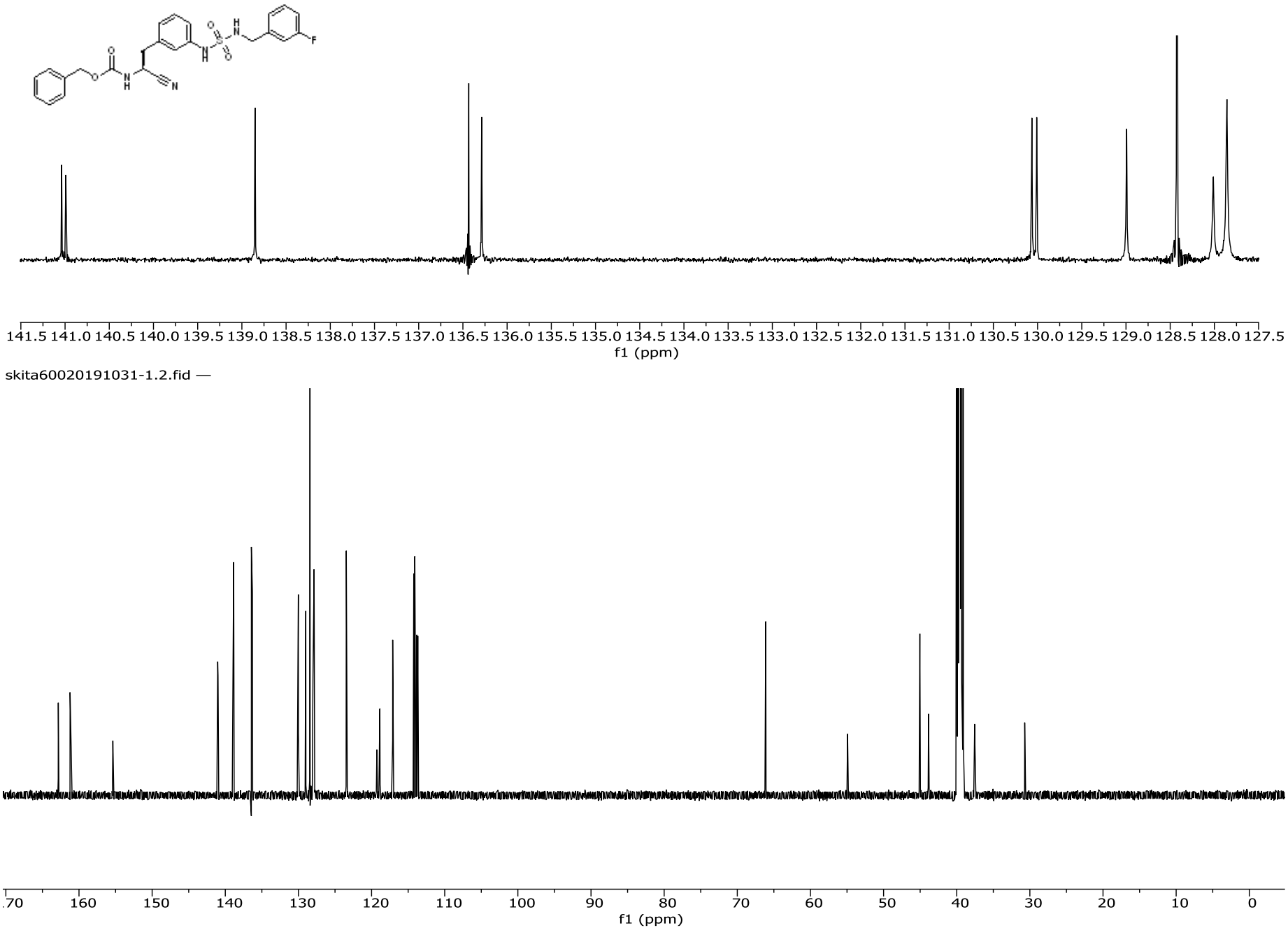

NMR spectra of compound **7**

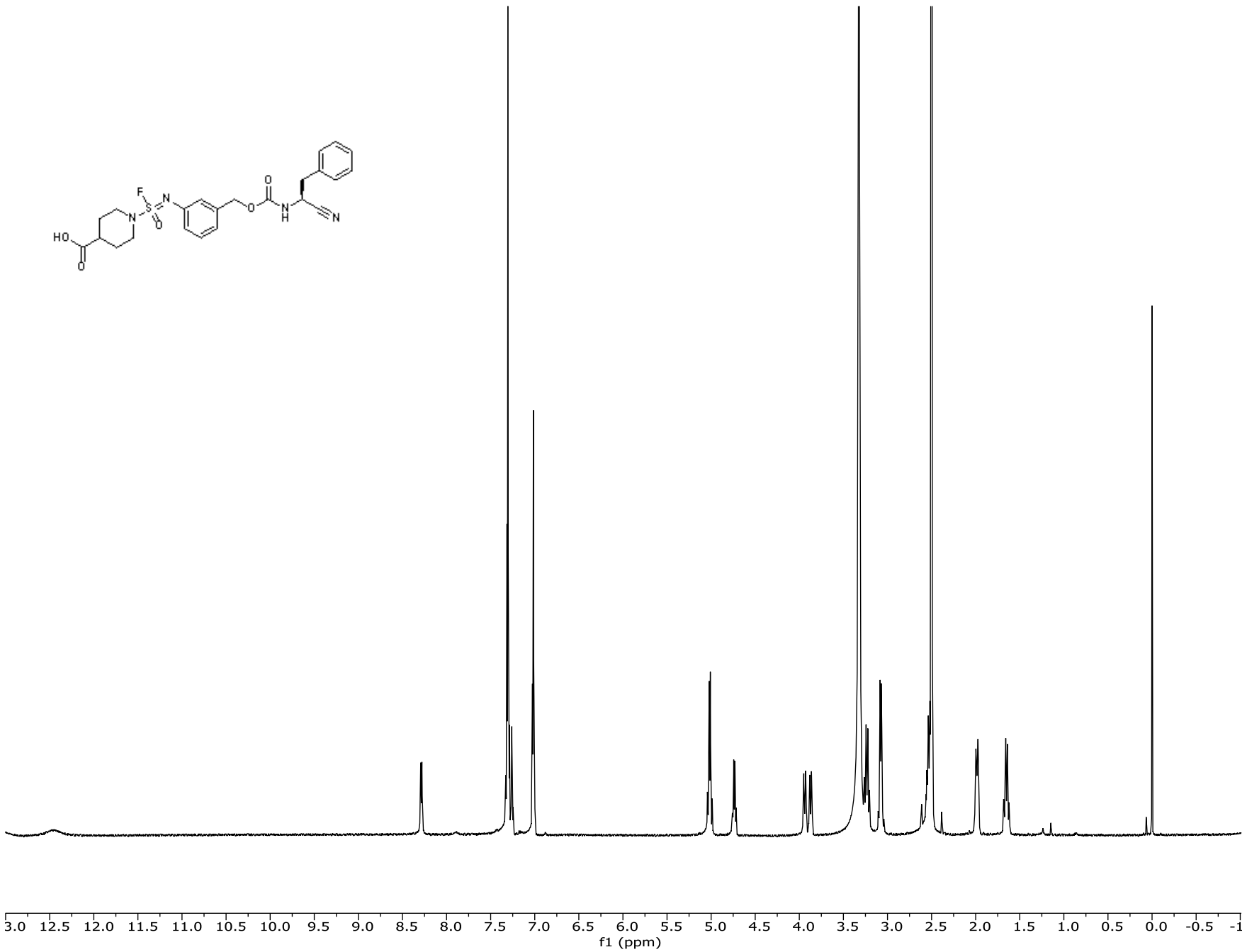

NMR spectra of compound **7**

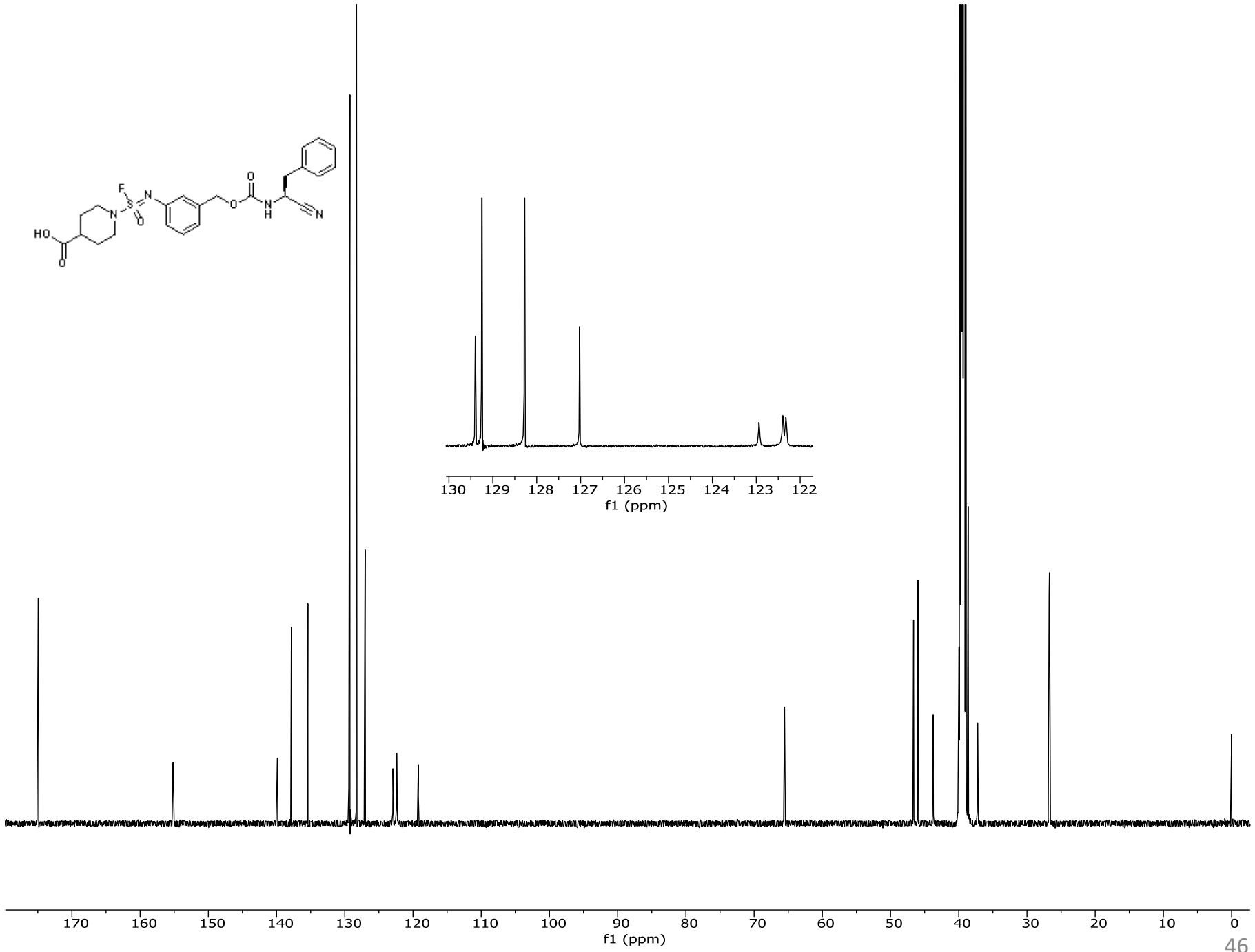

Kitamura et al. 2019 SI

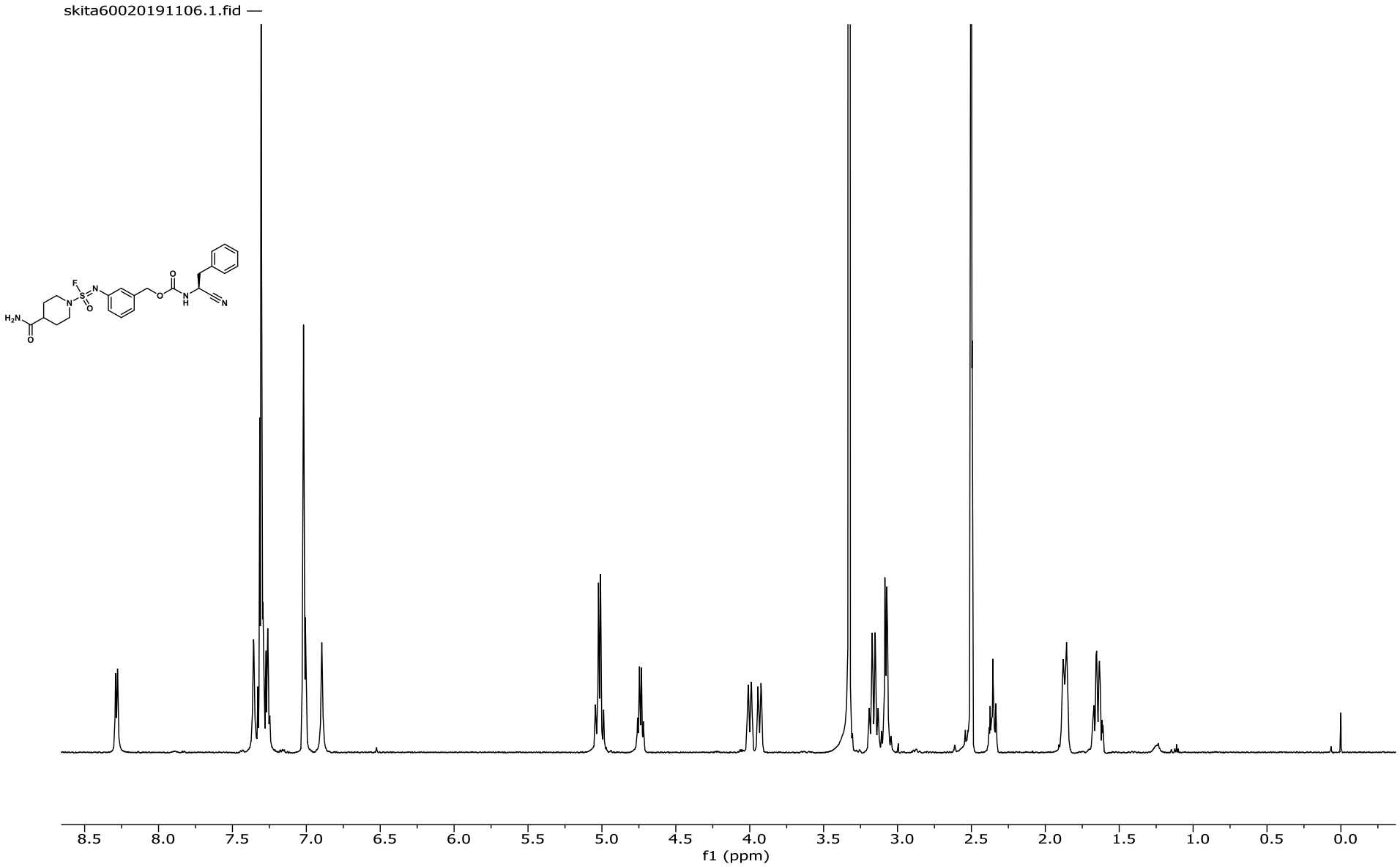
skita60020191106.1.fid
8.5
8.0
7.5
7.0
6.5
6.0
5.5
5.0
4.5
4.0
3.5
3.0
2.5
2.0
1.5
1.0
0.5
0.0
f1 (ppm)

skita60020191106.2.fid —

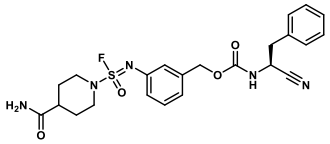

f1 (ppm)

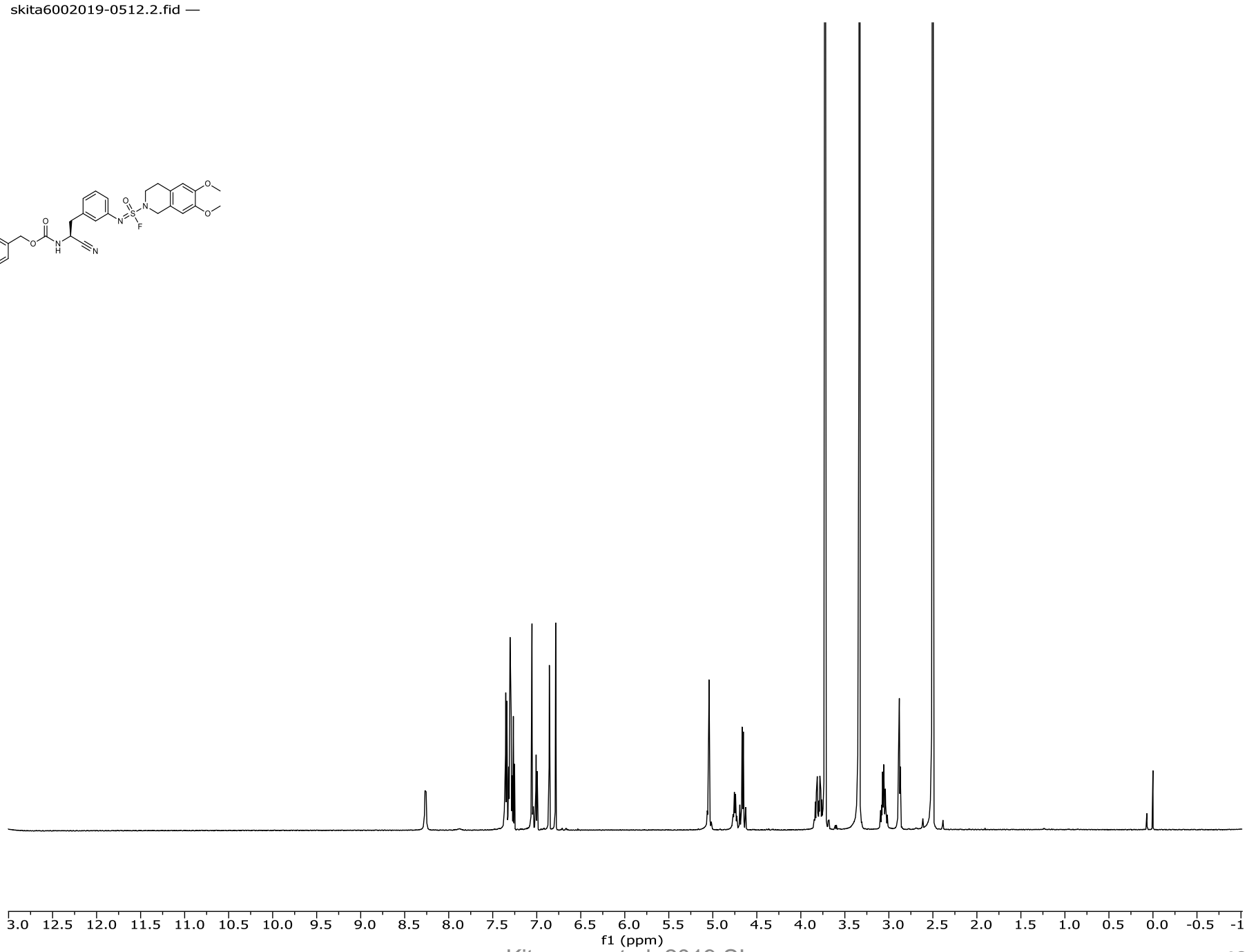
skita6002019-0512.2.fid —
3.0 12.5 12.0 11.5 11.0 10.5 10.0 9.5 9.0 8.5 8.0 7.5 7.0 6.5 6.0 5.5 5.0 4.5 4.0 3.5 3.0 2.5 2.0 1.5 1.0 0.5 0.0 -0.5 -1
f1 (ppm)

skita6002019-0512.20.fid —

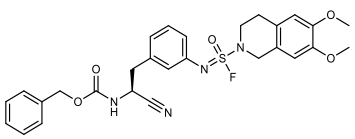

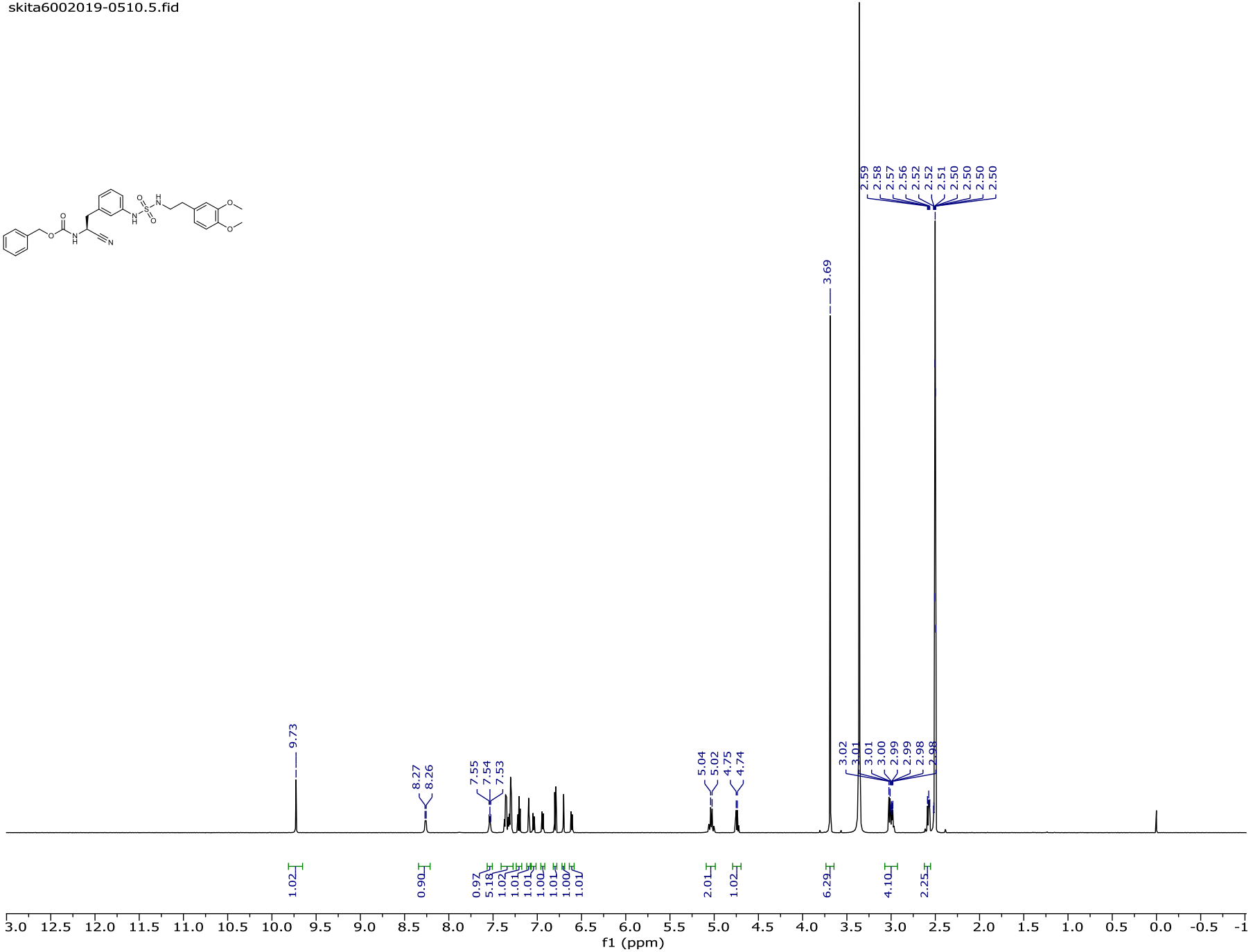
skita6002019-0510.5.fid
9.73
8.27
8.26
7.55
7.54
7.53
5.04
5.02
4.75
4.74
3.69
3.02
3.01
3.00
2.99
2.98
2.98
2.59
2.58
2.57
2.56
2.52
2.52
2.51
2.50
2.50
2.50
2.50
1.02
0.90
0.97
5.18
1.02
1.01
1.01
1.00
1.01
1.00
1.01
2.01
1.02
6.29
4.10
2.25
f1 (ppm)

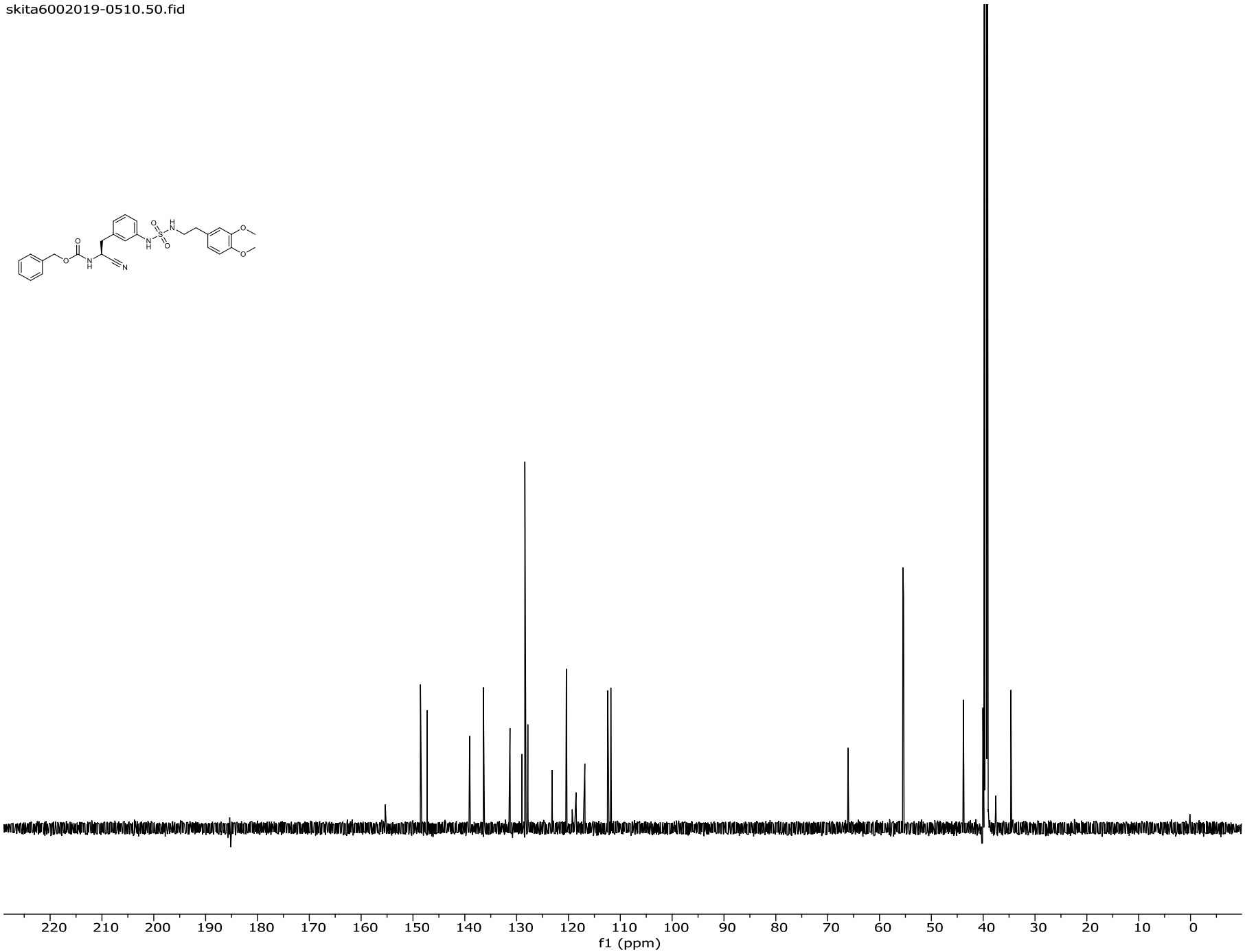
skita6002019-0510.50.fid
220
210
200
190
180
170
160
150
140
130
120
110
100
90
80
70
60
50
40
30
20
10
0
f1 (ppm)

skita6002019-0512.1.fid —

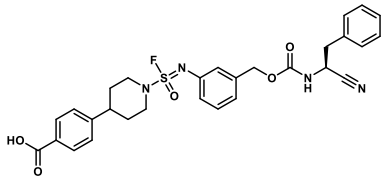

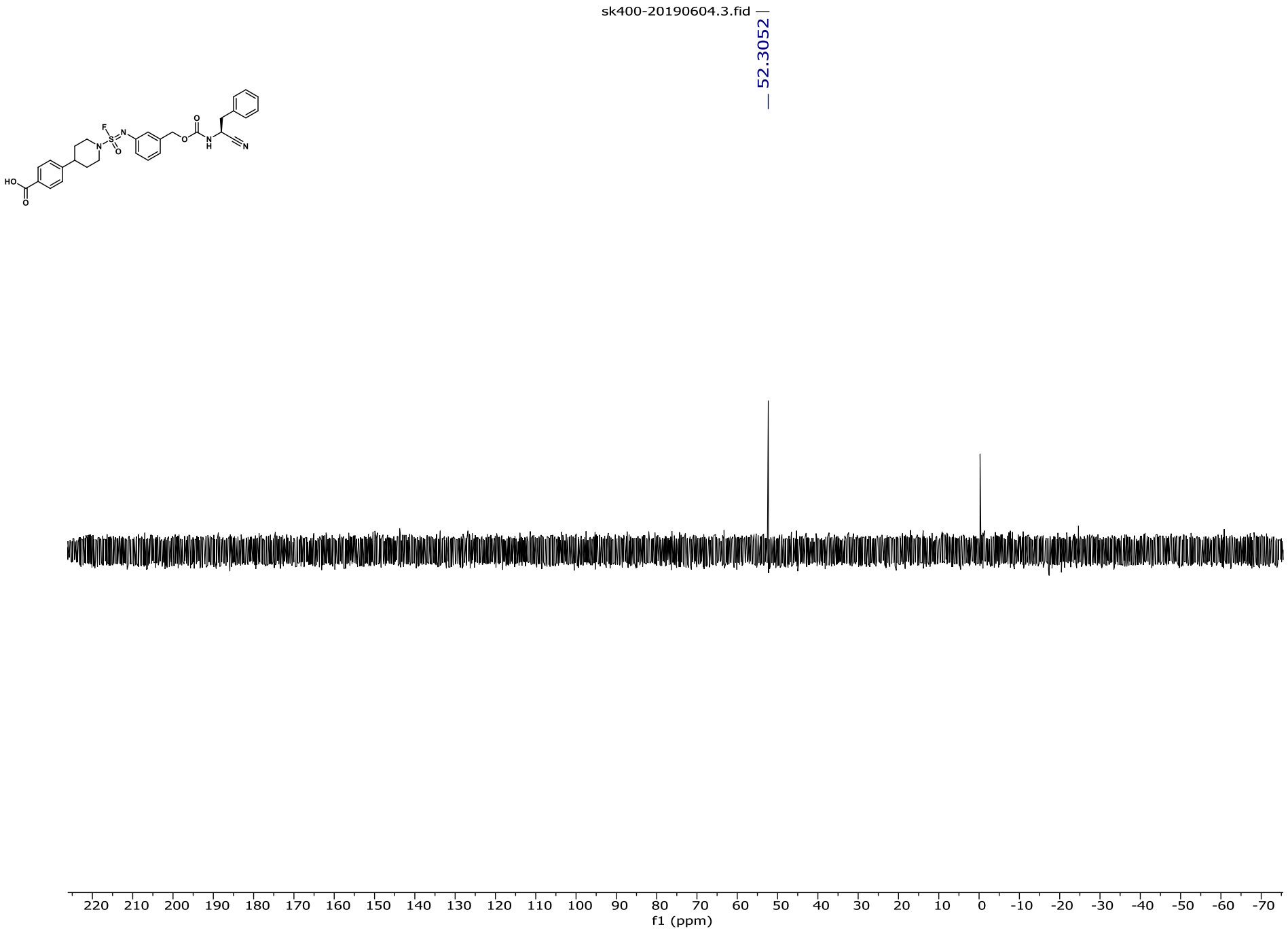
sk400-20190604.3.fid
52.3052
HO
O
F
S
O
N
N
O
O
N
H
N
220 210 200 190 180 170 160 150 140 130 120 110 100 90 80 70 60 50 40 30 20 10 0 -10 -20 -30 -40 -50 -60 -70
f1 (ppm)

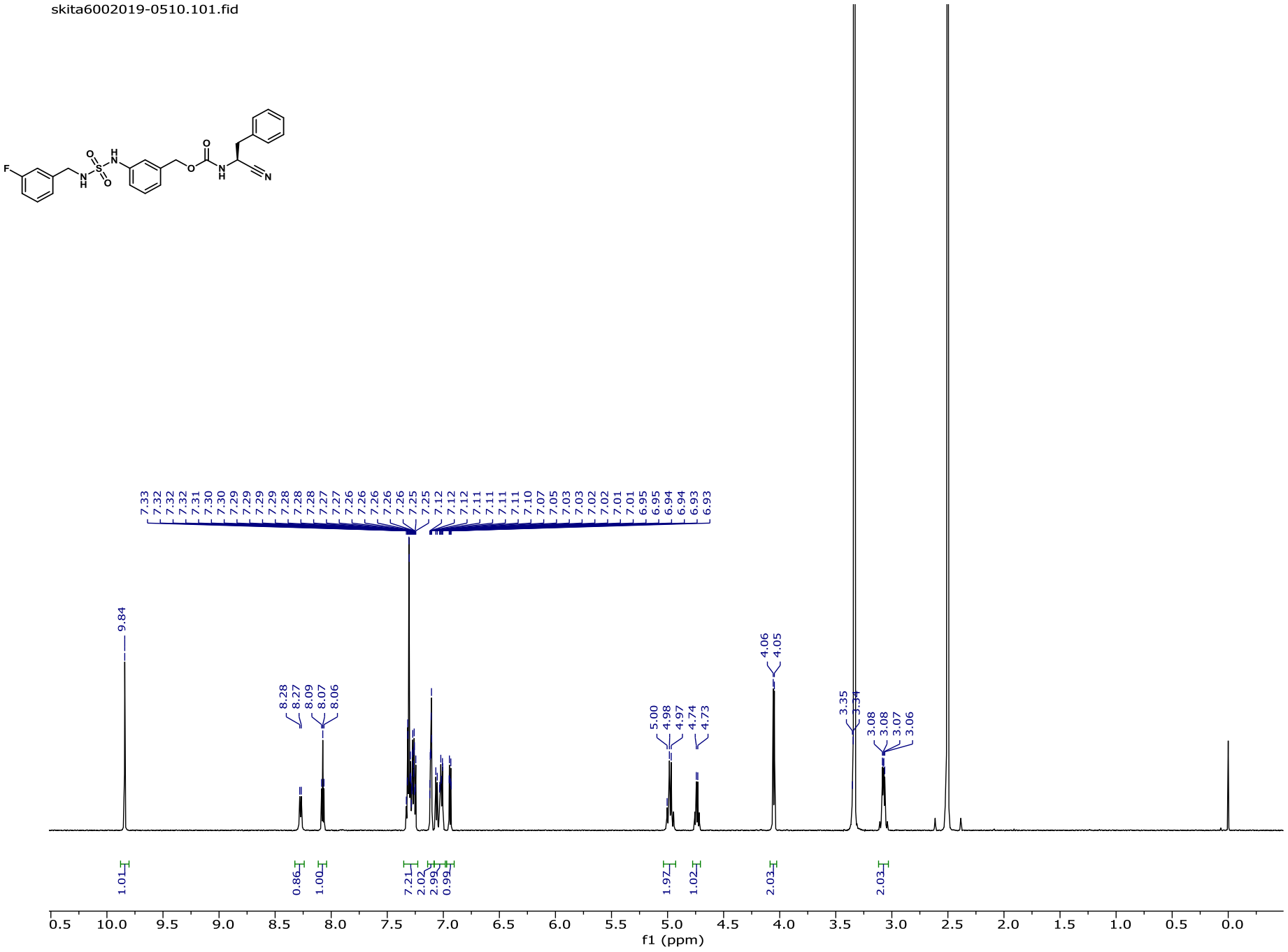
skita6002019-0510.101.fid
F
O
S
O
H
N
N
H
O
O
N
H
N
7.33 7.32 7.32 7.32 7.31 7.30 7.30 7.29 7.29 7.29 7.29 7.28 7.28 7.28 7.27 7.27 7.26 7.26 7.26 7.26 7.25 7.25 7.12 7.12 7.12 7.11 7.11 7.11 7.11 7.10 7.07 7.05 7.03 7.03 7.02 7.02 7.01 7.01 6.95 6.95 6.94 6.94 6.93 6.93
9.84
8.28 8.27 8.09 8.07 8.06
5.00 4.98 4.97 4.74 4.73
4.06 4.05
3.35 3.34
3.08 3.08 3.07 3.06
1.01 0.86 1.00 7.21 2.02 2.99 0.99 1.97 1.02 2.03 2.03
0.5 10.0 9.5 9.0 8.5 8.0 7.5 7.0 6.5 6.0 5.5 5.0 4.5 4.0 3.5 3.0 2.5 2.0 1.5 1.0 0.5 0.0
f1 (ppm)

skita6002019-0510.1010.fid

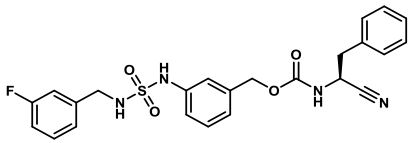

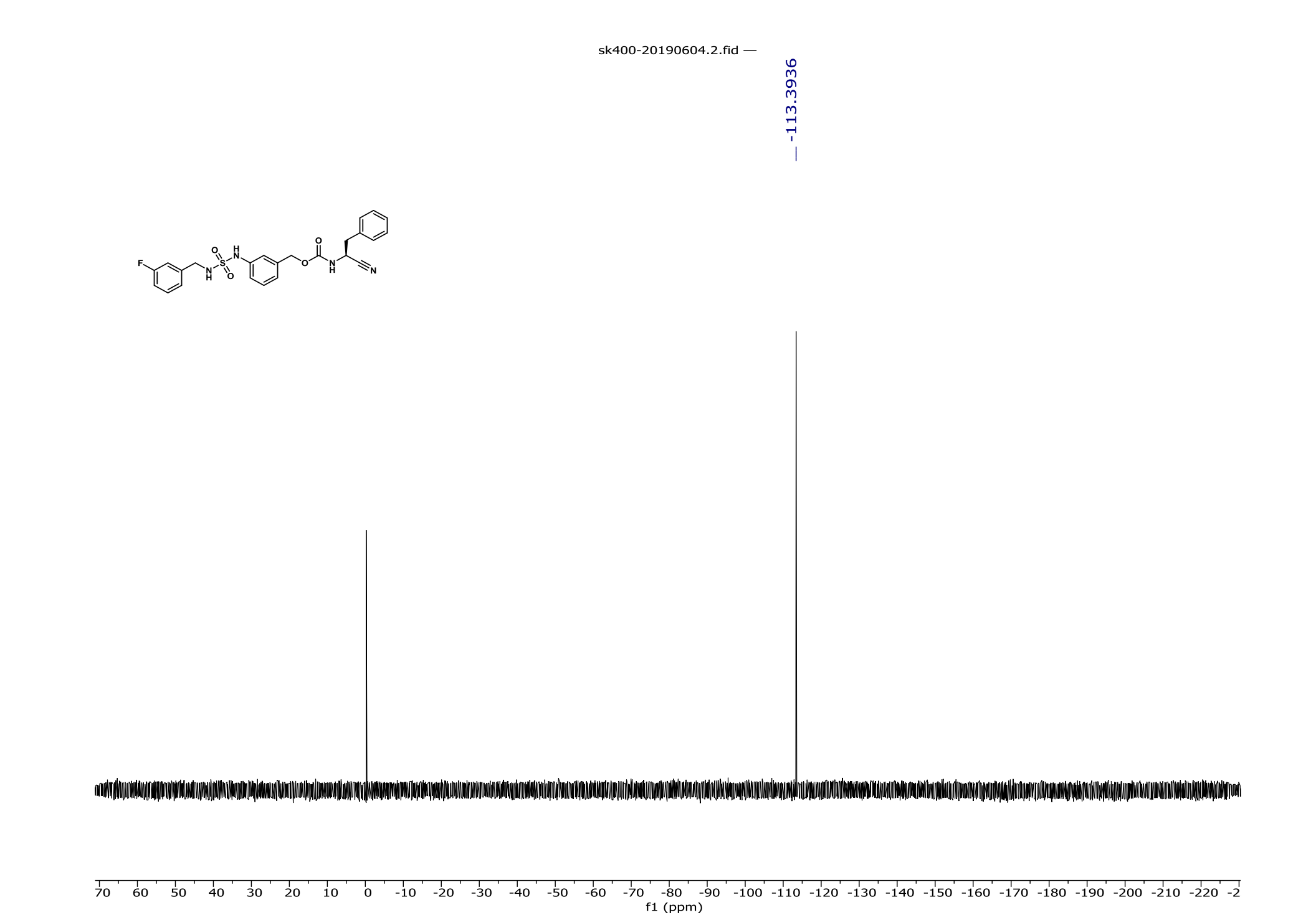
sk400-20190604.2.fid
-113.3936
F
O
H
N
S
O
N
H
O
O
O
N
H
N
70 60 50 40 30 20 10 0 -10 -20 -30 -40 -50 -60 -70 -80 -90 -100 -110 -120 -130 -140 -150 -160 -170 -180 -190 -200 -210 -220 -2
f1 (ppm)

skita6002019-0512.10.fid —

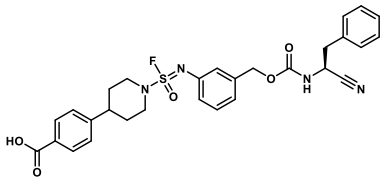

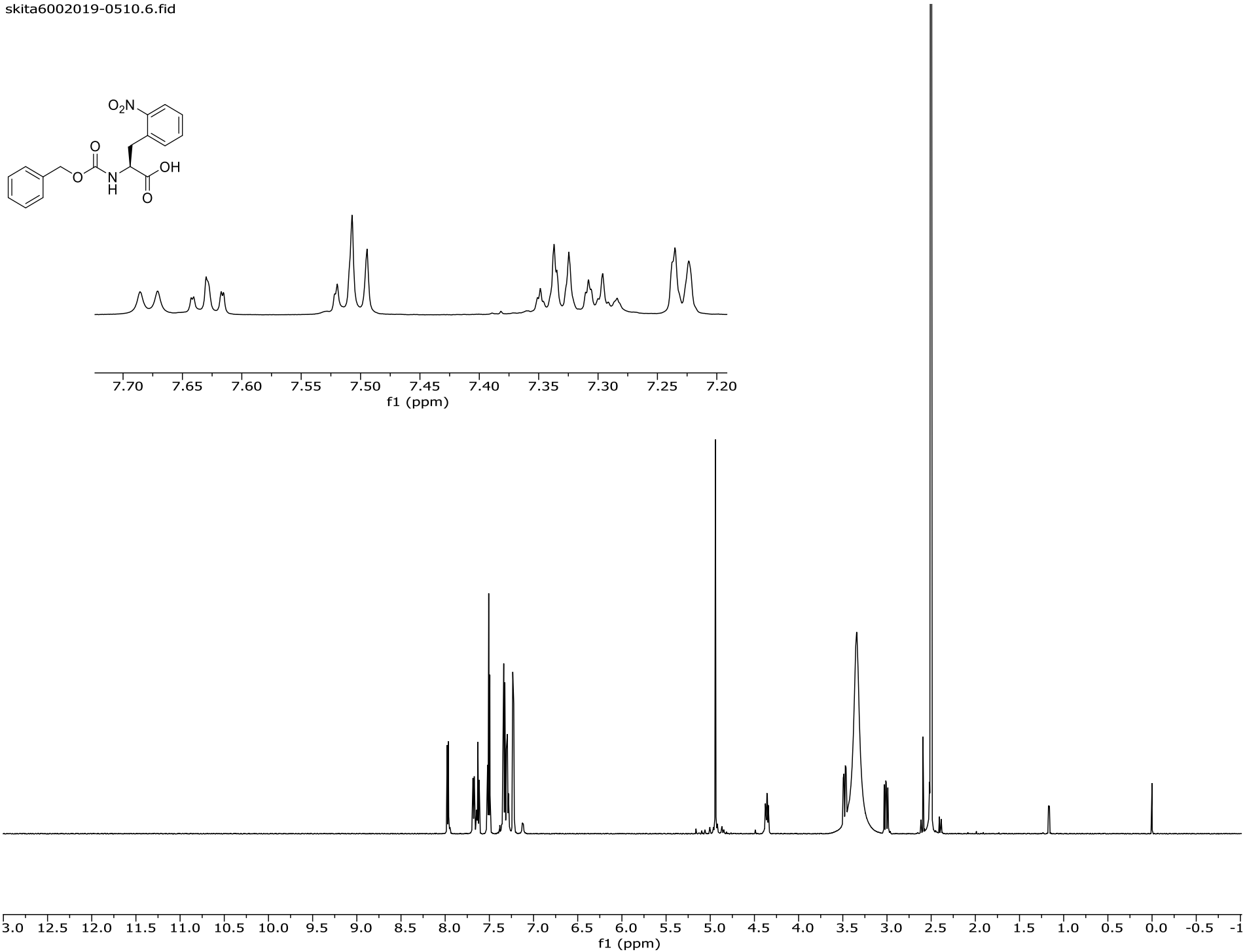
skita6002019-0510.6.fid
O2N
O
O
N
H
OH
O
7.70 7.65 7.60 7.55 7.50 7.45 7.40 7.35 7.30 7.25 7.20
f1 (ppm)
3.0 12.5 12.0 11.5 11.0 10.5 10.0 9.5 9.0 8.5 8.0 7.5 7.0 6.5 6.0 5.5 5.0 4.5 4.0 3.5 3.0 2.5 2.0 1.5 1.0 0.5 0.0 -0.5 -1
f1 (ppm)

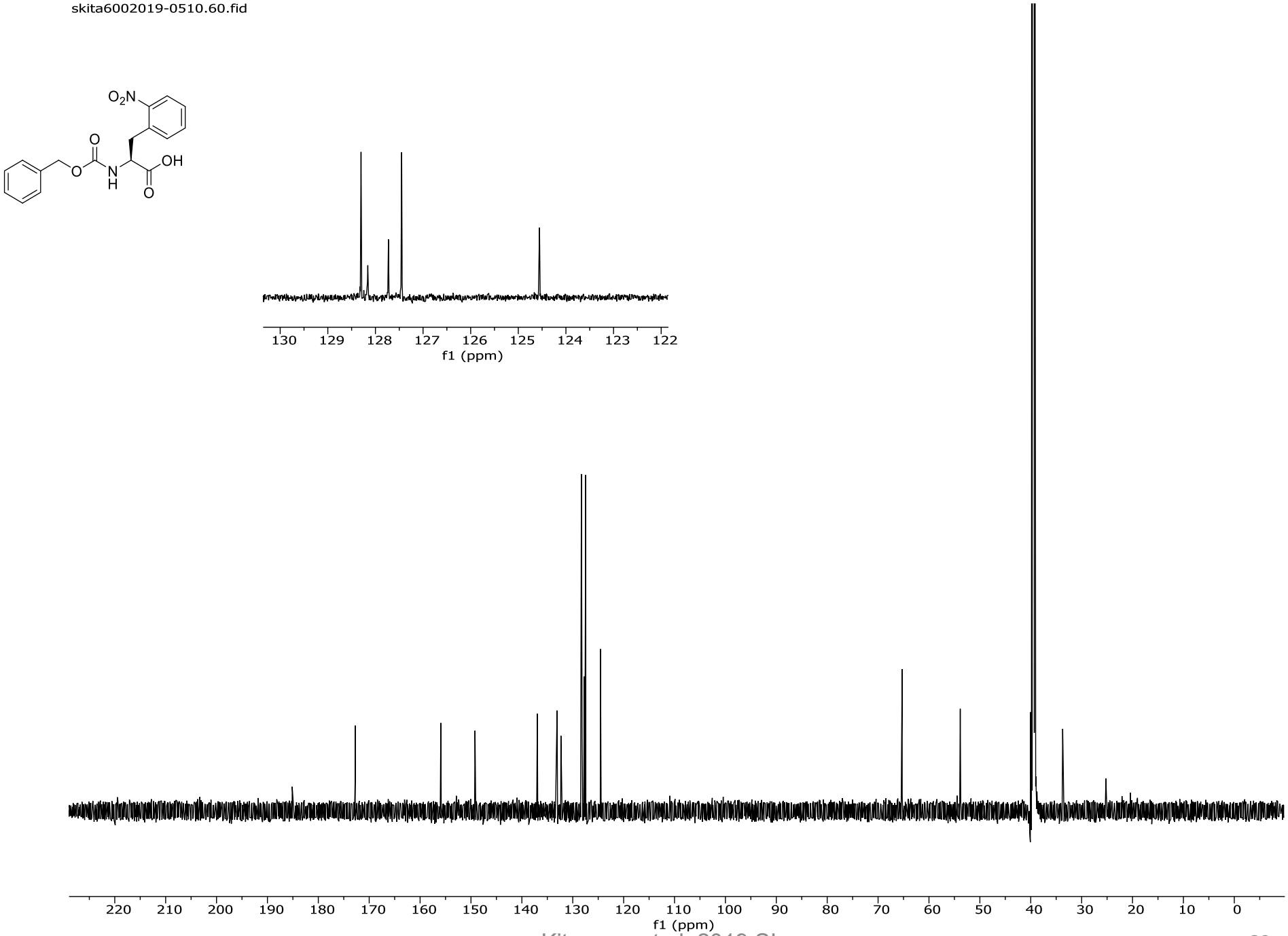
skita6002019-0510.60.fid
O2N
O
O
N
H
OH
O
130
129
128
127
126
125
124
123
122
f1 (ppm)
220
210
200
190
180
170
160
150
140
130
120
110
100
90
80
70
60
50
40
30
20
10
0
f1 (ppm)

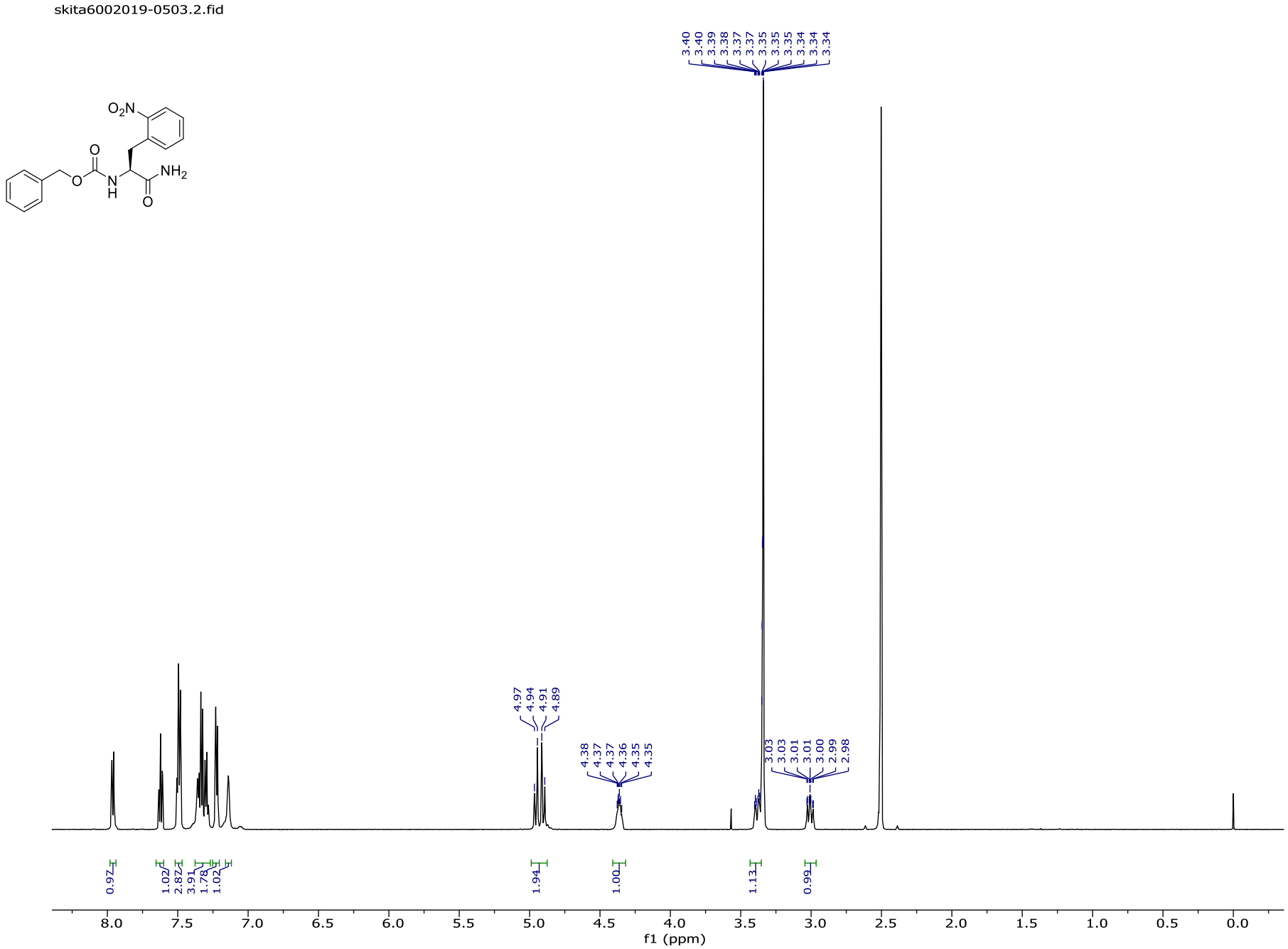
skita6002019-0503.2.fid
O2N
O
O
N
H
NH2
O
3.40
3.40
3.39
3.38
3.37
3.37
3.35
3.35
3.34
3.34
3.34
4.97
4.94
4.91
4.89
4.38
4.37
4.37
4.36
4.35
4.35
3.03
3.03
3.01
3.01
3.00
2.99
2.98
0.97
1.02
2.82
3.91
1.78
1.02
1.94
1.00
1.13
0.99
8.0
7.5
7.0
6.5
6.0
5.5
5.0
4.5
4.0
3.5
3.0
2.5
2.0
1.5
1.0
0.5
0.0
f1 (ppm)

skita6002019-0503.20.fid

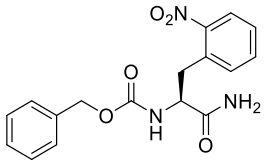

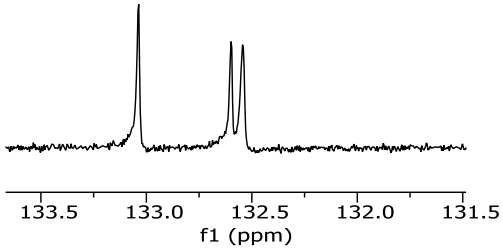

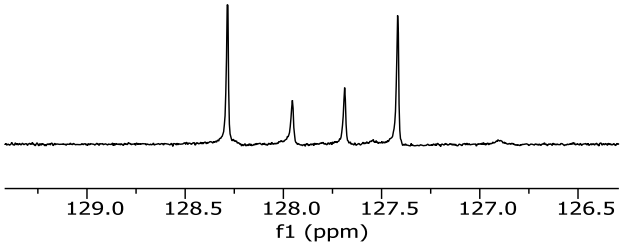

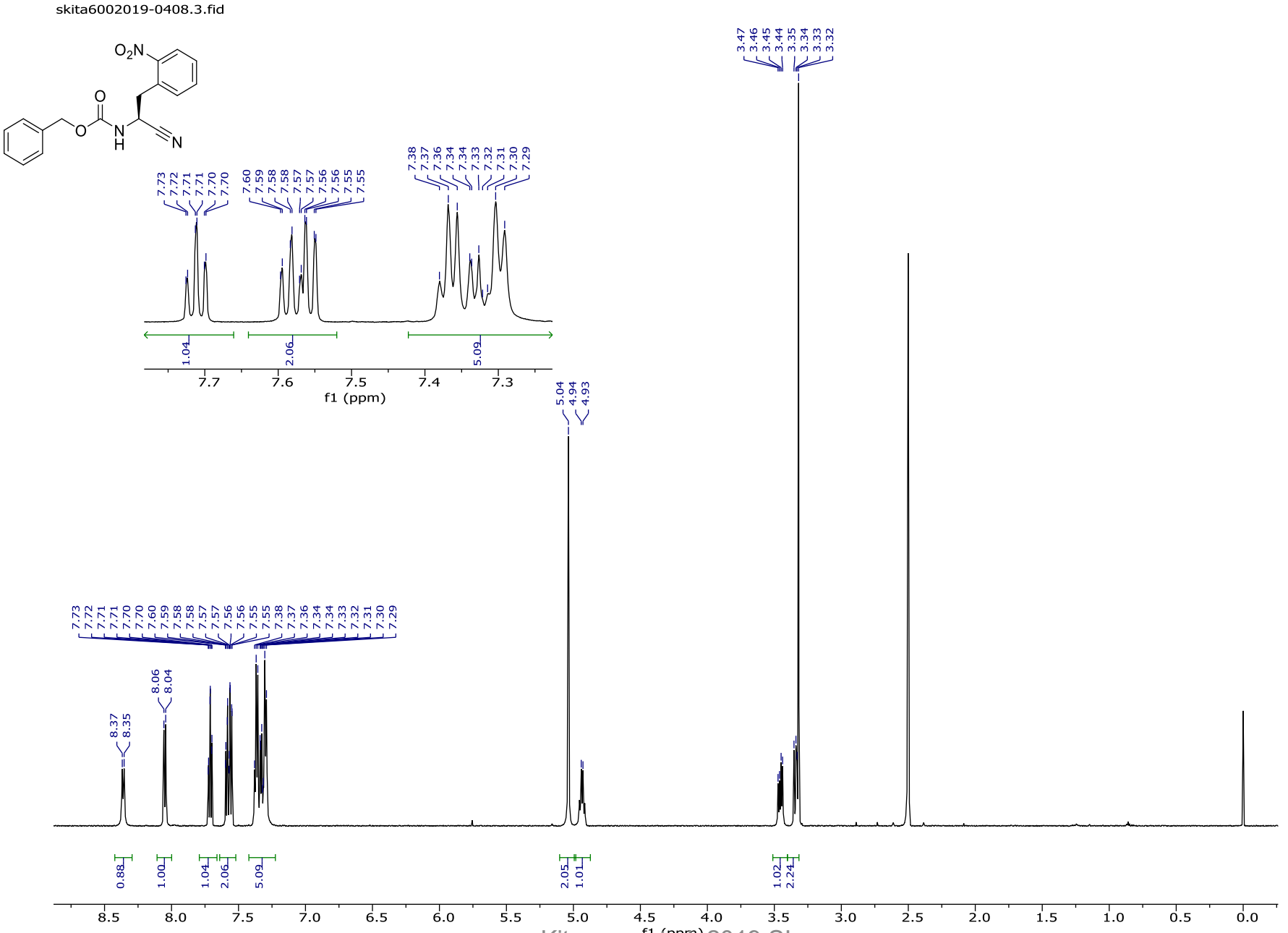
skita6002019-0408.3.fid
f1 (ppm)

skita6002019-0408.31.fid

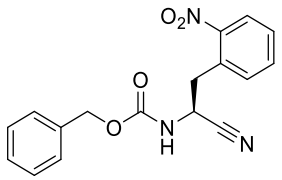

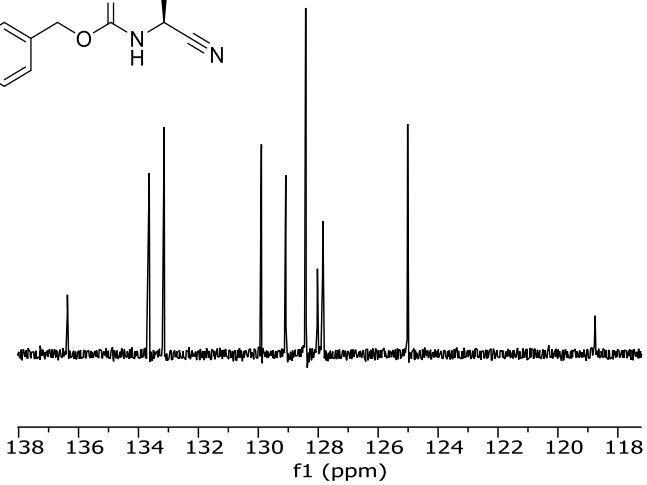

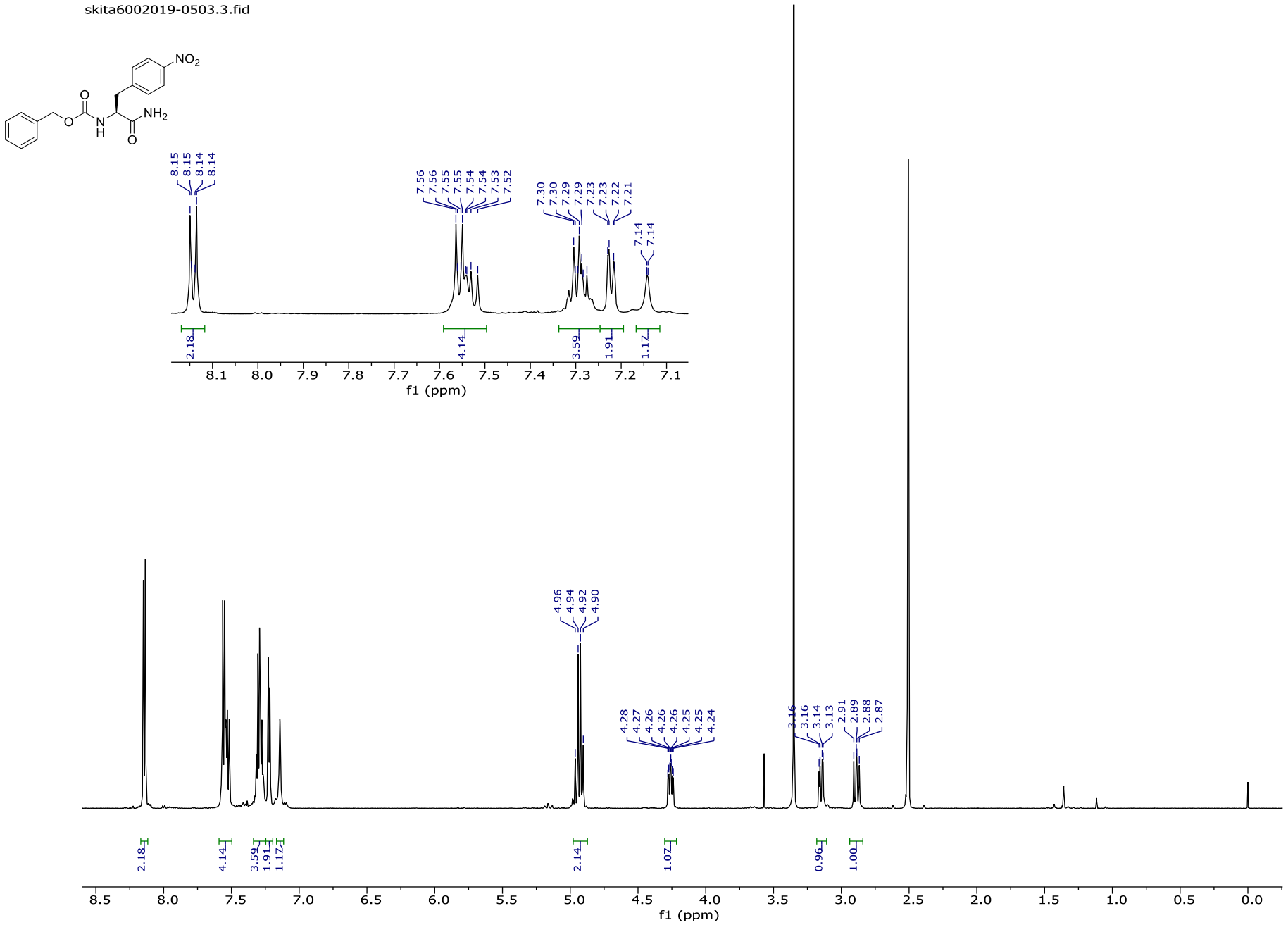
skita6002019-0503.3.fid
NO2
NH2
O
N
H
8.15
8.15
8.14
8.14
7.56
7.56
7.55
7.55
7.54
7.54
7.53
7.52
7.30
7.30
7.29
7.29
7.23
7.23
7.22
7.21
7.14
7.14
2.18
4.14
3.59
1.91
1.17
8.1
8.0
7.9
7.8
7.7
7.6
7.5
7.4
7.3
7.2
7.1
f1 (ppm)
4.96
4.94
4.92
4.90
4.28
4.27
4.26
4.26
4.26
4.25
4.25
4.24
3.16
3.16
3.14
3.13
2.91
2.89
2.88
2.87
2.18
4.14
3.59
1.91
1.12
2.14
1.07
0.96
1.00
8.5
8.0
7.5
7.0
6.5
6.0
5.5
5.0
4.5
4.0
3.5
3.0
2.5
2.0
1.5
1.0
0.5
0.0
f1 (ppm)

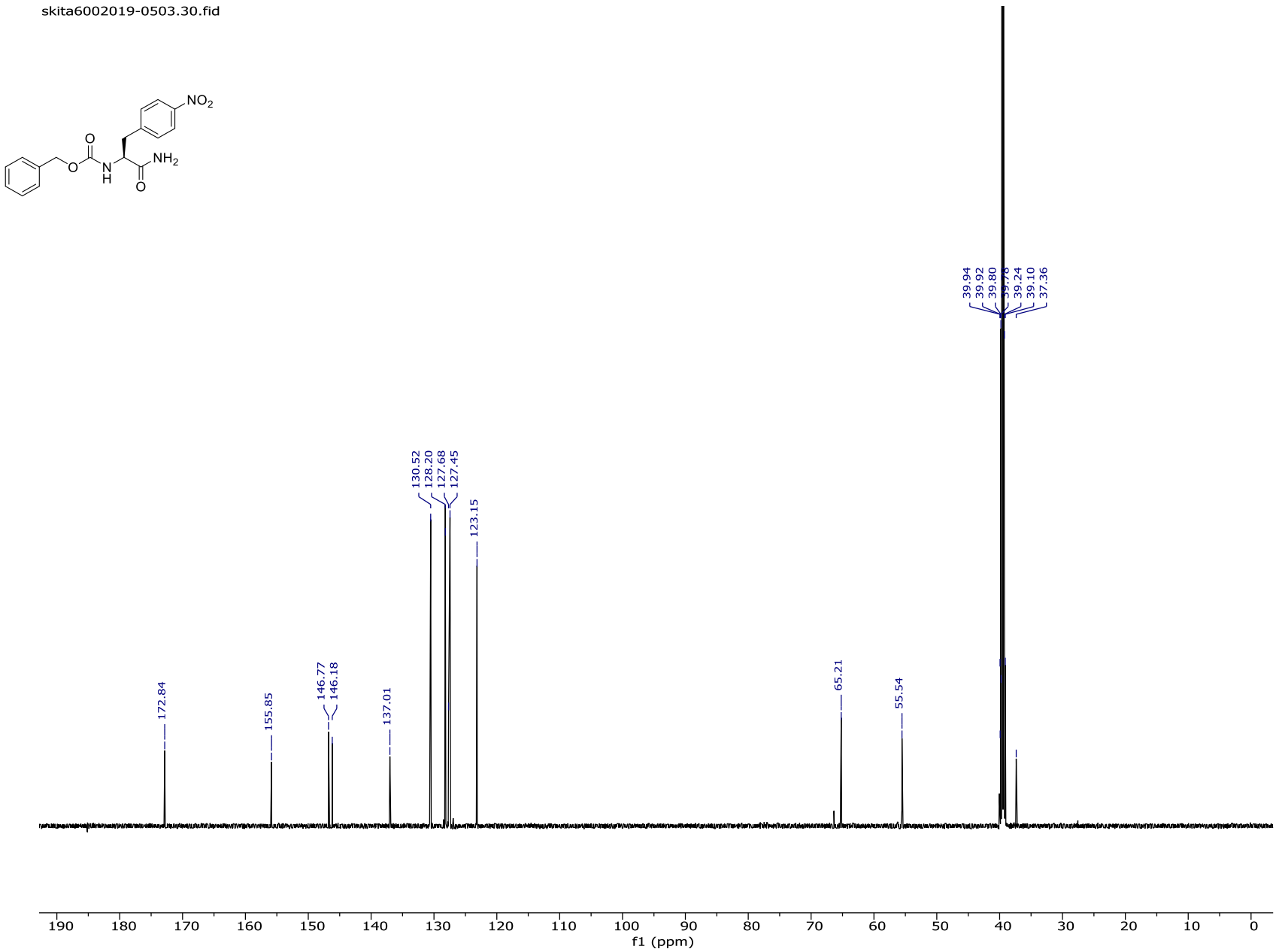
skita6002019-0503.30.fid
NO2
O
O
N
H
NH2
O
39.94
39.92
39.80
39.24
39.10
37.36
130.52
128.20
127.68
127.45
123.15
172.84
155.85
146.77
146.18
137.01
65.21
55.54
190
180
170
160
150
140
130
120
110
100
90
80
70
60
50
40
30
20
10
0
f1 (ppm)

skita6002019-0429.2.fid

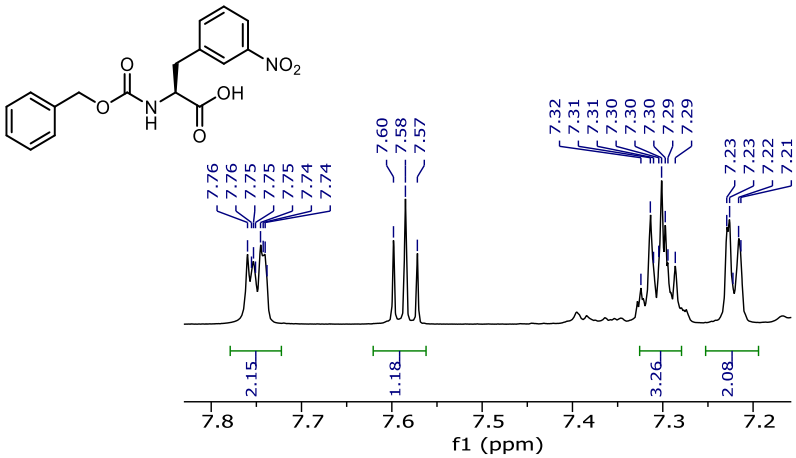

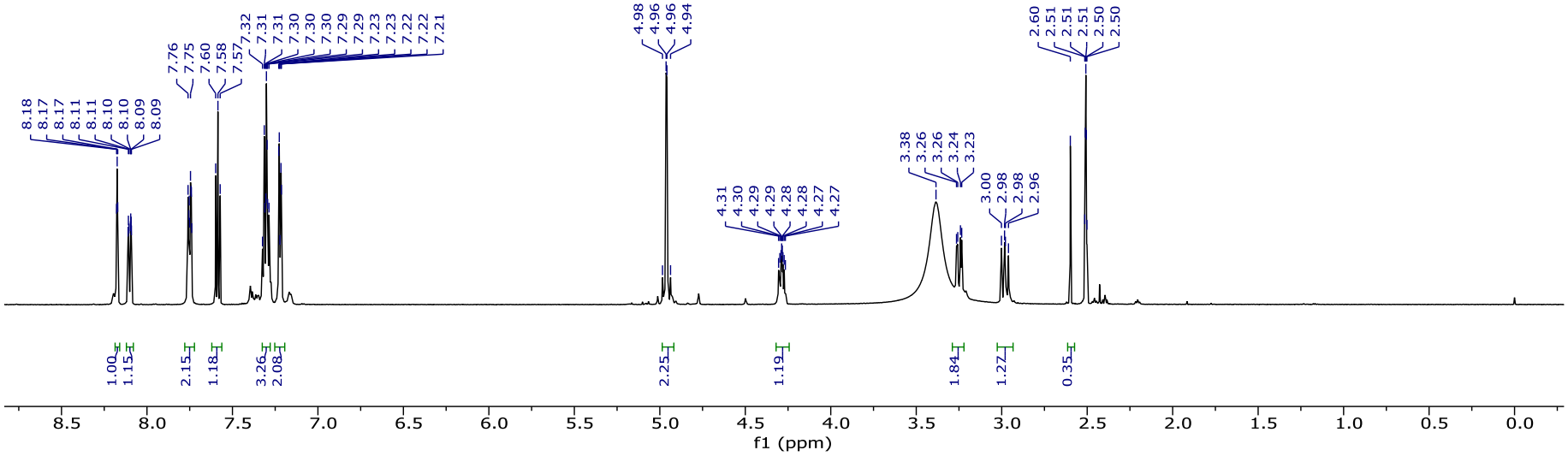

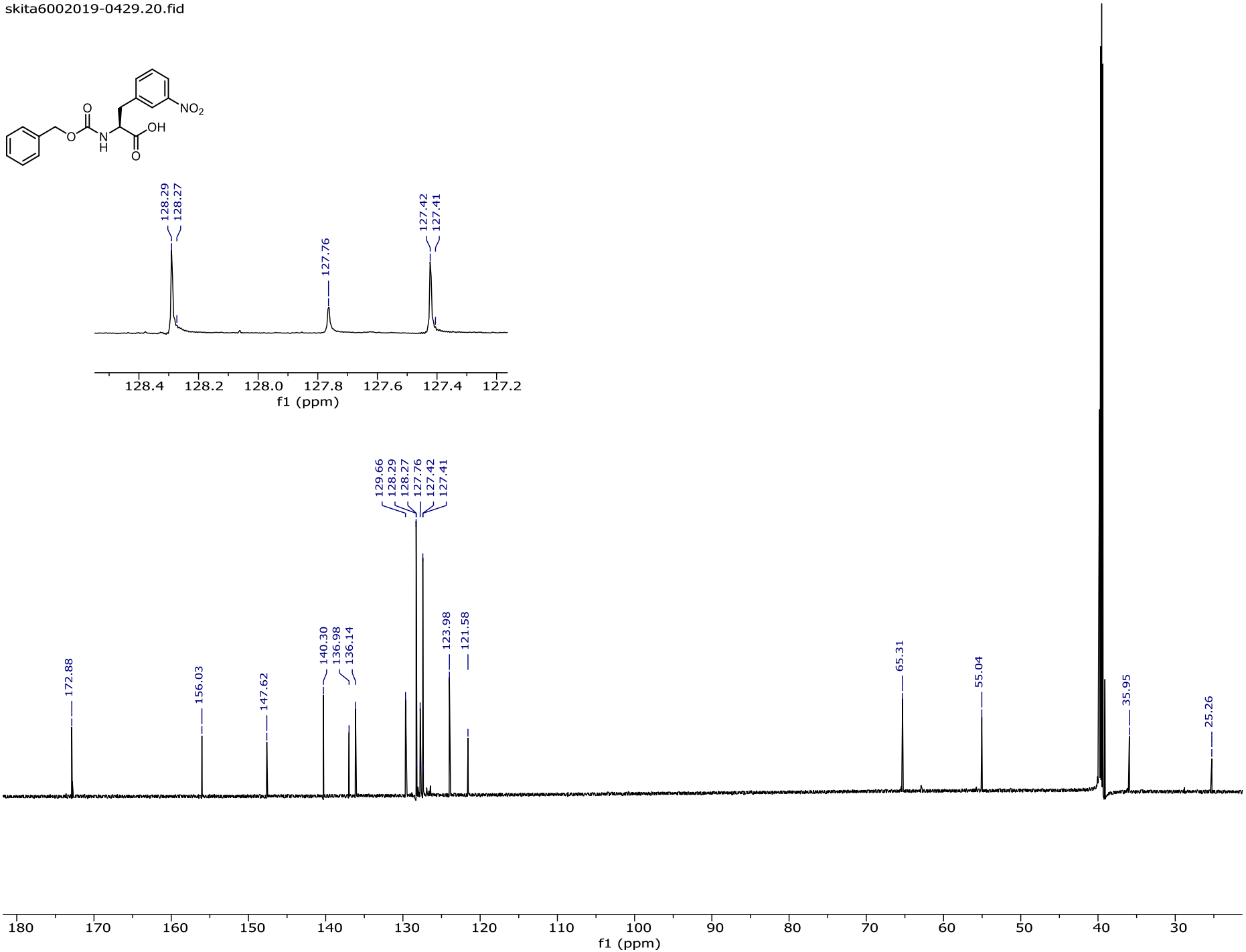
skita6002019-0429.20.fid
NO2
OH
O
N
H
O
O
O
128.29
128.27
127.76
127.42
127.41
128.4
128.2
128.0
127.8
127.6
127.4
127.2
f1 (ppm)
129.66
128.29
128.27
127.76
127.42
127.41
172.88
156.03
147.62
140.30
136.98
136.14
123.98
121.58
65.31
55.04
35.95
25.26
180
170
160
150
140
130
120
110
100
90
80
70
60
50
40
30
f1 (ppm)

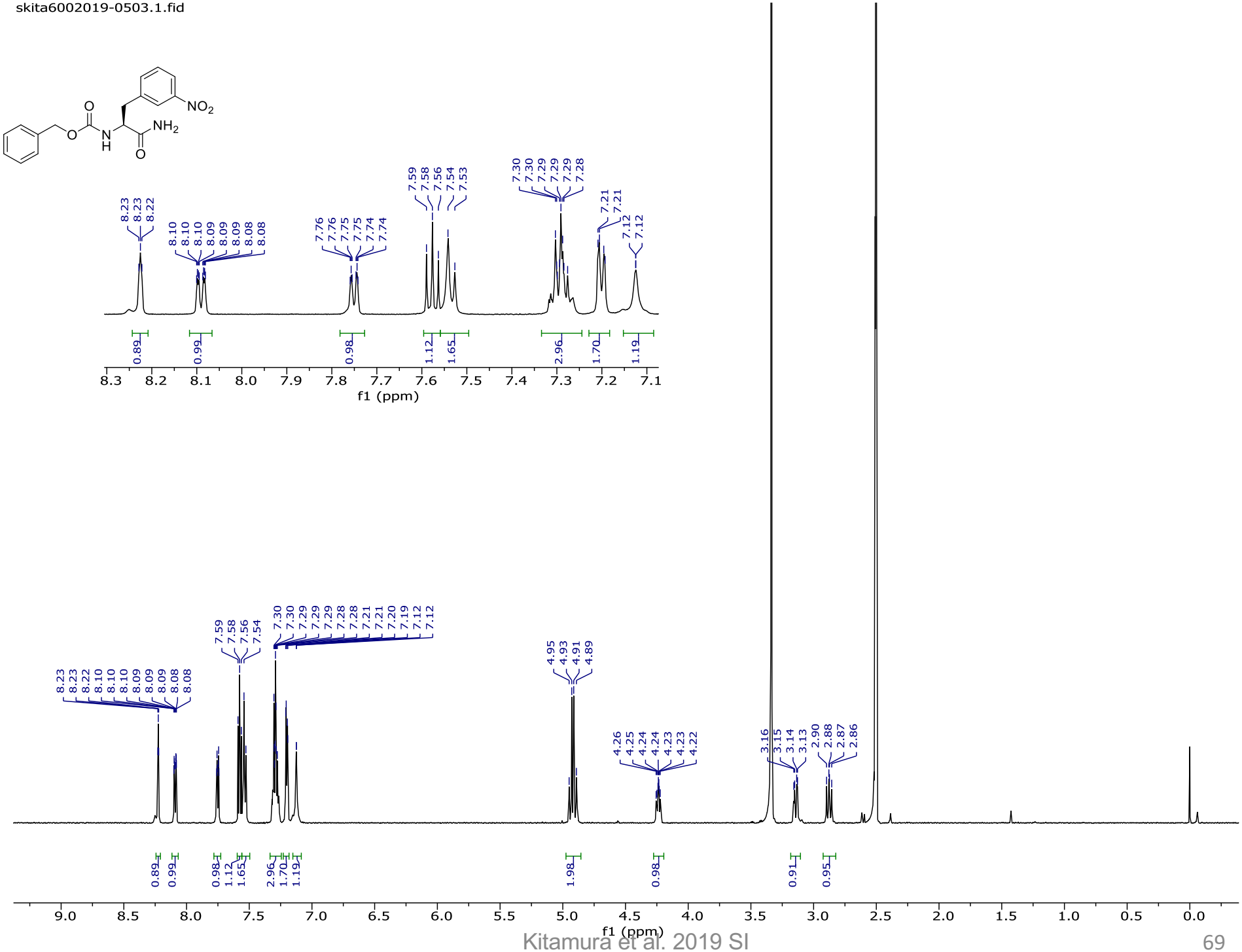
skita6002019-0503.1.fid
NO2
NH2
O
N
H
f1 (ppm)

skita6002019-0503.10.fid

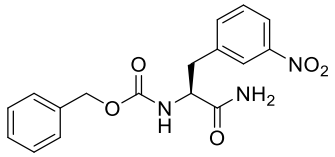

skita6002019-0510.100.fid

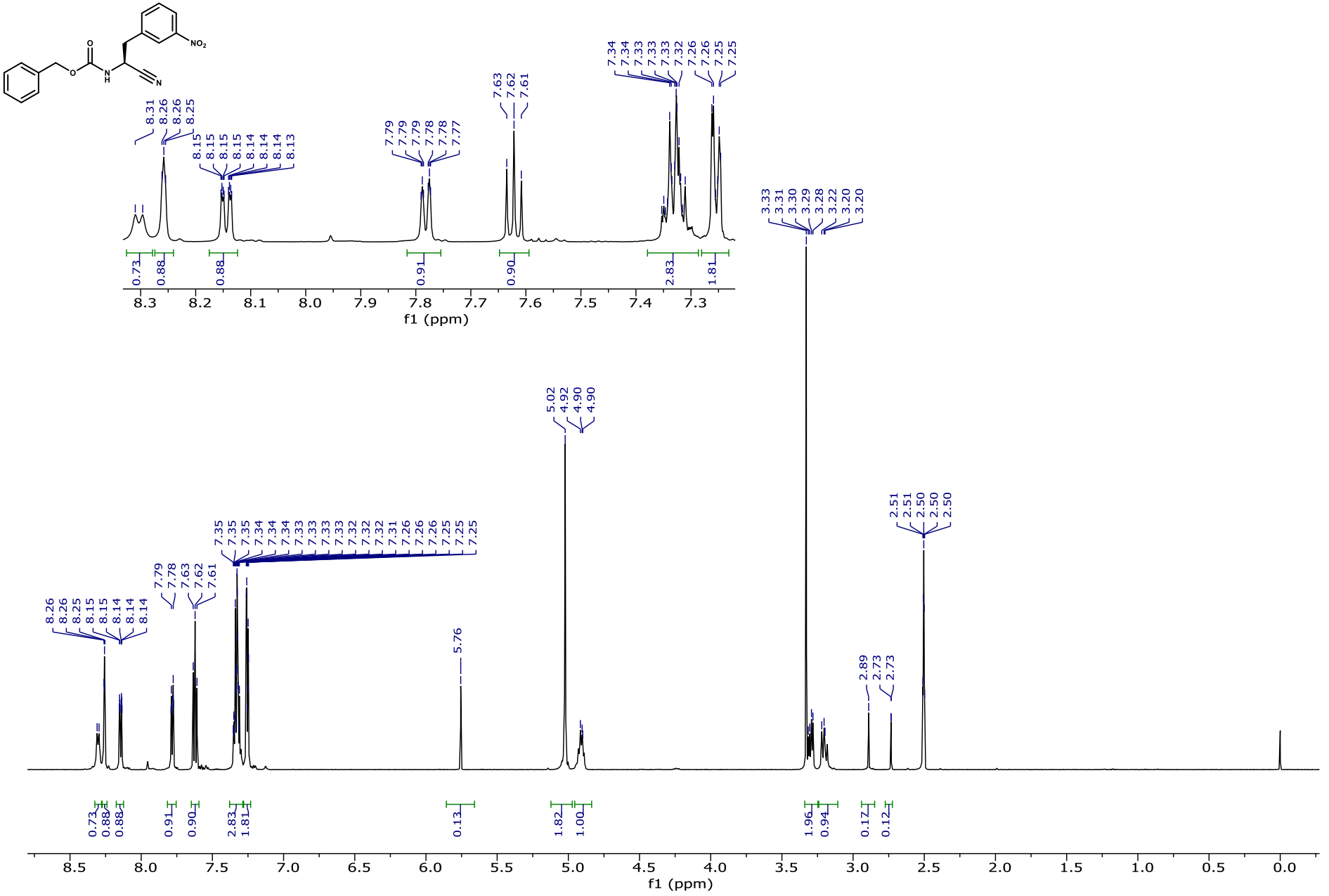

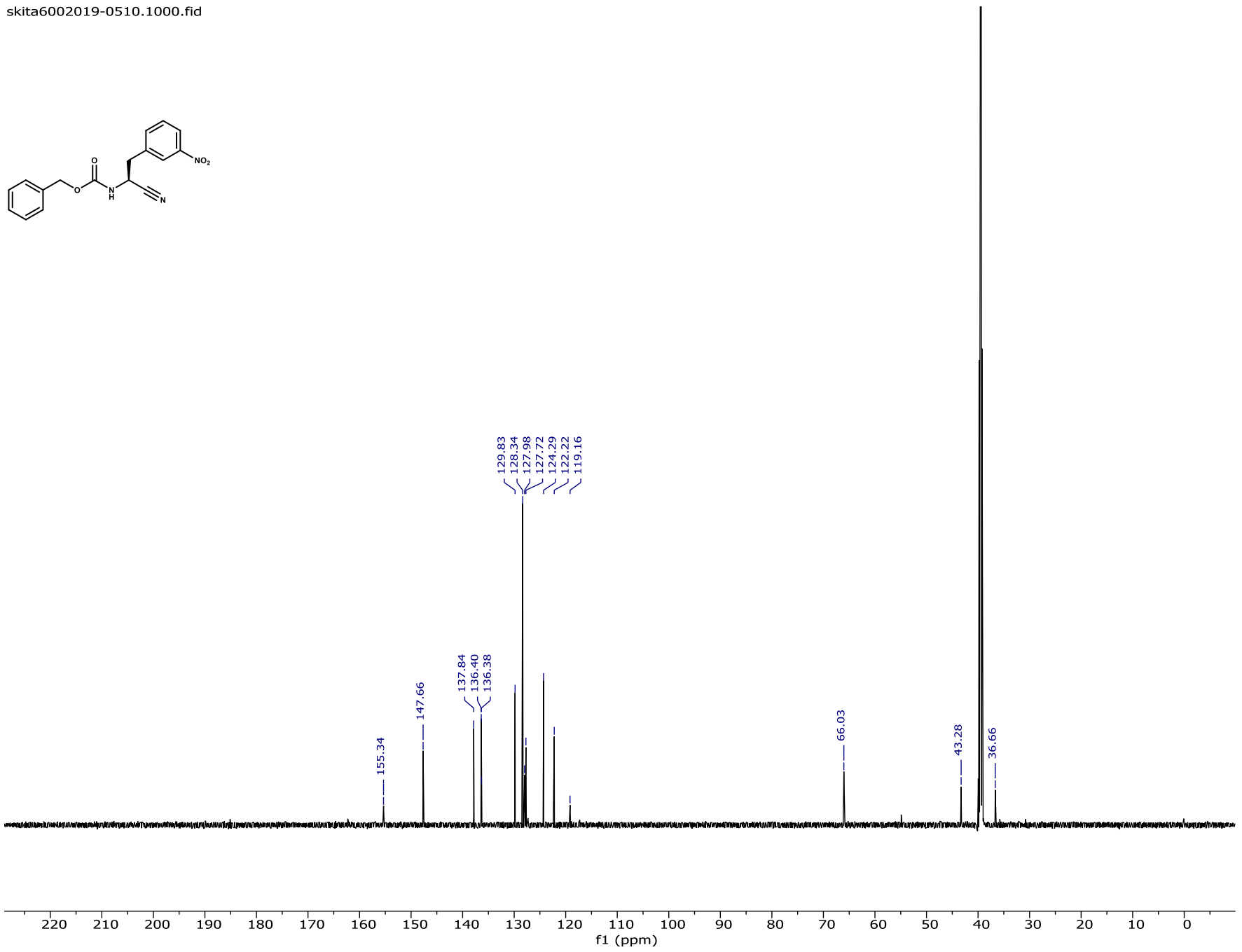
skita6002019-0510.1000.fid
O
O
N
H
N
NO2
155.34
147.66
137.84
136.40
136.38
129.83
128.34
127.98
127.72
124.29
122.22
119.16
66.03
43.28
36.66
220
210
200
190
180
170
160
150
140
130
120
110
100
90
80
70
60
50
40
30
20
10
0
f1 (ppm)

skita6002019-0429.1.fid

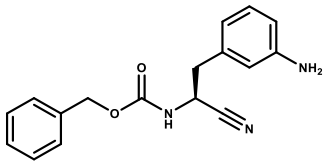

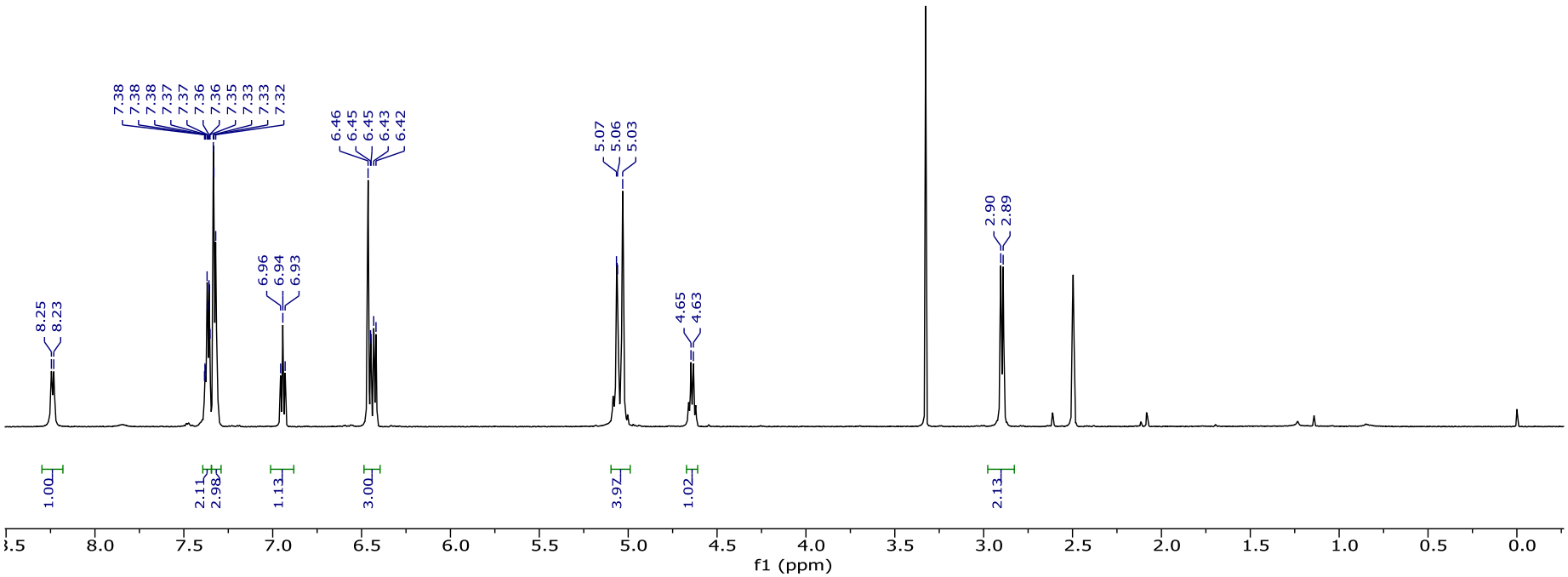

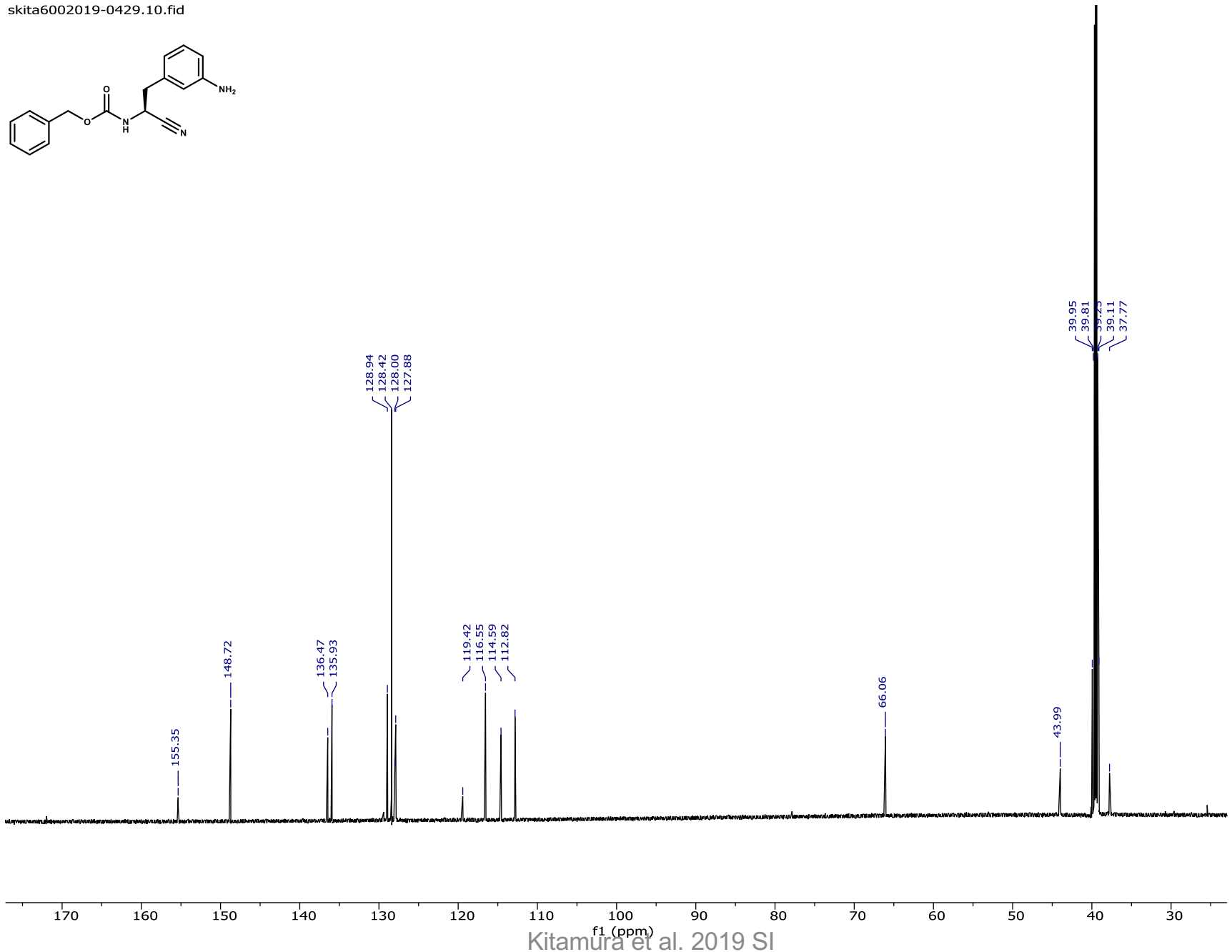
skita6002019-0429.10.fid
NH2
O
O
N
H
N
155.35
148.72
136.47
135.93
128.94
128.42
128.00
127.88
119.42
116.55
114.59
112.82
66.06
43.99
39.95
39.81
39.25
39.11
37.77
170
160
150
140
130
120
110
100
90
80
70
60
50
40
30
f1 (ppm)

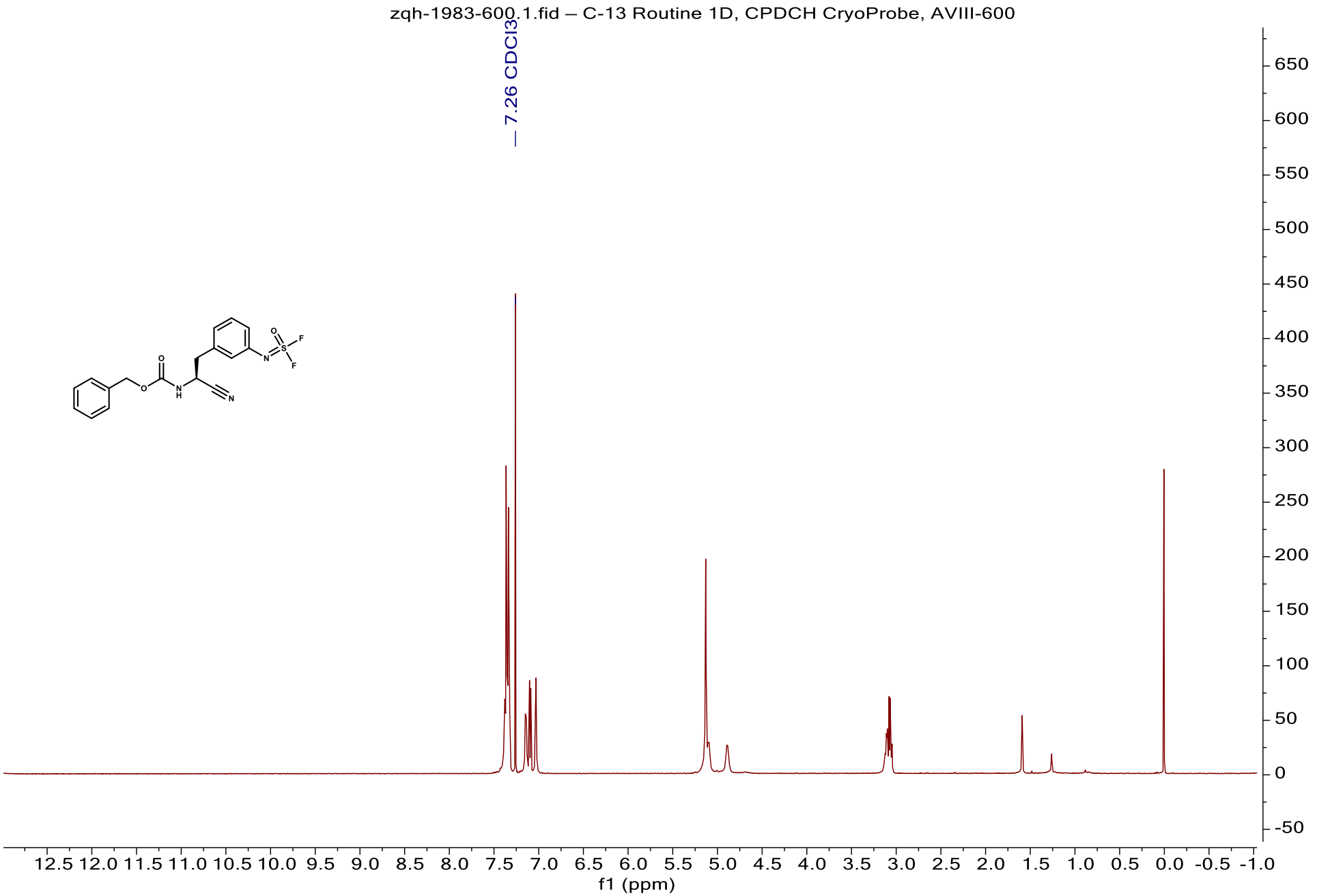
zqh-1983-600.1.fid – C-13 Routine 1D, CPDCH CryoProbe, AVIII-600
7.26 CDCl3
650
600
550
500
450
400
350
300
250
200
150
100
50
0
-50
12.5 12.0 11.5 11.0 10.5 10.0 9.5 9.0 8.5 8.0 7.5 7.0 6.5 6.0 5.5 5.0 4.5 4.0 3.5 3.0 2.5 2.0 1.5 1.0 0.5 0.0 -0.5 -1.0
f1 (ppm)

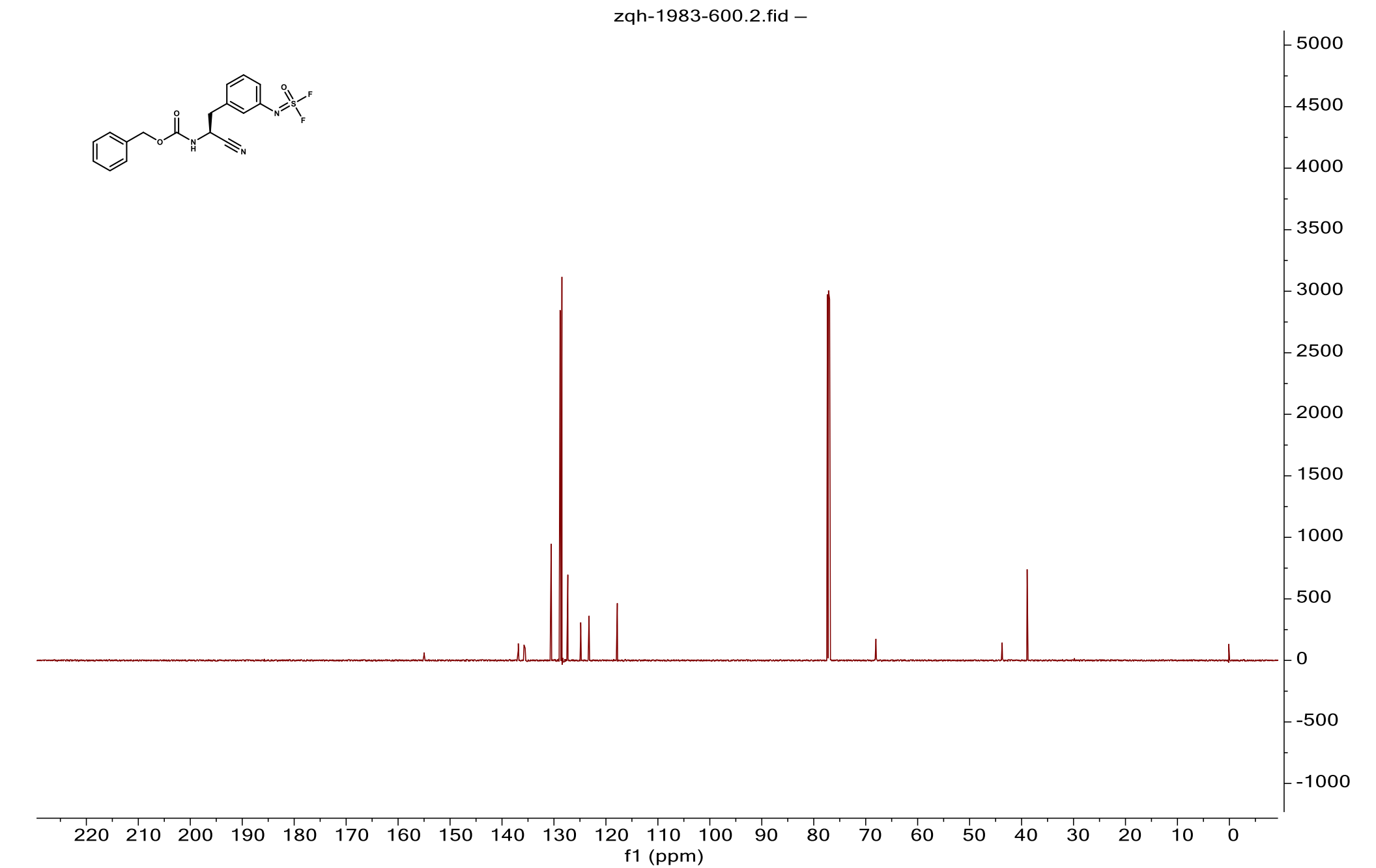
zqh-1983-600.2.fid
5000
4500
4000
3500
3000
2500
2000
1500
1000
500
0
-500
-1000
220 210 200 190 180 170 160 150 140 130 120 110 100 90 80 70 60 50 40 30 20 10 0
f1 (ppm)

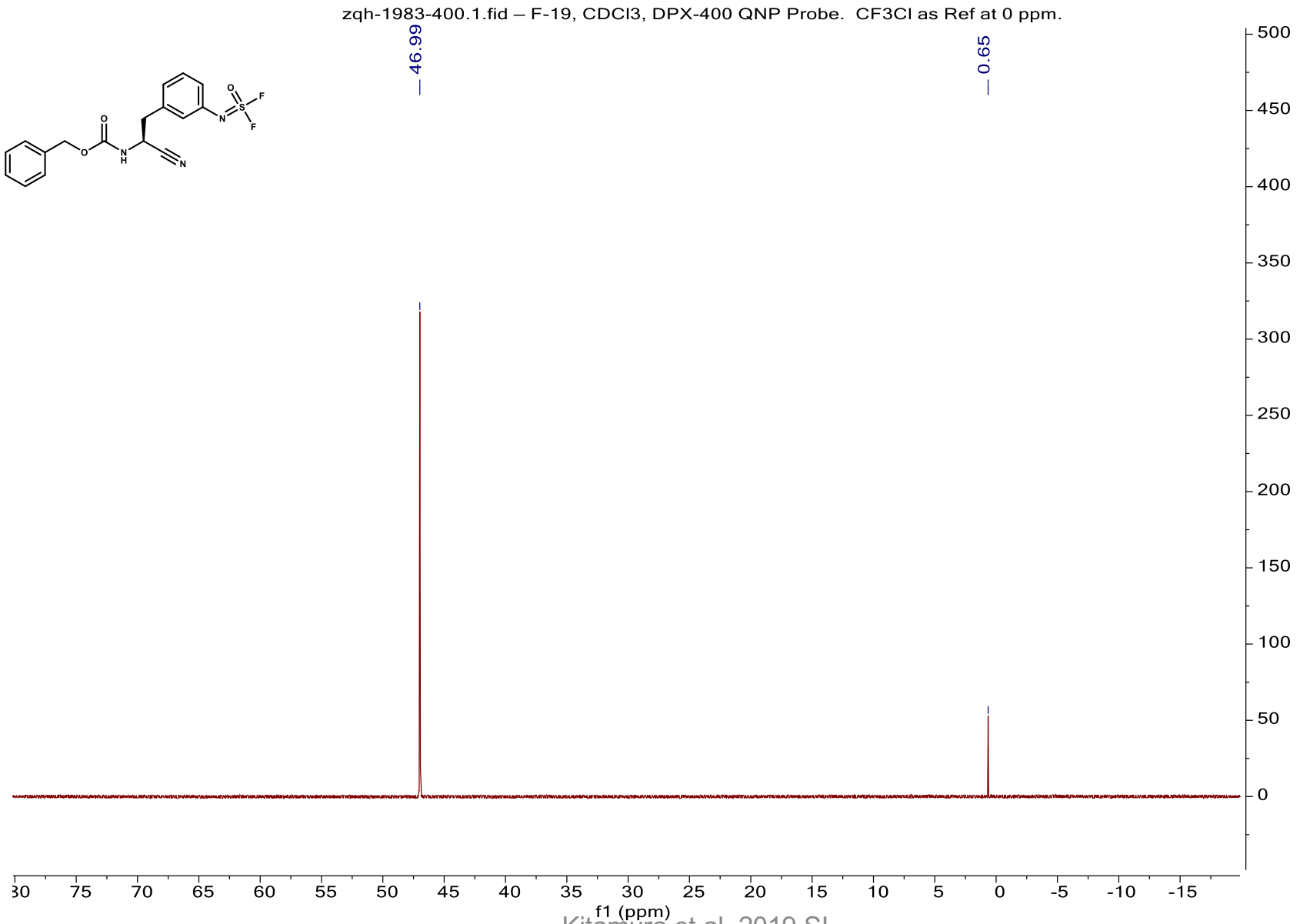
zqh-1983-400.1.fid – F-19, CDCl3, DPX-400 QNP Probe. CF3Cl as Ref at 0 ppm.
46.99
0.65
f1 (ppm)

skita6002019-0503.4.fid

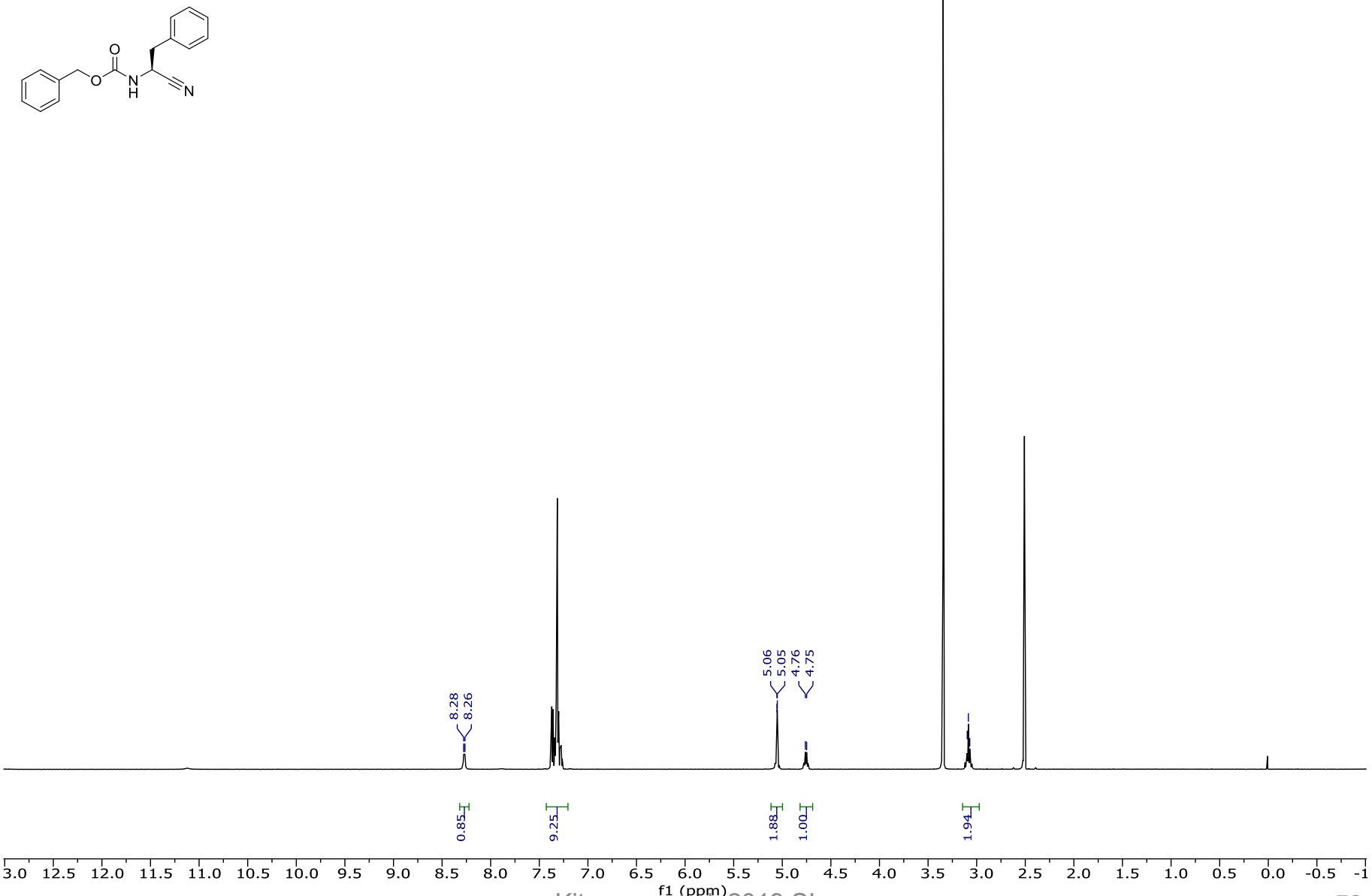

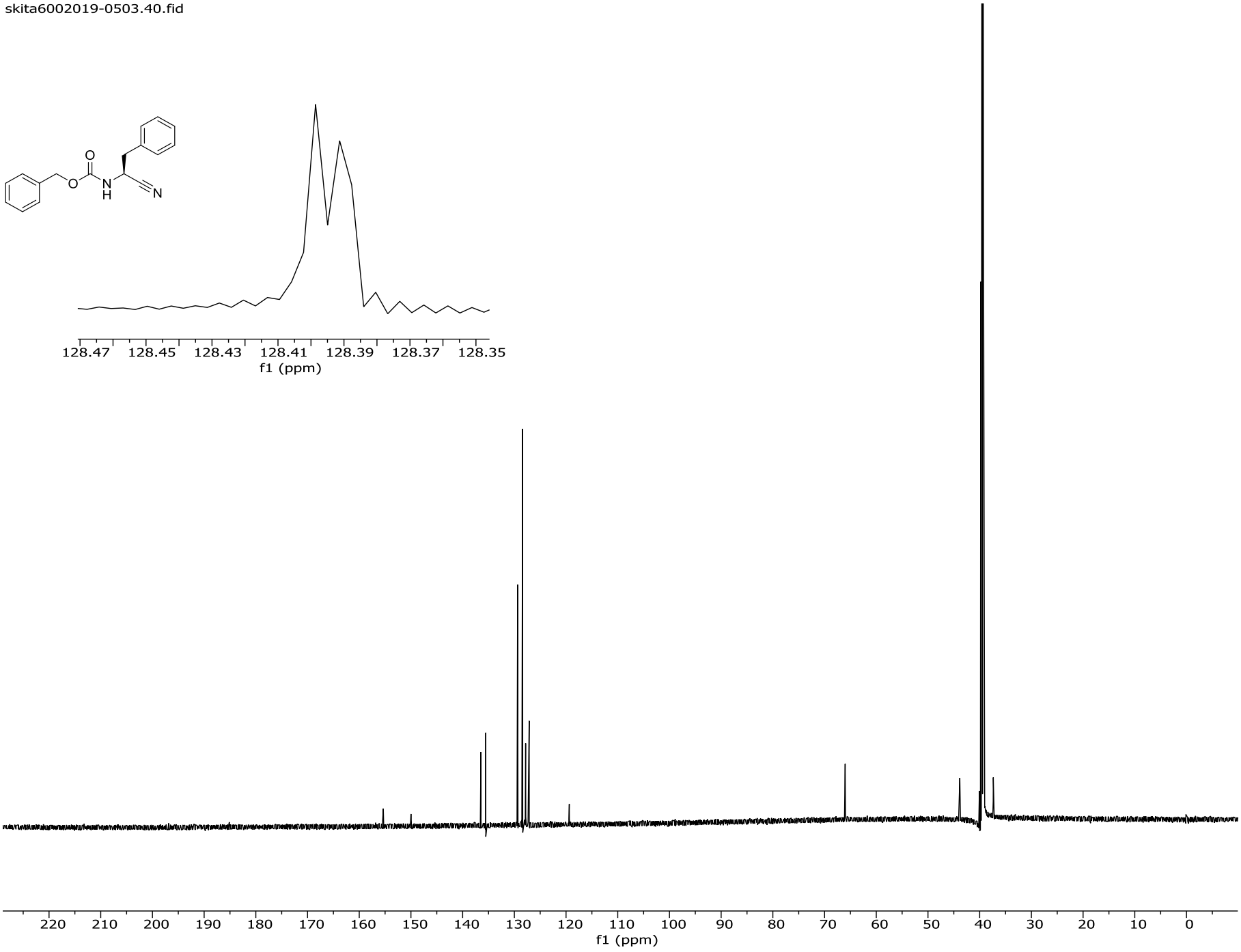
skita6002019-0503.40.fid
O
O
N
H
N
128.47
128.45
128.43
128.41
128.39
128.37
128.35
f1 (ppm)
220
210
200
190
180
170
160
150
140
130
120
110
100
90
80
70
60
50
40
30
20
10
0
f1 (ppm)

skita6002019-0510.9.fid

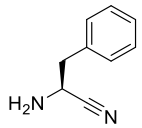

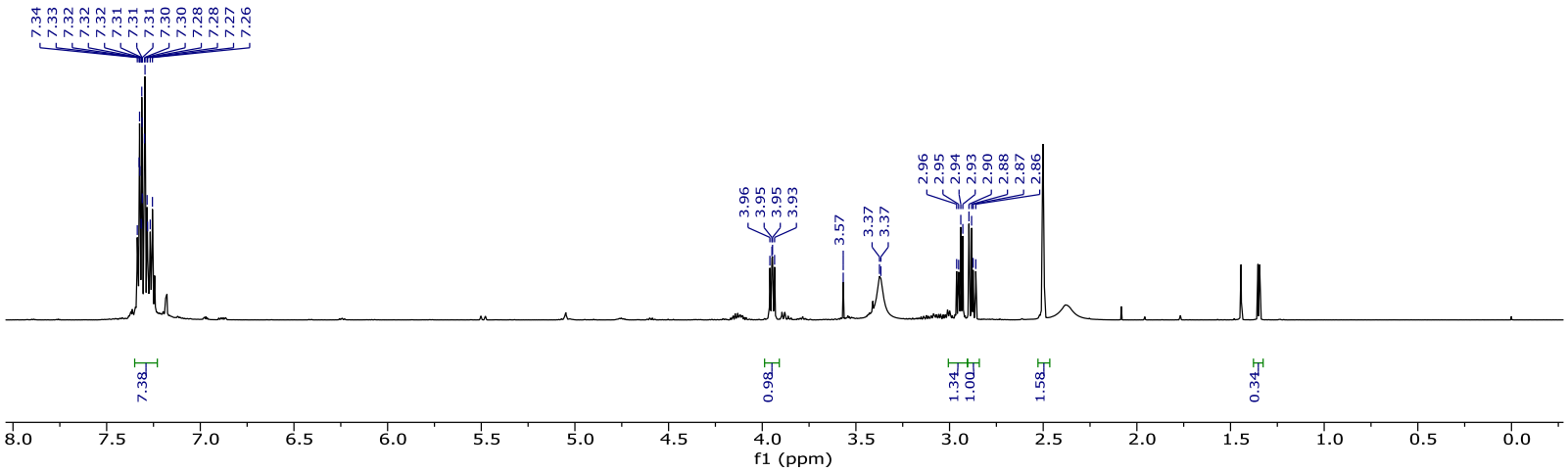

skita6002019-0510.90.fid

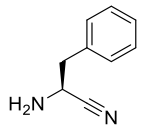

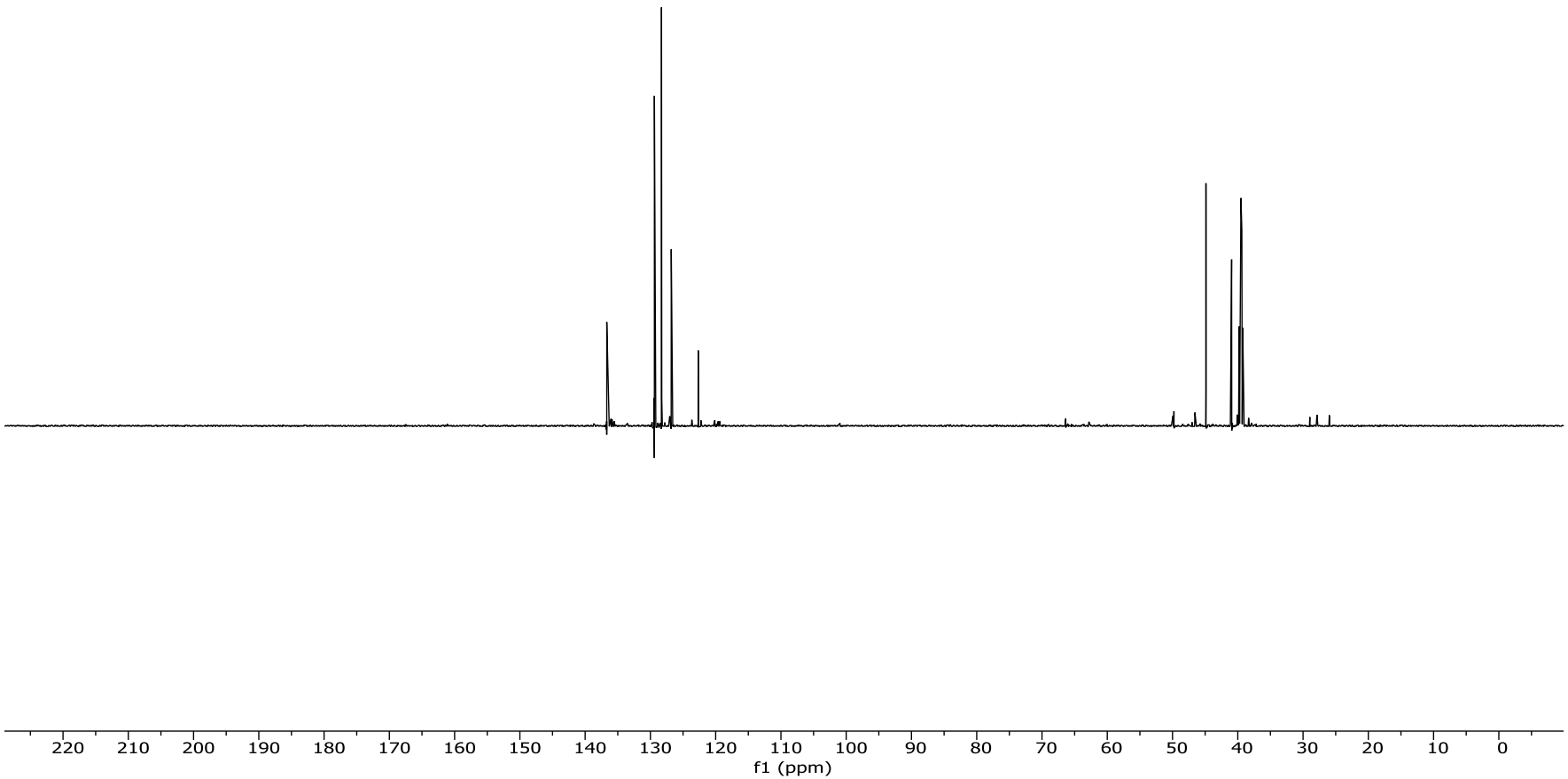

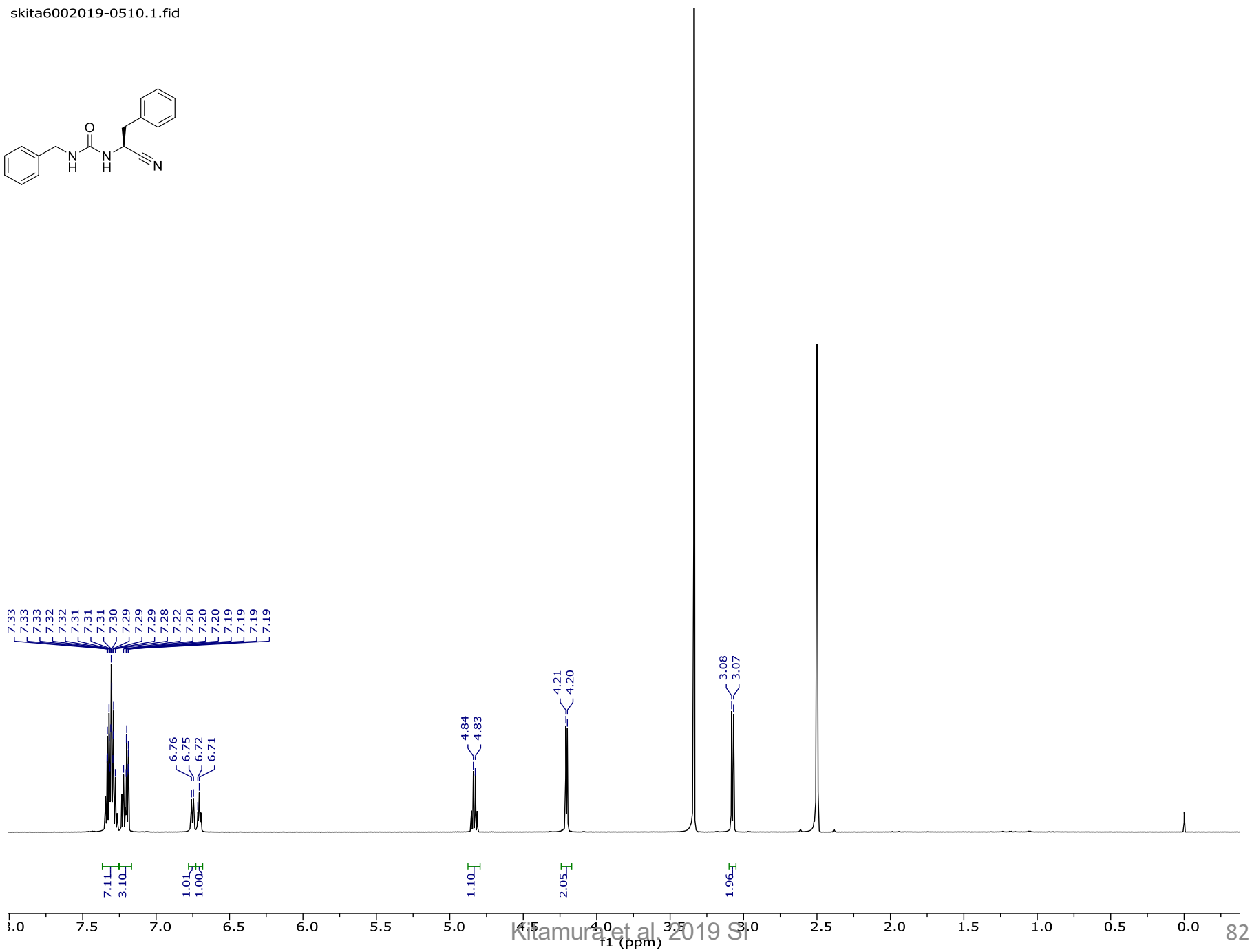
skita6002019-0510.1.fid
O
N
H
N
H
N
7.33
7.33
7.33
7.32
7.32
7.31
7.31
7.31
7.30
7.29
7.29
7.29
7.28
7.22
7.20
7.20
7.20
7.19
7.19
7.19
7.19
6.76
6.75
6.72
6.71
4.84
4.83
4.21
4.20
3.08
3.07
7.11
3.10
1.01
1.00
1.10
2.05
1.96
8.0
7.5
7.0
6.5
6.0
5.5
5.0
4.5
4.0
3.5
3.0
2.5
2.0
1.5
1.0
0.5
0.0
f1 (ppm)

skita6002019-0510.10.fid

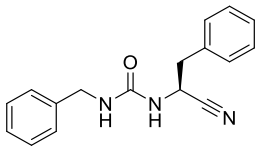

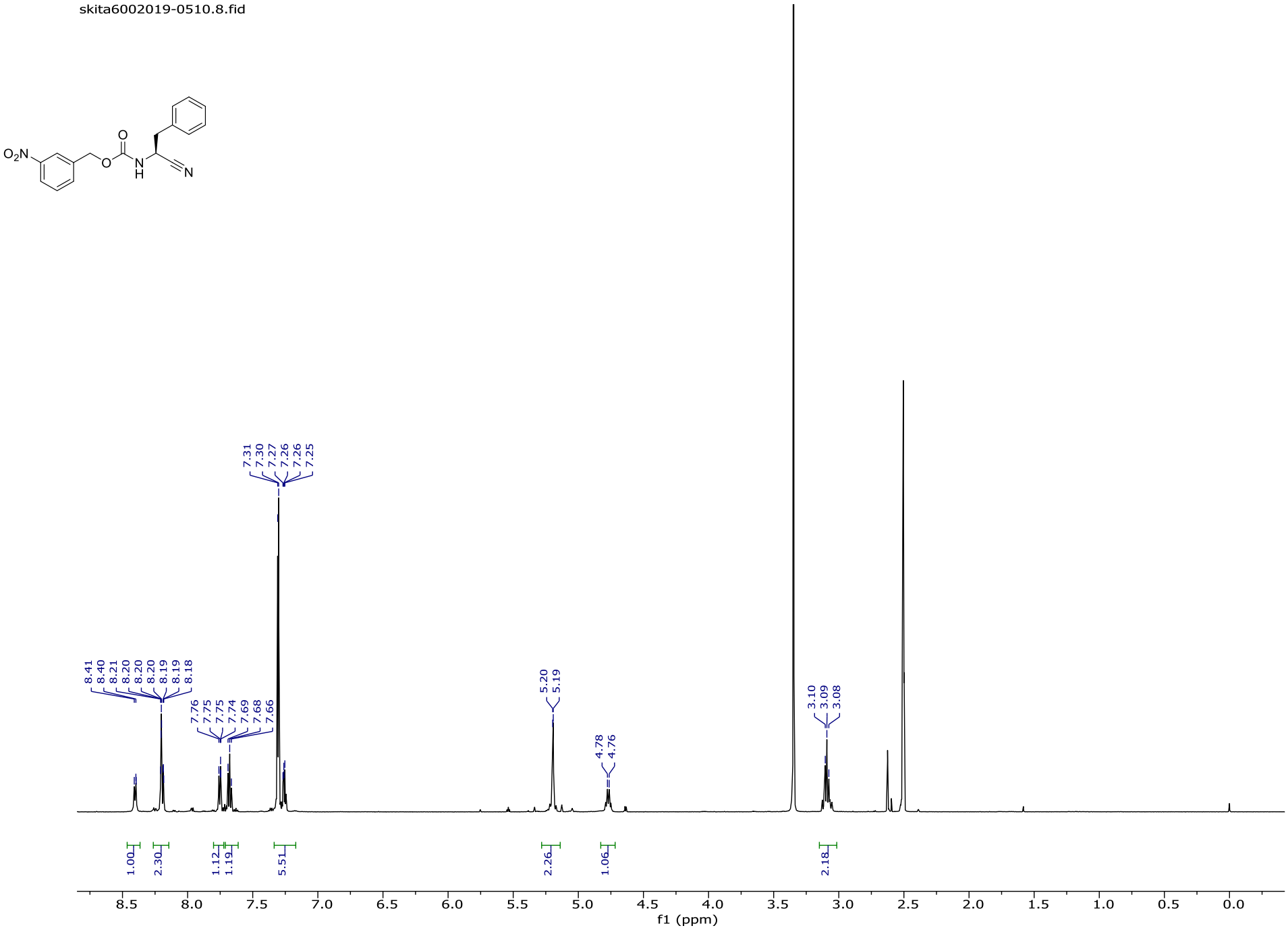
skita6002019-0510.8.fid
O2N
O
O
N
H
N
8.41
8.40
8.21
8.20
8.20
8.20
8.19
8.19
8.18
7.76
7.75
7.75
7.74
7.69
7.68
7.66
7.31
7.30
7.27
7.26
7.26
7.25
5.20
5.19
4.78
4.76
3.10
3.09
3.08
1.00
2.30
1.12
1.19
5.51
2.26
1.06
2.18
8.5
8.0
7.5
7.0
6.5
6.0
5.5
5.0
4.5
4.0
3.5
3.0
2.5
2.0
1.5
1.0
0.5
0.0
f1 (ppm)

skita6002019-0510.80.fid

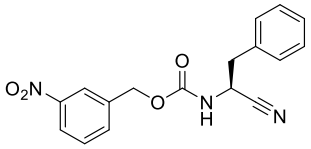

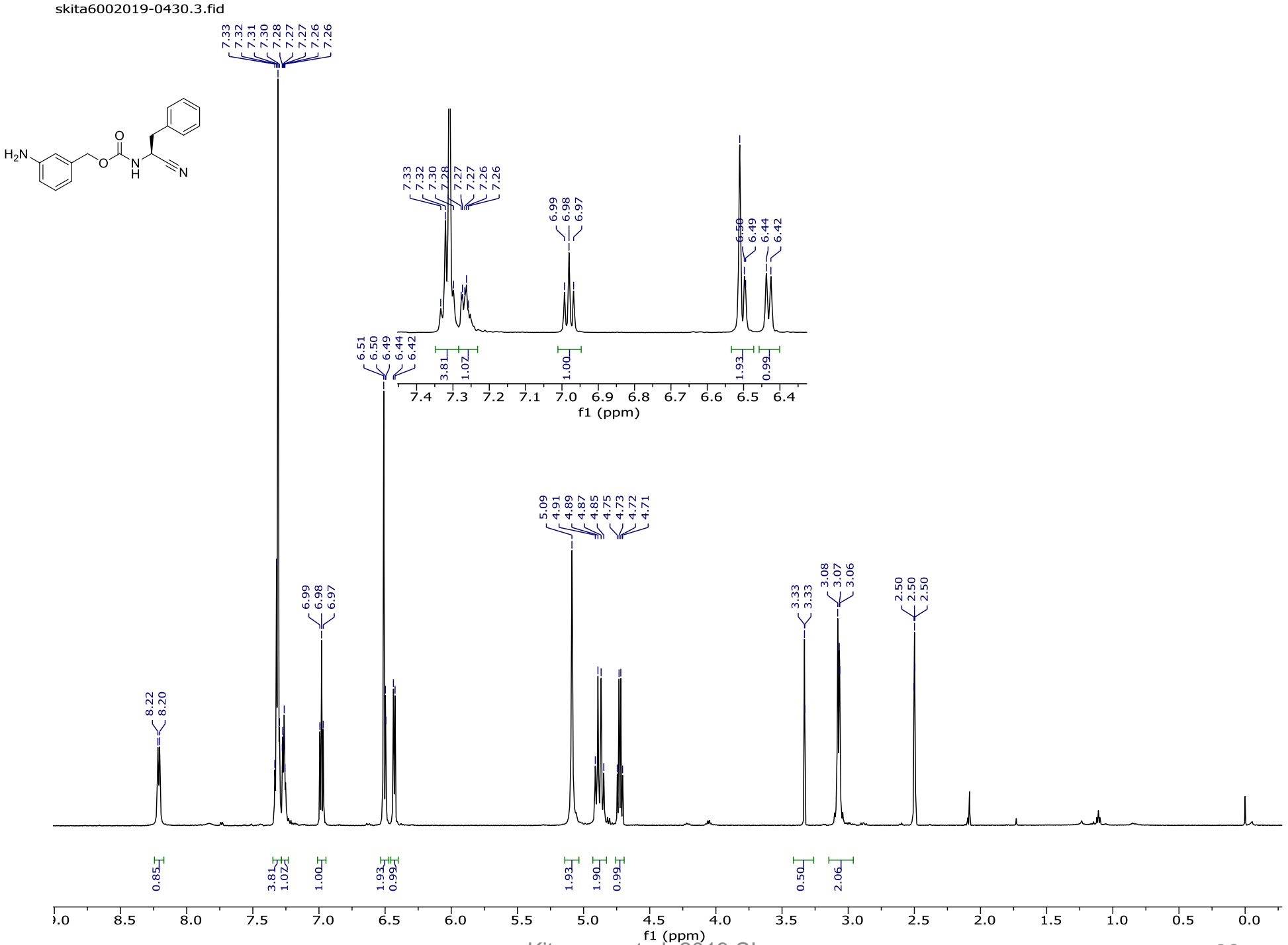
skita6002019-0430.3.fid
f1 (ppm)

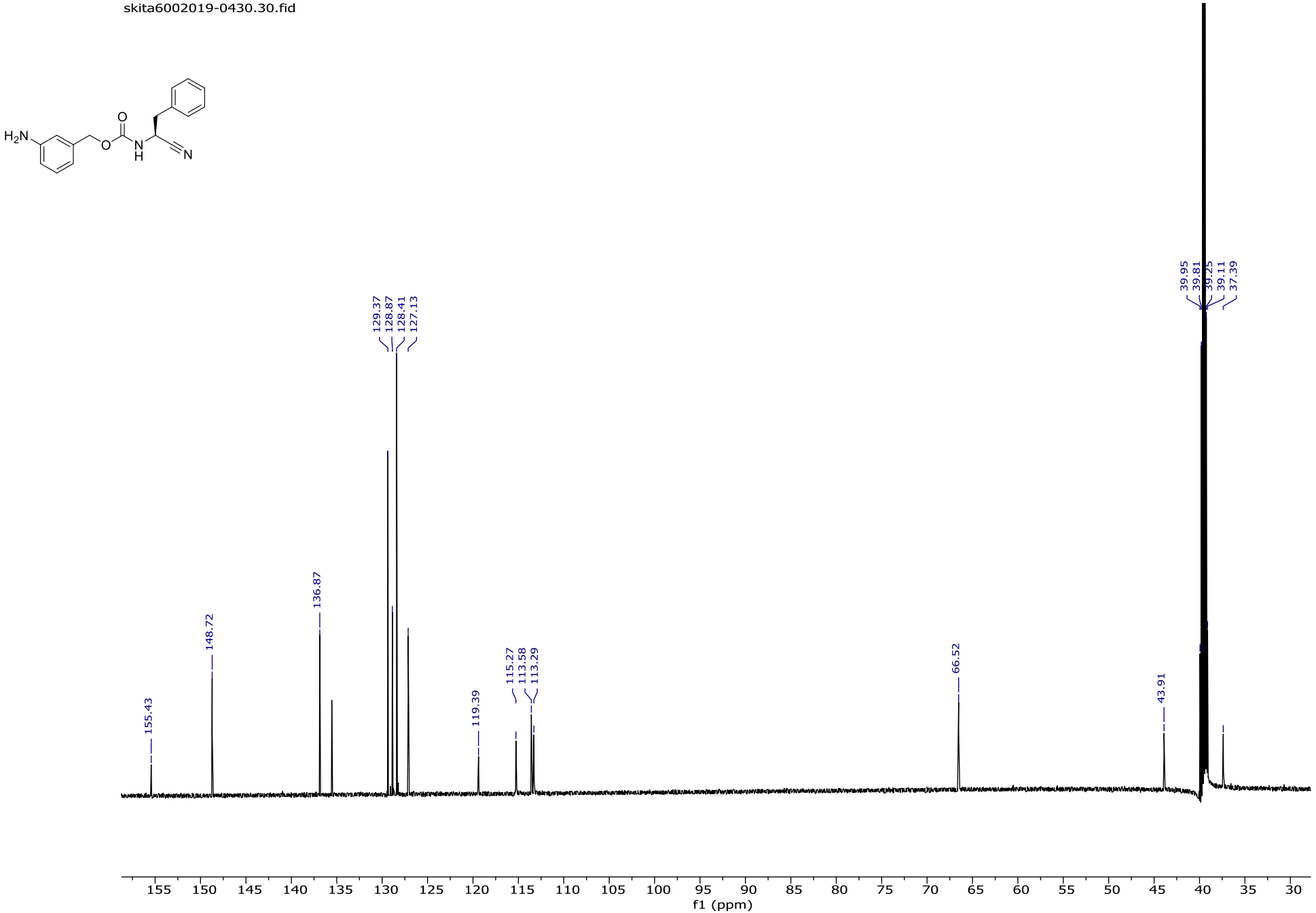
skita6002019-0430.30.fid
H2N
O
O
N
H
N
155.43
148.72
136.87
129.37
128.87
128.41
127.13
119.39
115.27
113.58
113.29
66.52
43.91
39.95
39.81
39.25
39.11
37.39
155 150 145 140 135 130 125 120 115 110 105 100 95 90 85 80 75 70 65 60 55 50 45 40 35 30
f1 (ppm)

skita600C20191107.1.fid —

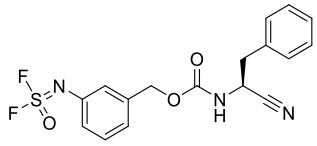

skita600C20191107.1.fid —

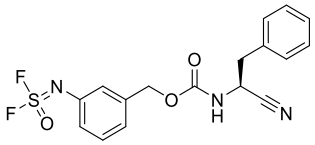

skita60020191023-1.1.fid

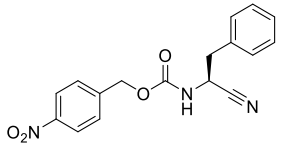

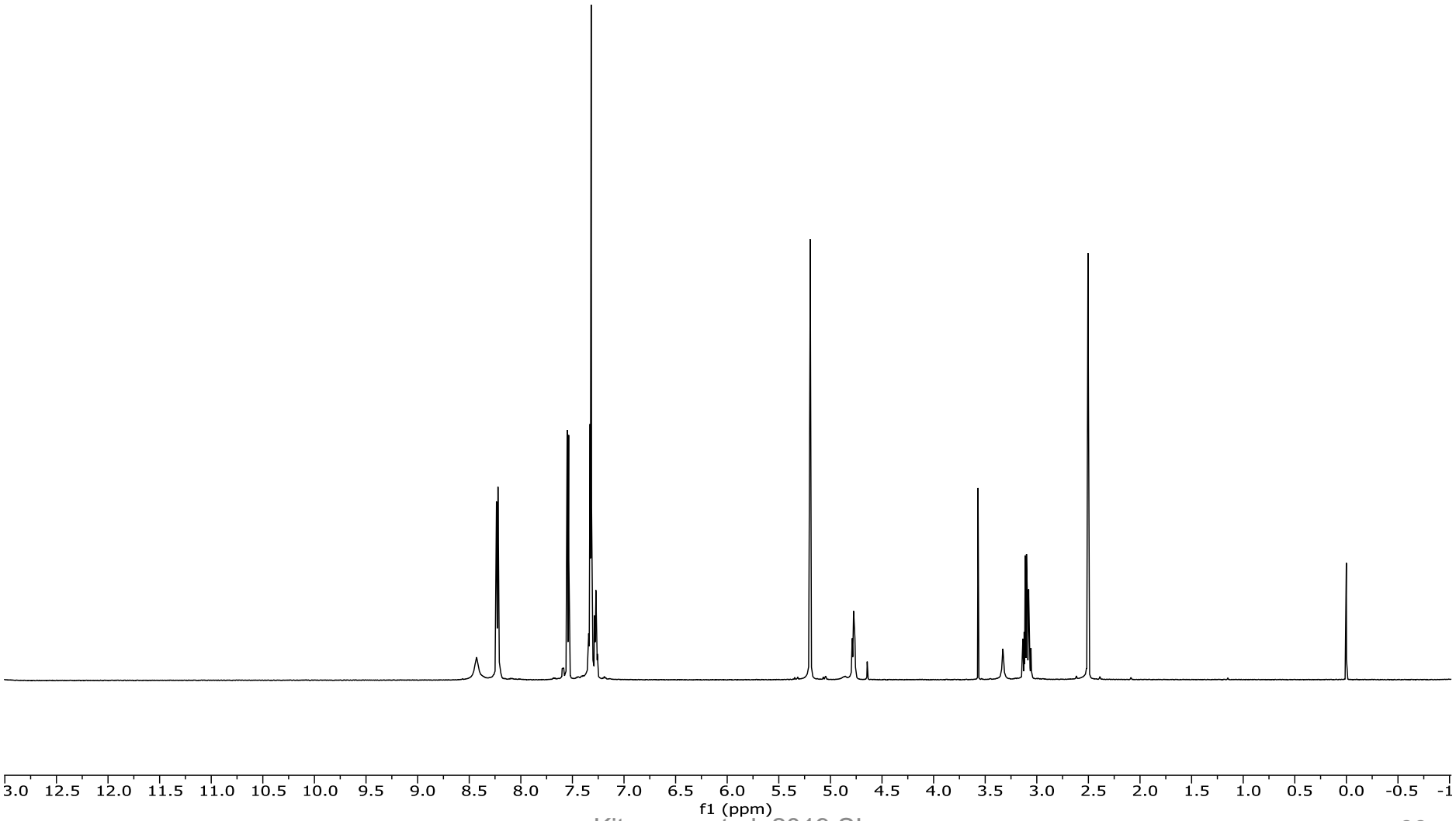

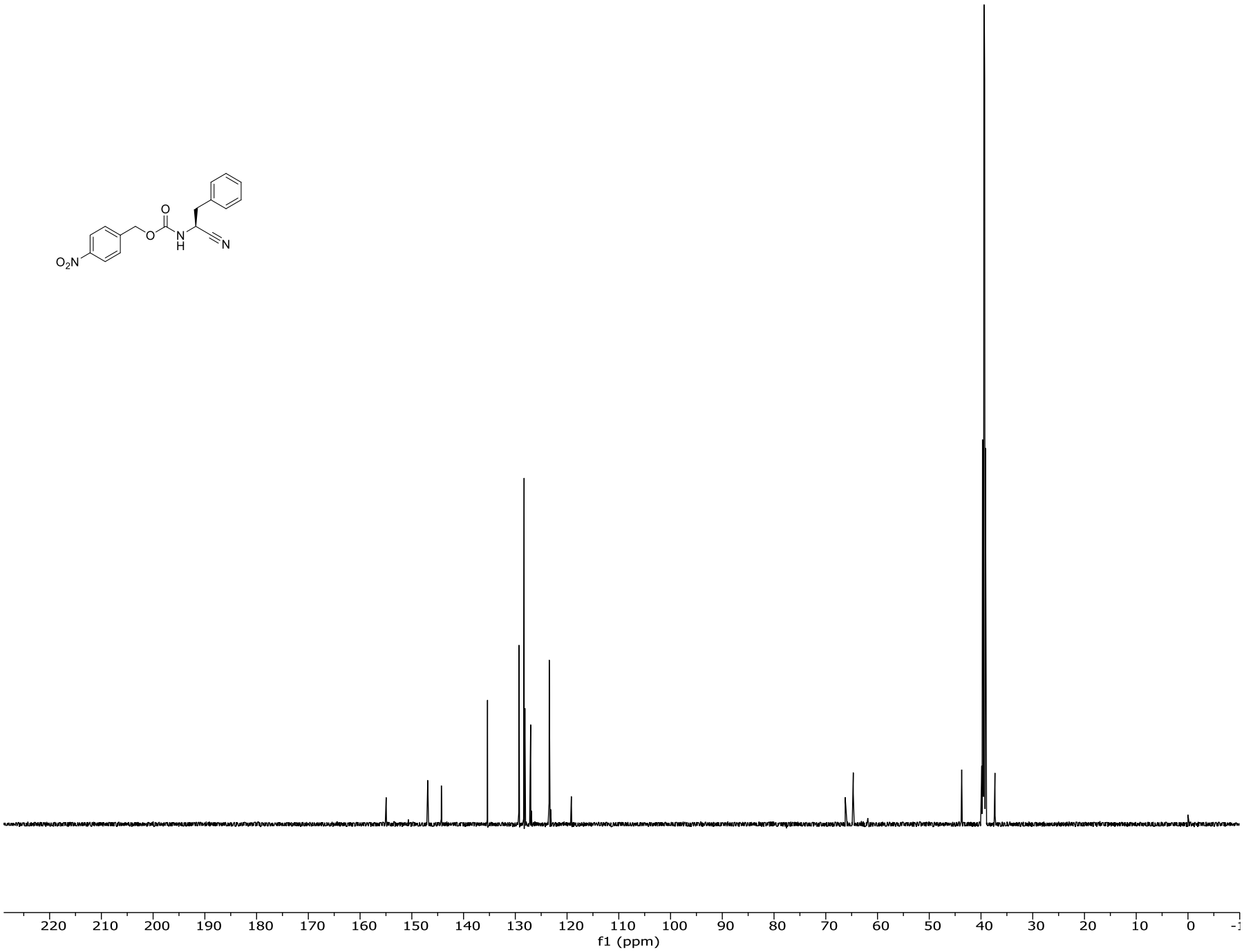
O
O
N
H
N
O_2N
220
210
200
190
180
170
160
150
140
130
120
110
100
90
80
70
60
50
40
30
20
10
0
f1 (ppm)

skita6002019-0510.4.fid

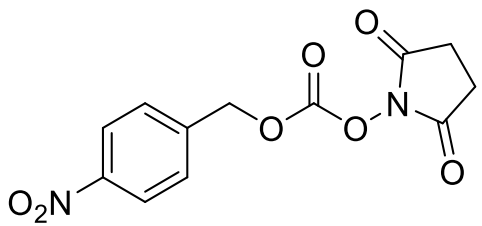

skita6002019-0510.40.fid

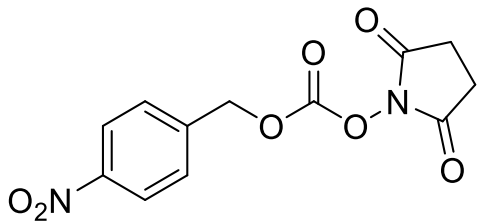

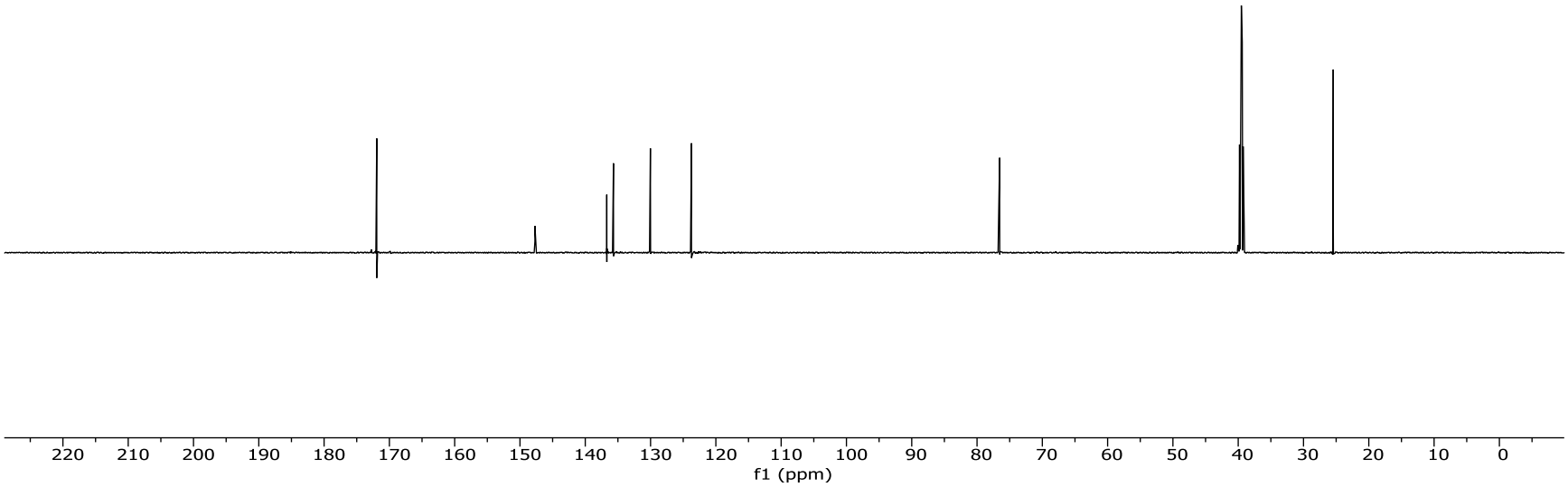

Supplementary Data LC-CAD trace of the SuFEx reaction

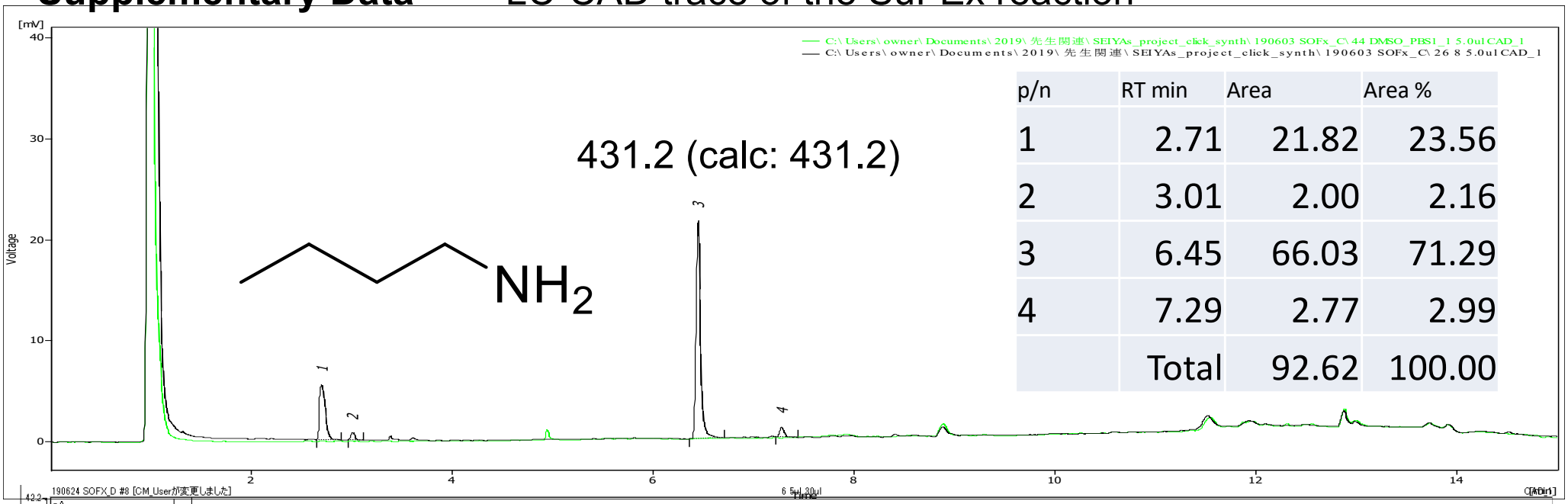

p/n	RT min	Area	Area %
1	2.71	21.82	23.56
2	3.01	2.00	2.16
3	6.45	66.03	71.29
4	7.29	2.77	2.99
	Total	92.62	100.00

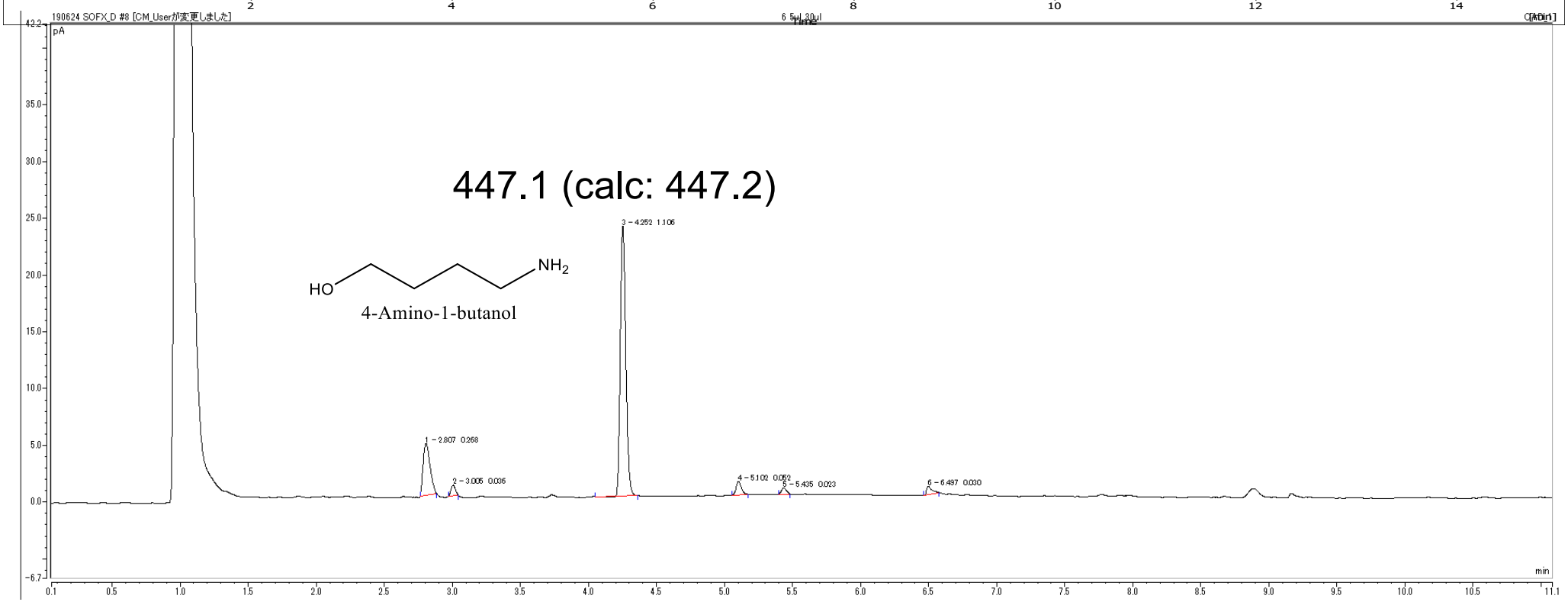

Supplementary Data LC-CAD trace of the SuFEx reaction

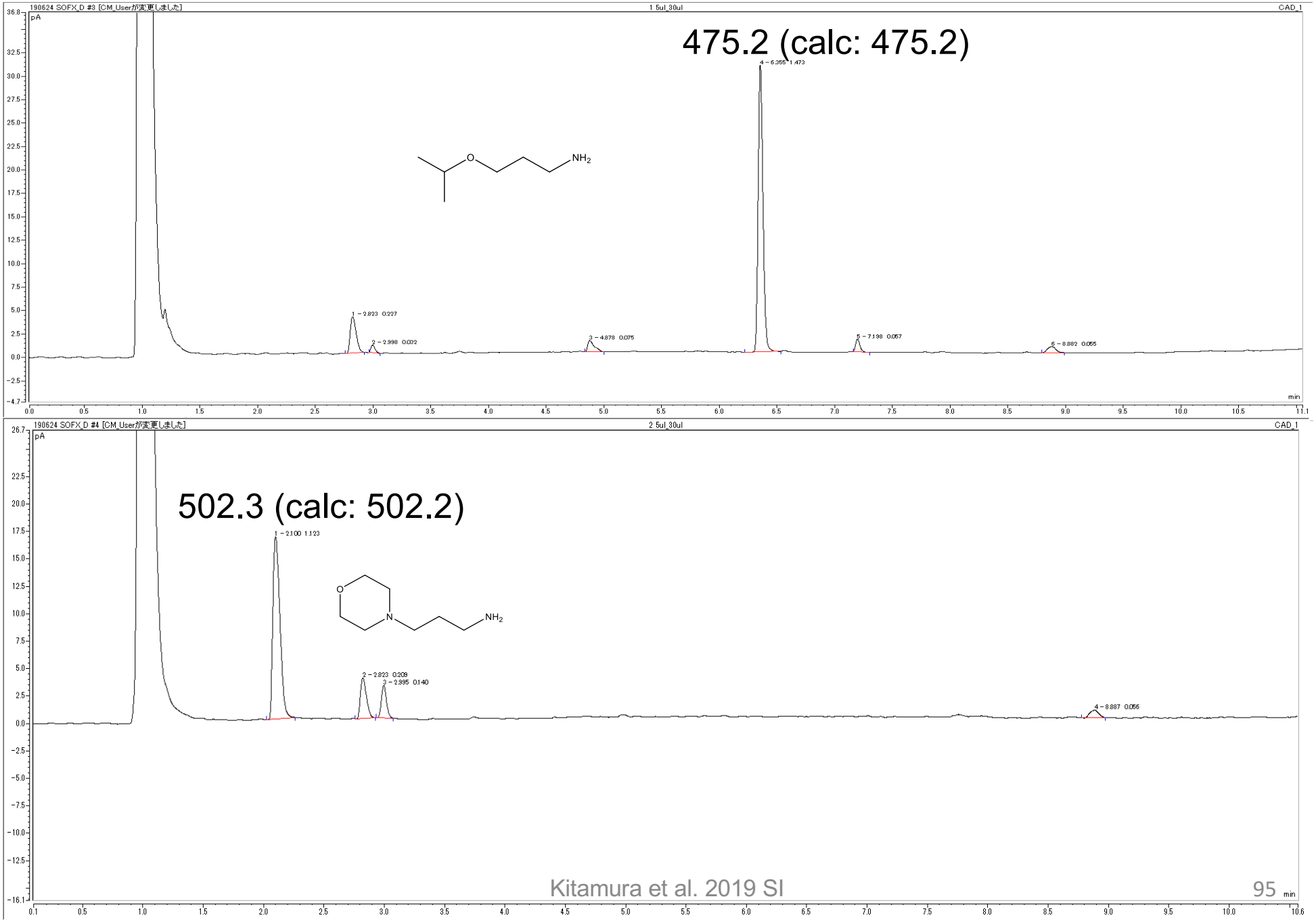

Supplementary Data LC-CAD trace of the SuFEx reaction

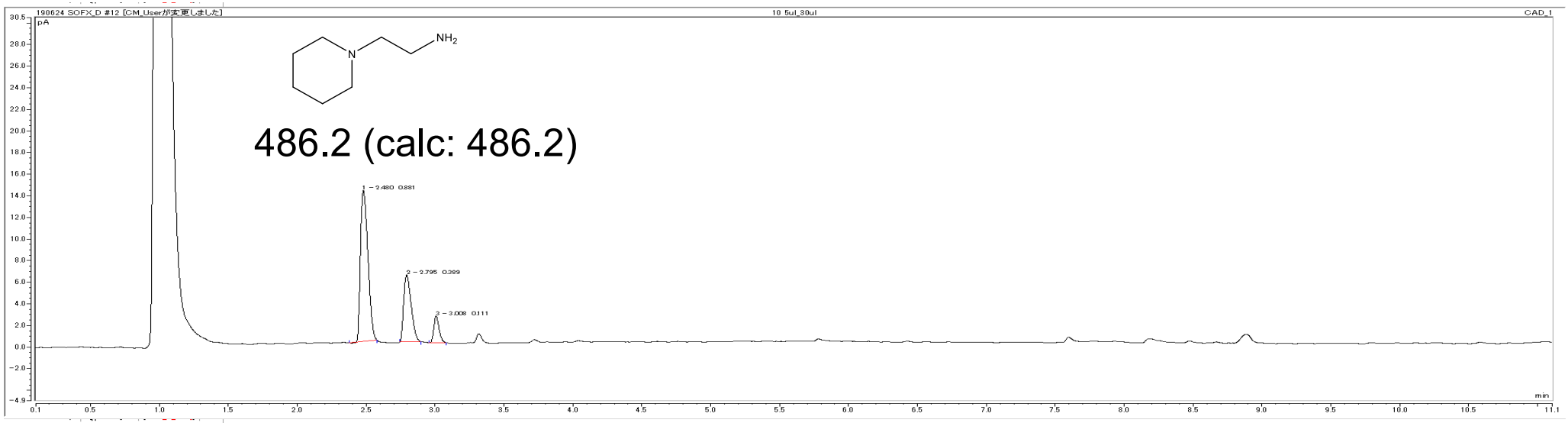

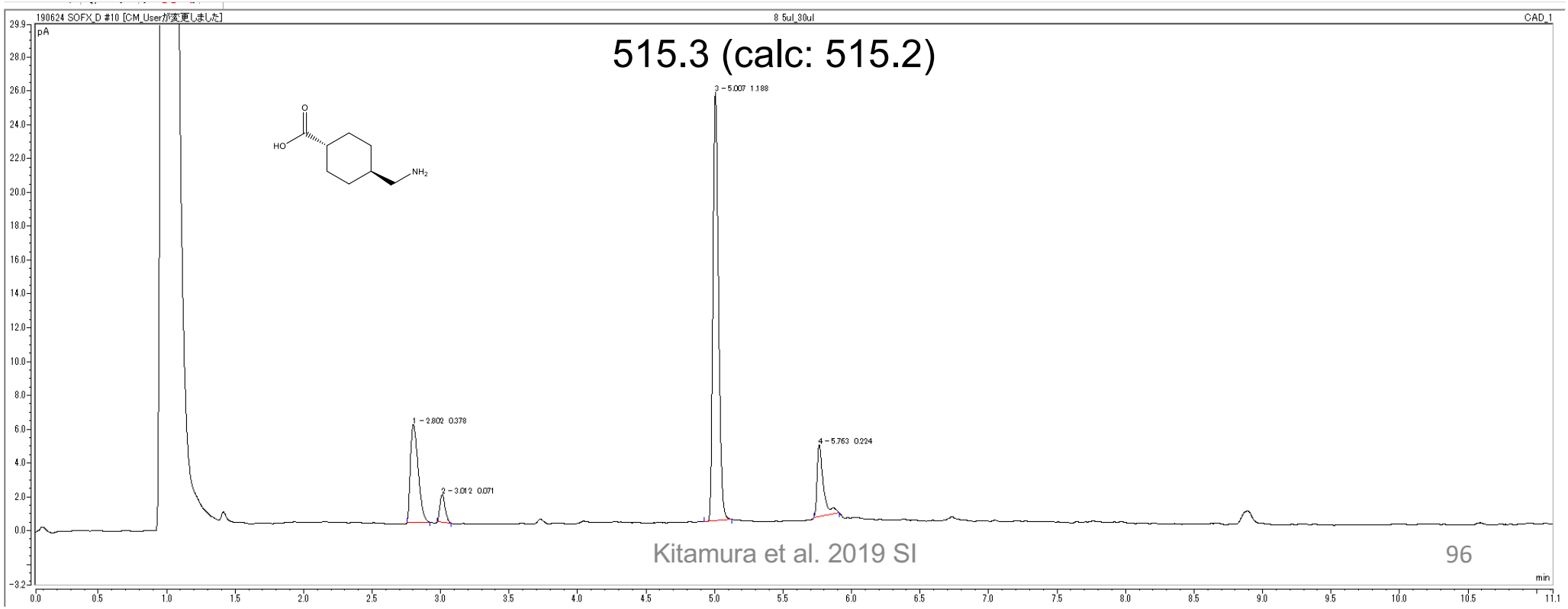

Supplementary Data LC-CAD trace of the SuFEx reaction

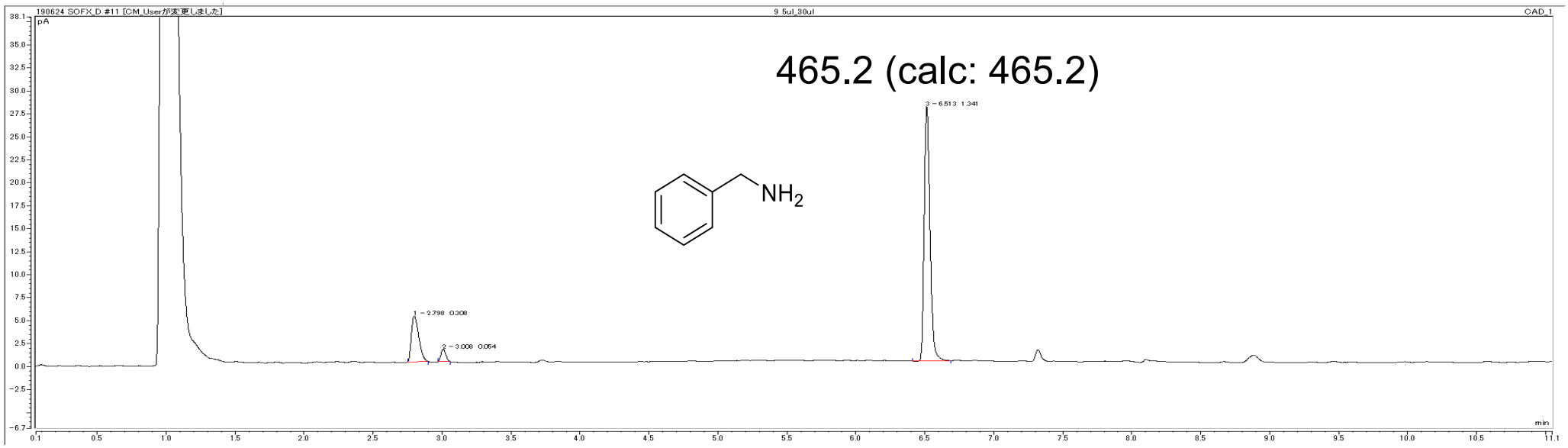

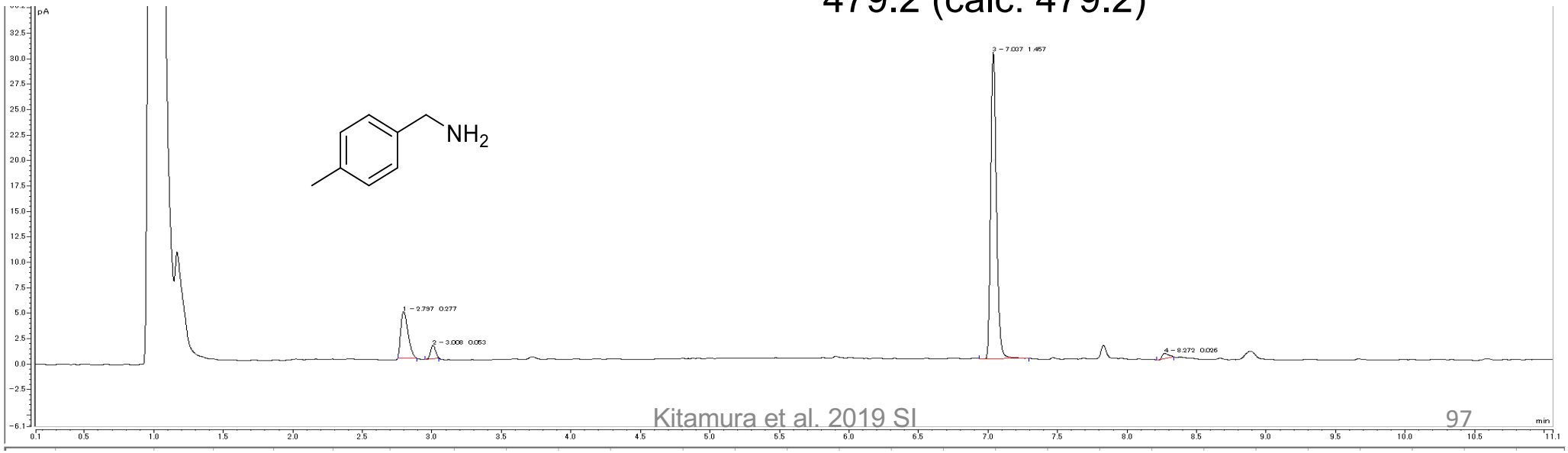

Supplementary Data LC-CAD trace of the SuFEx reaction

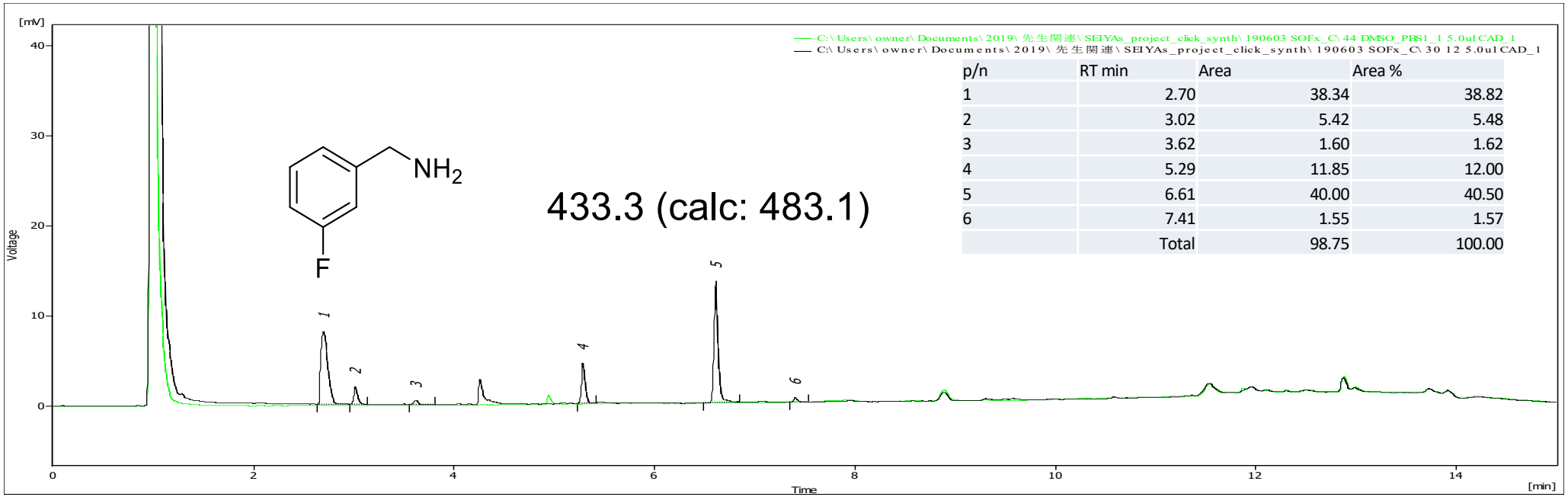

p/n	RT min	Area	Area %
1	2.70	38.34	38.82
2	3.02	5.42	5.48
3	3.62	1.60	1.62
4	5.29	11.85	12.00
5	6.61	40.00	40.50
6	7.41	1.55	1.57
	Total	98.75	100.00

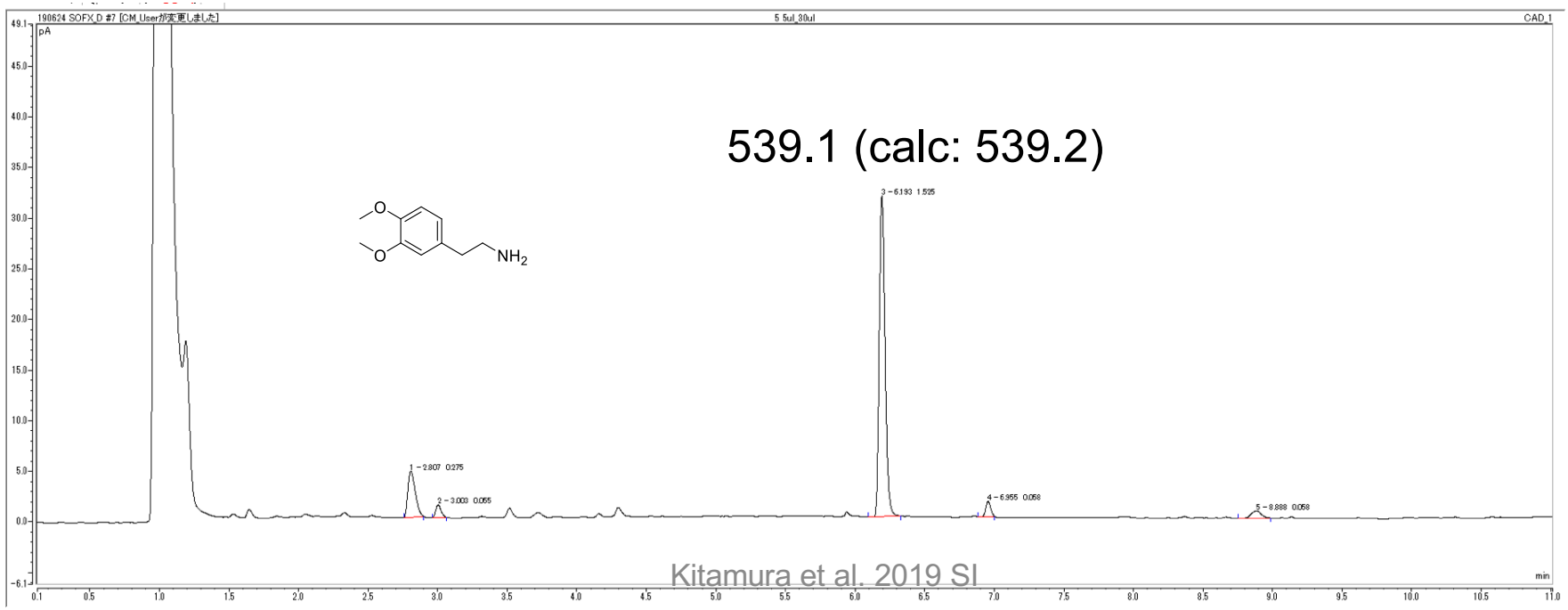

Supplementary Data LC-CAD trace of the SuFEx reaction

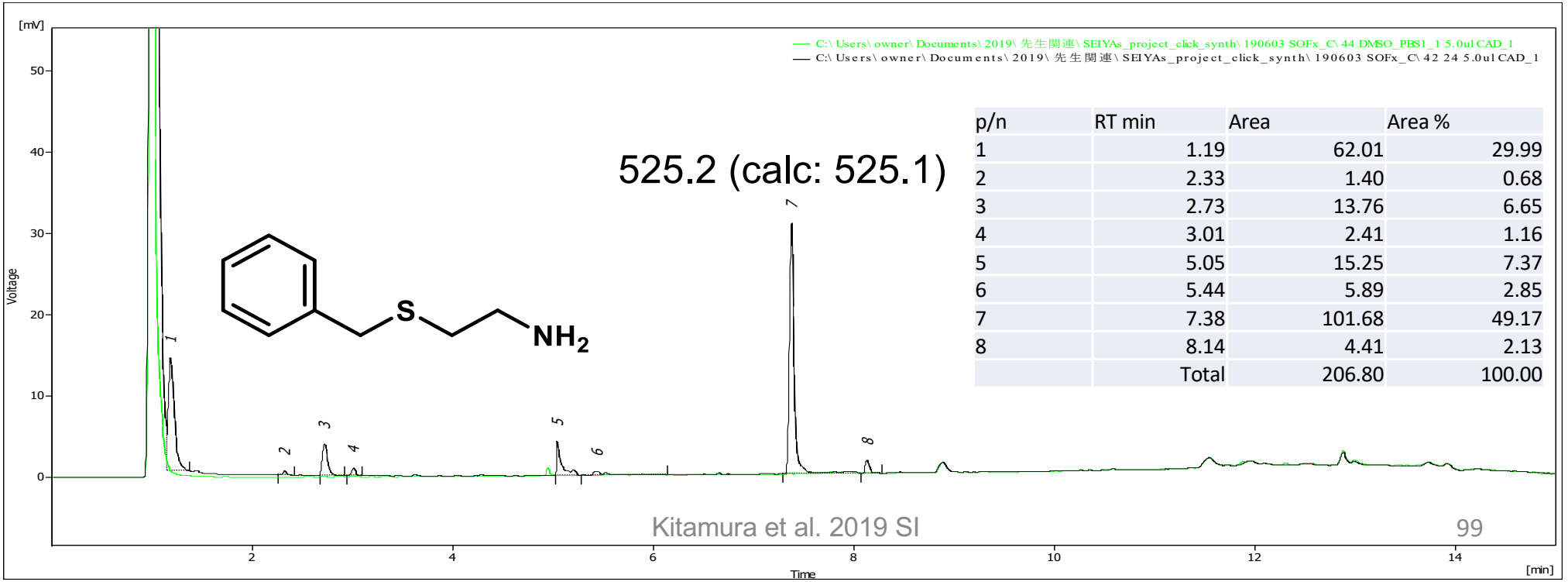

p/n	RT min	Area	Area %
1	1.19	62.01	29.99
2	2.33	1.40	0.68
3	2.73	13.76	6.65
4	3.01	2.41	1.16
5	5.05	15.25	7.37
6	5.44	5.89	2.85
7	7.38	101.68	49.17
8	8.14	4.41	2.13
	Total	206.80	100.00

Supplementary Data LC-CAD trace of the SuFEx reaction

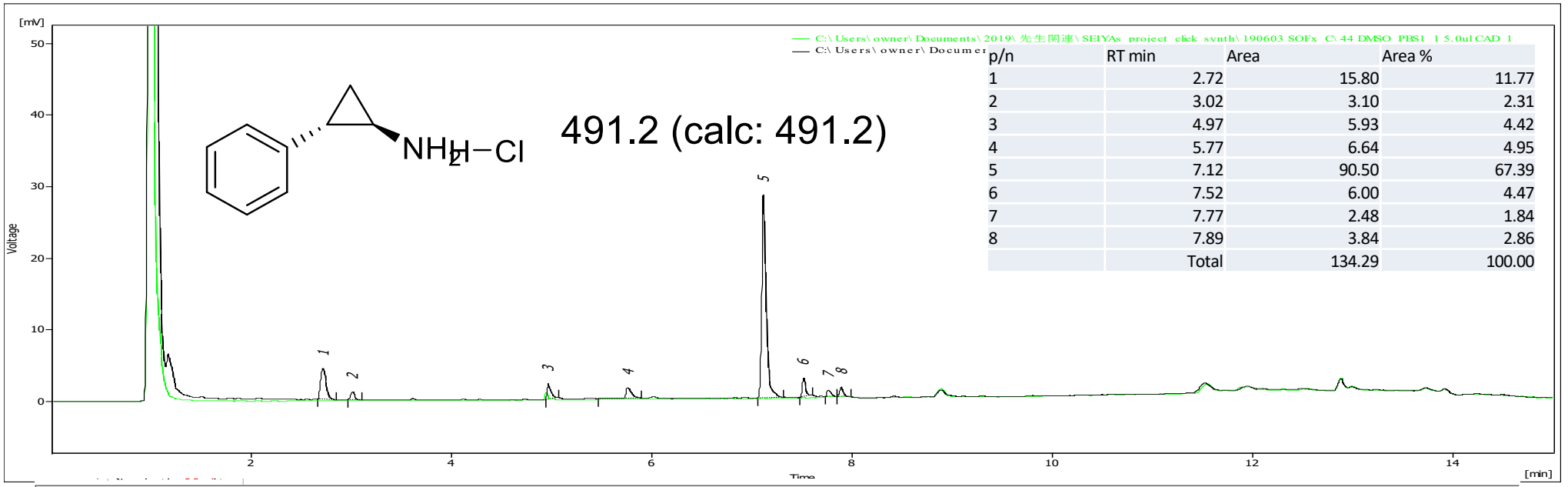

p/n	RT min	Area	Area %
1	2.72	15.80	11.77
2	3.02	3.10	2.31
3	4.97	5.93	4.42
4	5.77	6.64	4.95
5	7.12	90.50	67.39
6	7.52	6.00	4.47
7	7.77	2.48	1.84
8	7.89	3.84	2.86
	Total	134.29	100.00

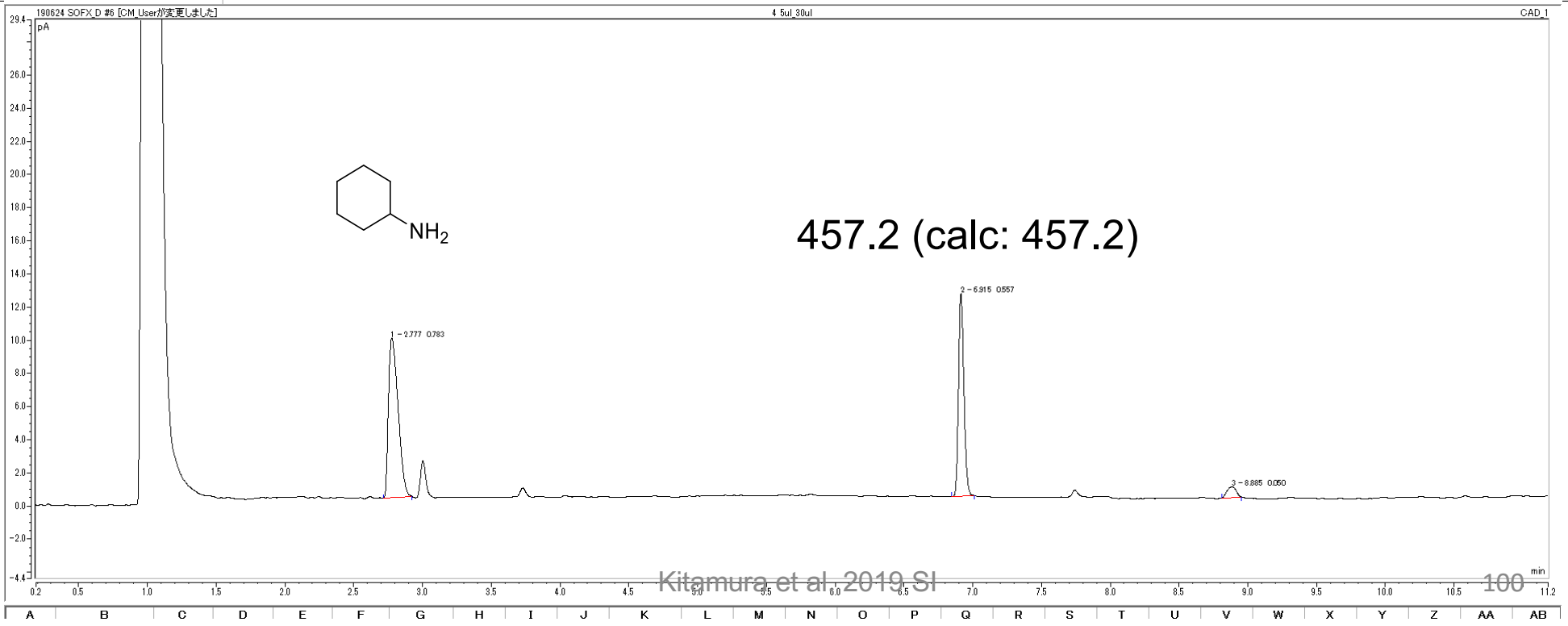

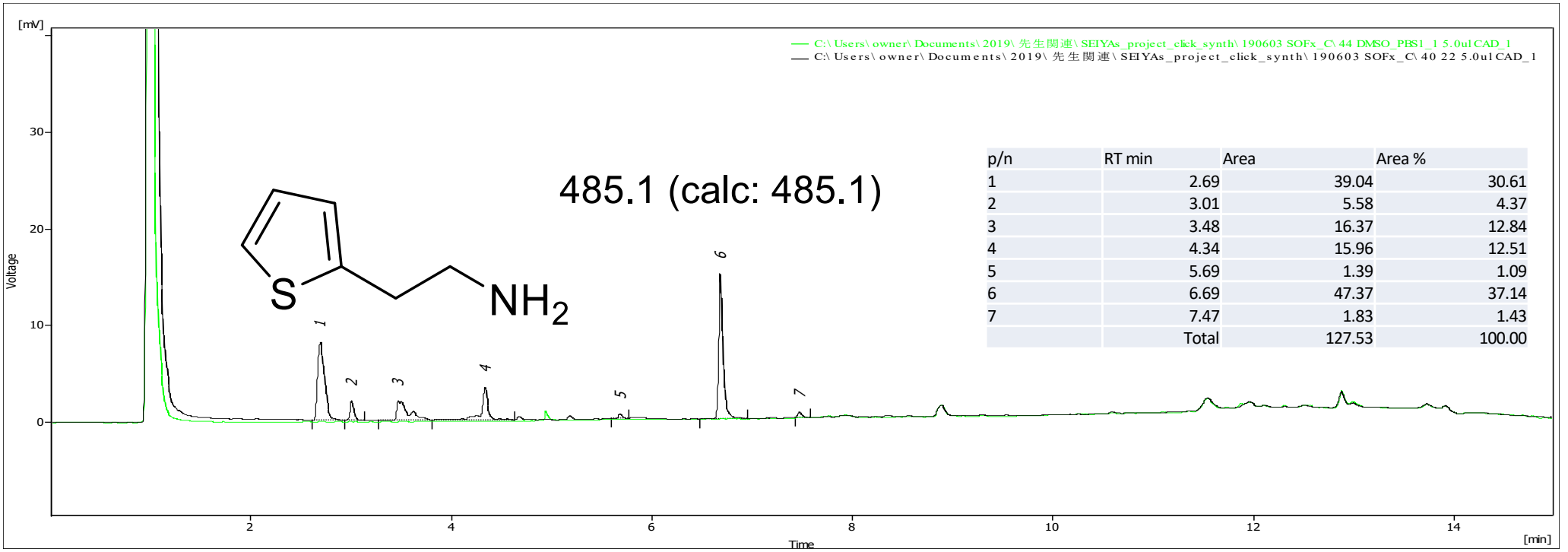

p/n	RT min	Area	Area %
1	2.69	39.04	30.61
2	3.01	5.58	4.37
3	3.48	16.37	12.84
4	4.34	15.96	12.51
5	5.69	1.39	1.09
6	6.69	47.37	37.14
7	7.47	1.83	1.43
	Total	127.53	100.00

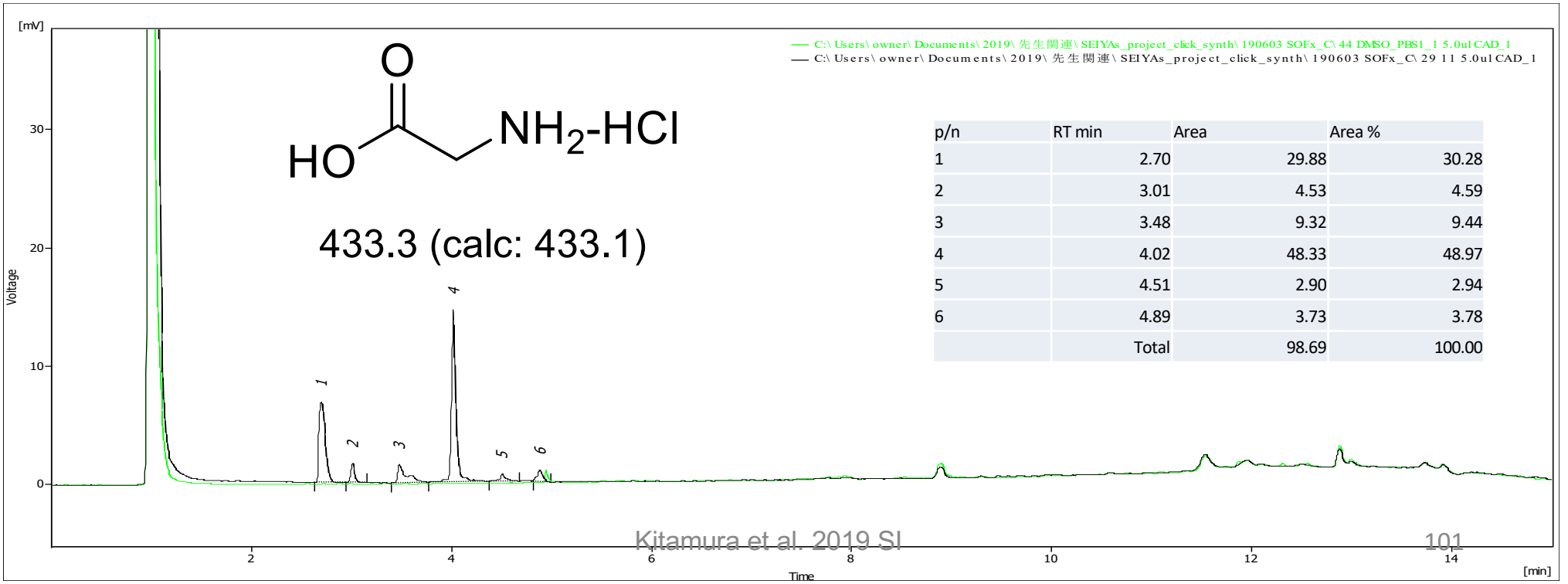

p/n	RT min	Area	Area %
1	2.70	29.88	30.28
2	3.01	4.53	4.59
3	3.48	9.32	9.44
4	4.02	48.33	48.97
5	4.51	2.90	2.94
6	4.89	3.73	3.78
	Total	98.69	100.00

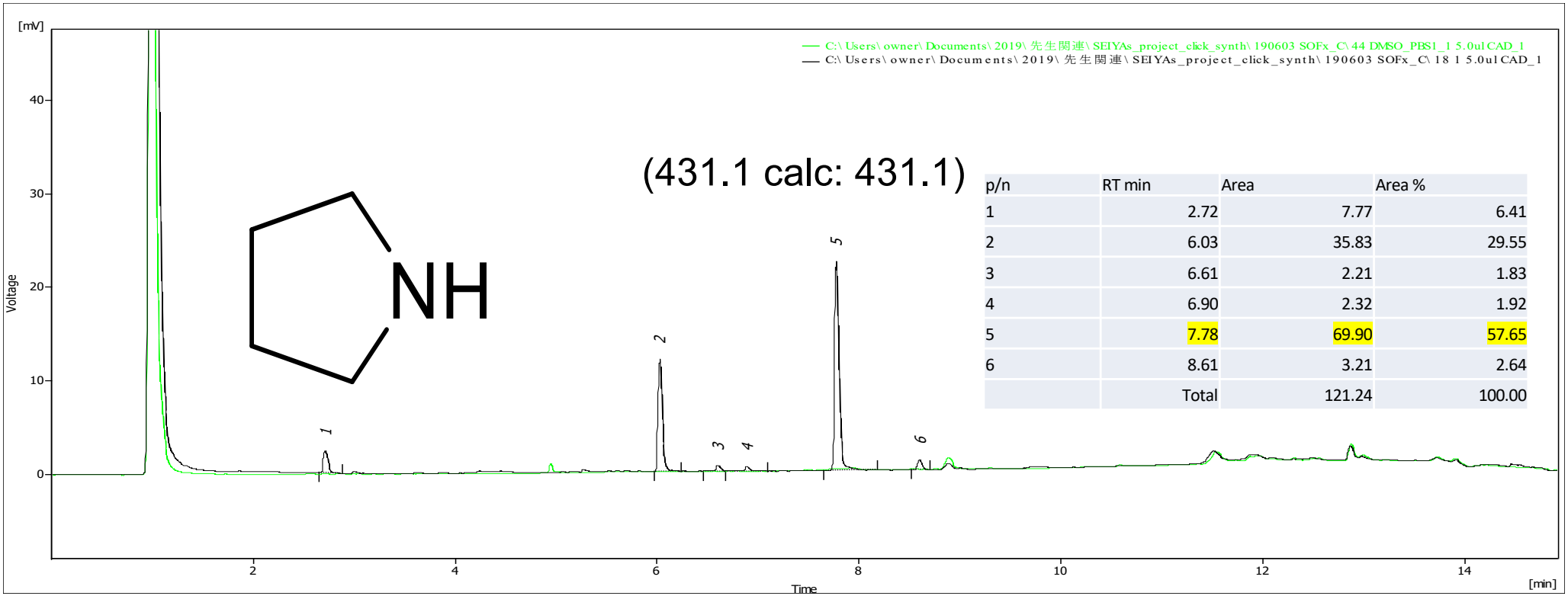

p/n	RT min	Area	Area %
1	2.72	7.77	6.41
2	6.03	35.83	29.55
3	6.61	2.21	1.83
4	6.90	2.32	1.92
5	7.78	69.90	57.65
6	8.61	3.21	2.64
	Total	121.24	100.00

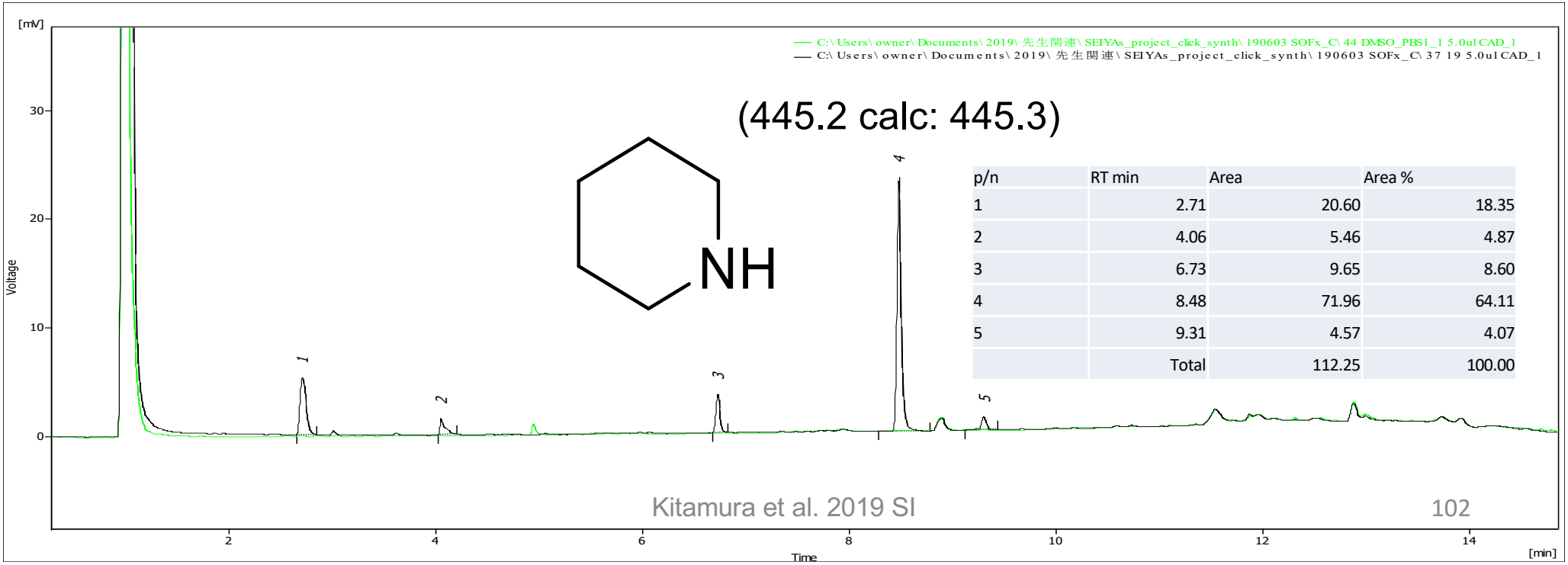

p/n	RT min	Area	Area %
1	2.71	20.60	18.35
2	4.06	5.46	4.87
3	6.73	9.65	8.60
4	8.48	71.96	64.11
5	9.31	4.57	4.07
	Total	112.25	100.00

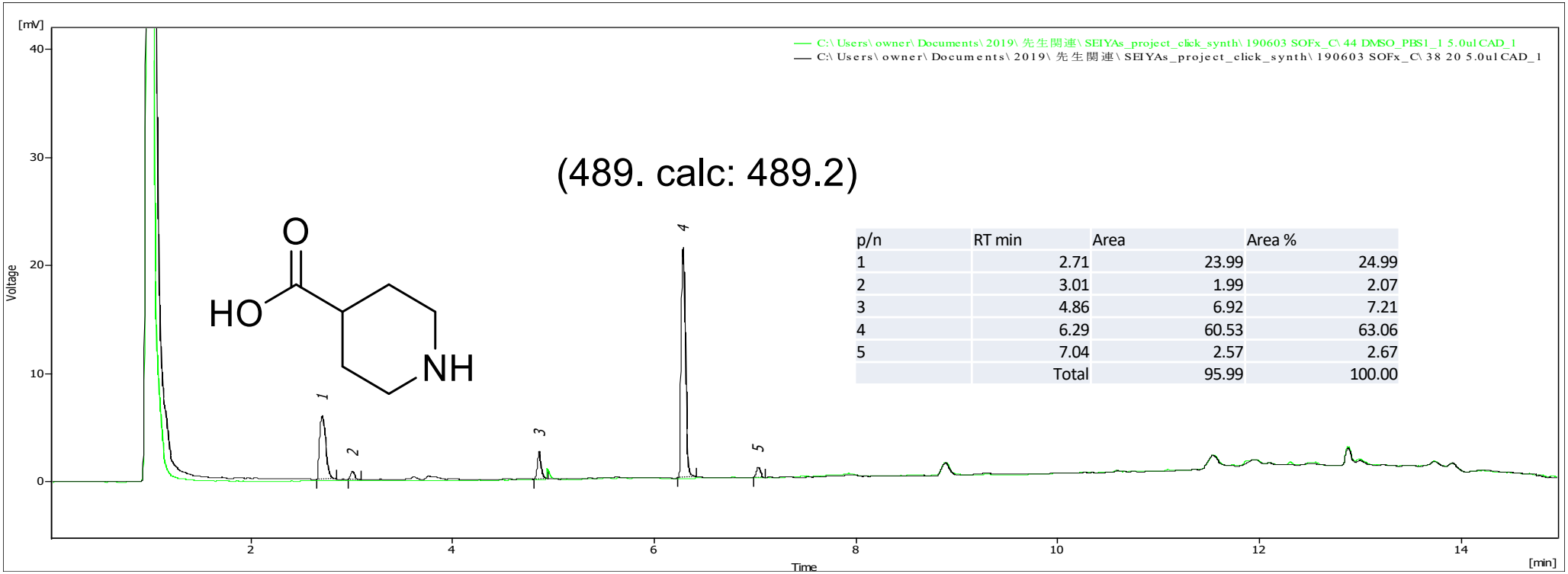

p/n	RT min	Area	Area %
1	2.71	23.99	24.99
2	3.01	1.99	2.07
3	4.86	6.92	7.21
4	6.29	60.53	63.06
5	7.04	2.57	2.67
	Total	95.99	100.00

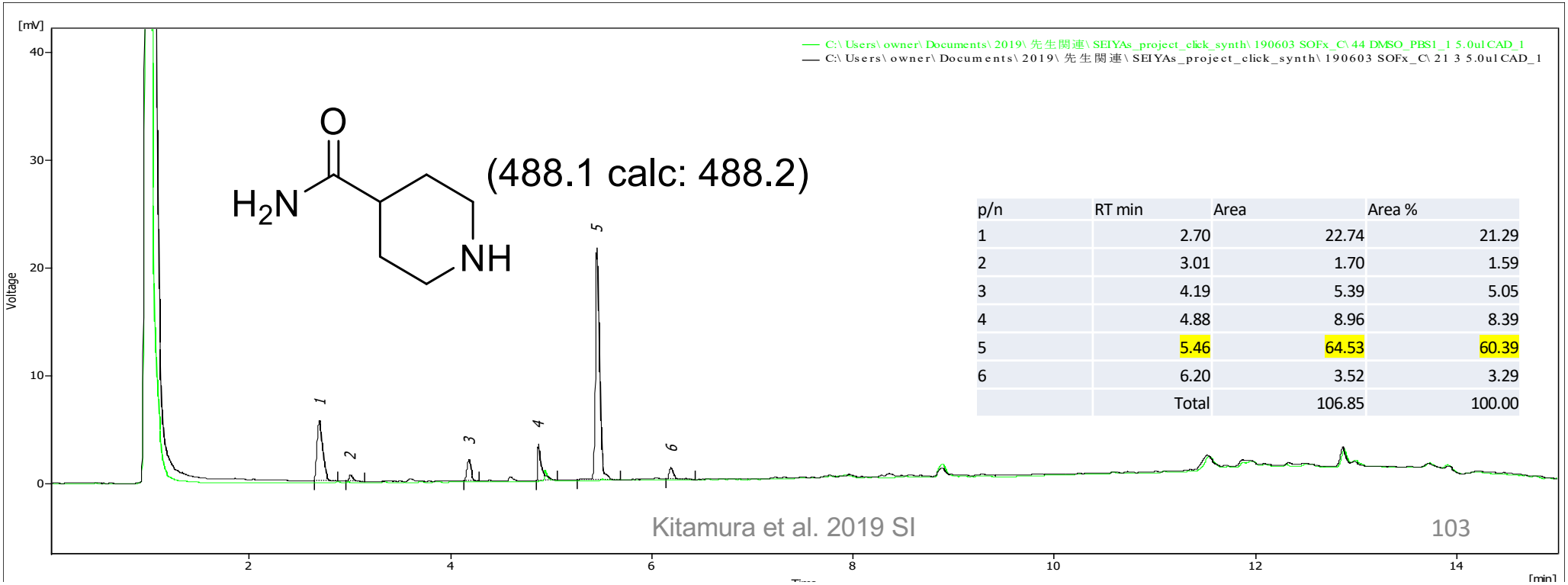

p/n	RT min	Area	Area %
1	2.70	22.74	21.29
2	3.01	1.70	1.59
3	4.19	5.39	5.05
4	4.88	8.96	8.39
5	5.46	64.53	60.39
6	6.20	3.52	3.29
	Total	106.85	100.00

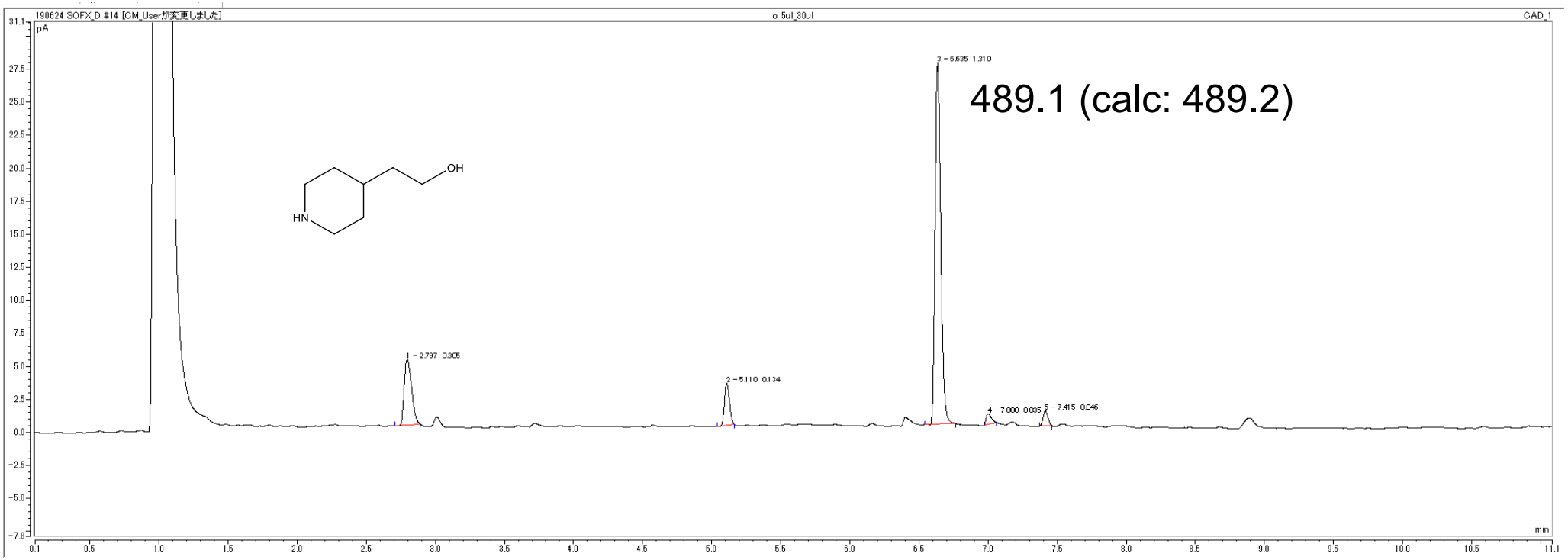

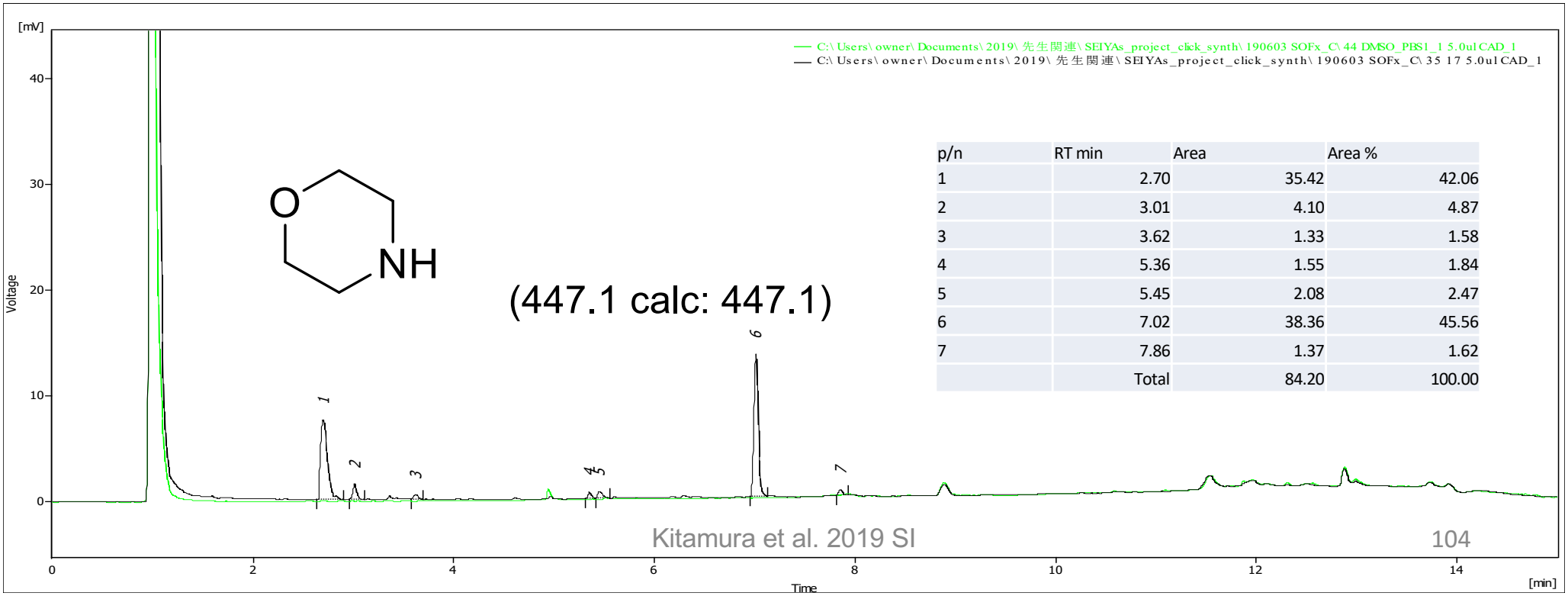

p/n	RT min	Area	Area %
1	2.70	35.42	42.06
2	3.01	4.10	4.87
3	3.62	1.33	1.58
4	5.36	1.55	1.84
5	5.45	2.08	2.47
6	7.02	38.36	45.56
7	7.86	1.37	1.62
	Total	84.20	100.00

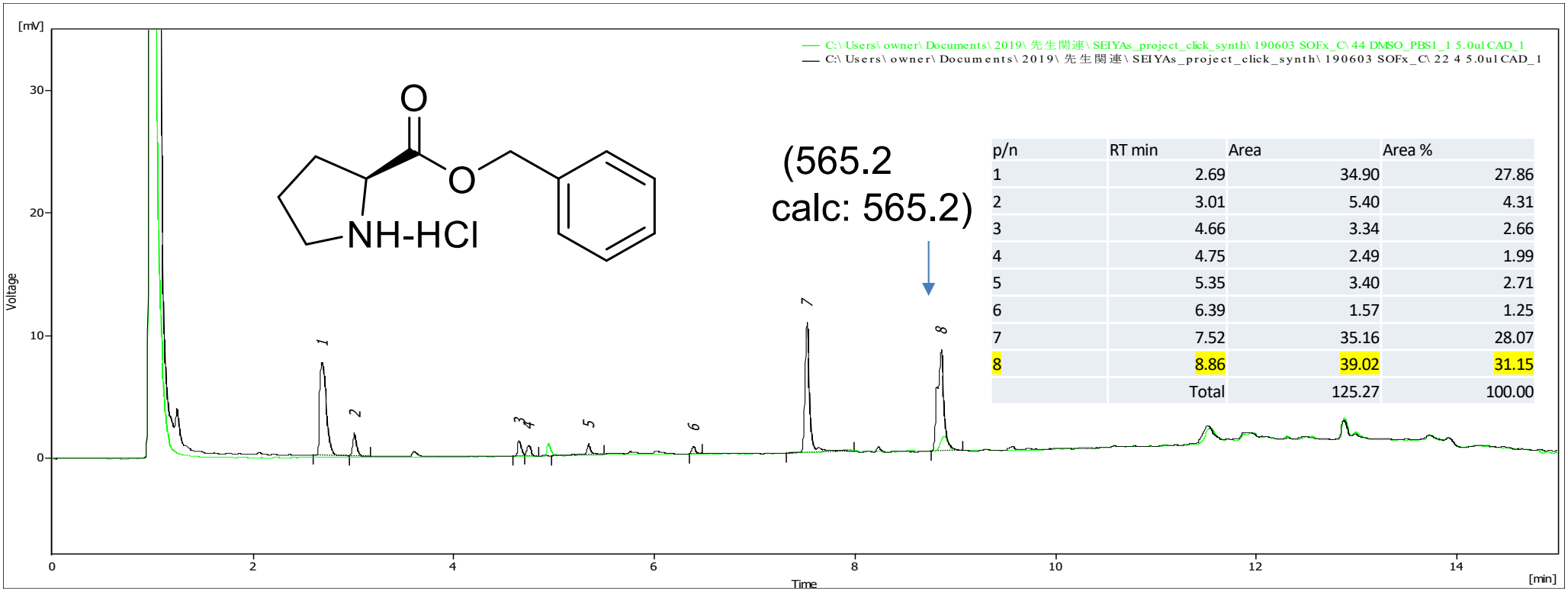

p/n	RT min	Area	Area %
1	2.69	34.90	27.86
2	3.01	5.40	4.31
3	4.66	3.34	2.66
4	4.75	2.49	1.99
5	5.35	3.40	2.71
6	6.39	1.57	1.25
7	7.52	35.16	28.07
8	8.86	39.02	31.15
	Total	125.27	100.00

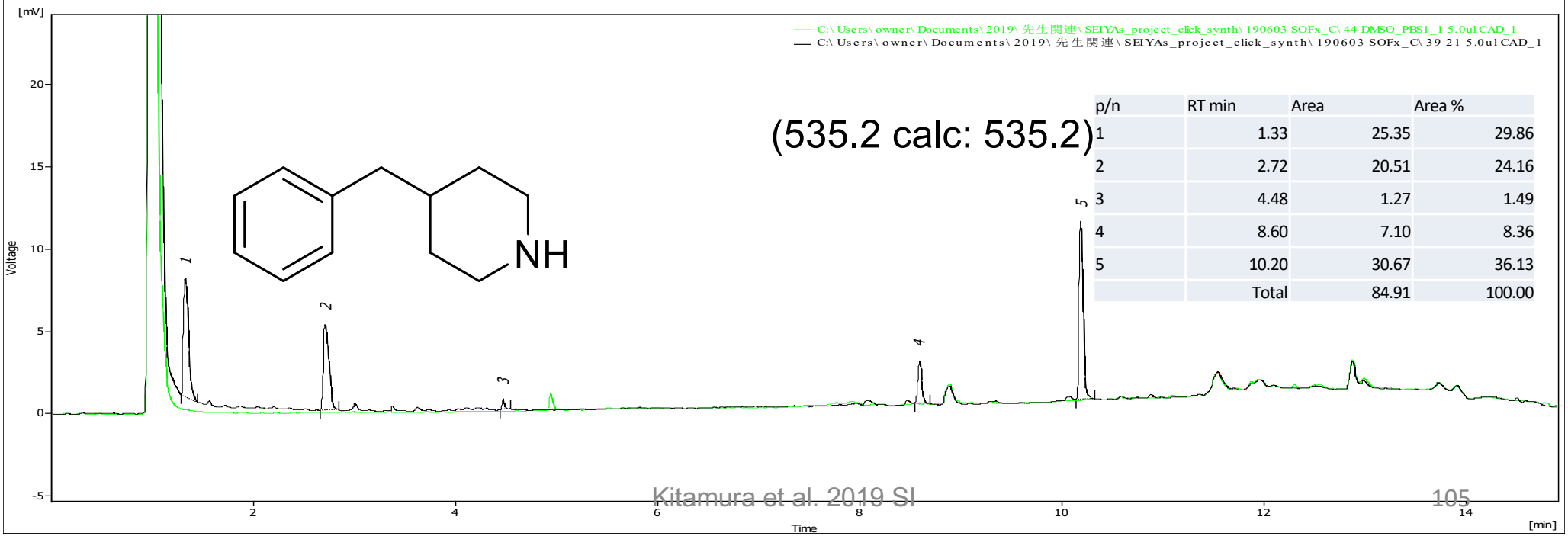

p/n	RT min	Area	Area %
1	1.33	25.35	29.86
2	2.72	20.51	24.16
3	4.48	1.27	1.49
4	8.60	7.10	8.36
5	10.20	30.67	36.13
	Total	84.91	100.00

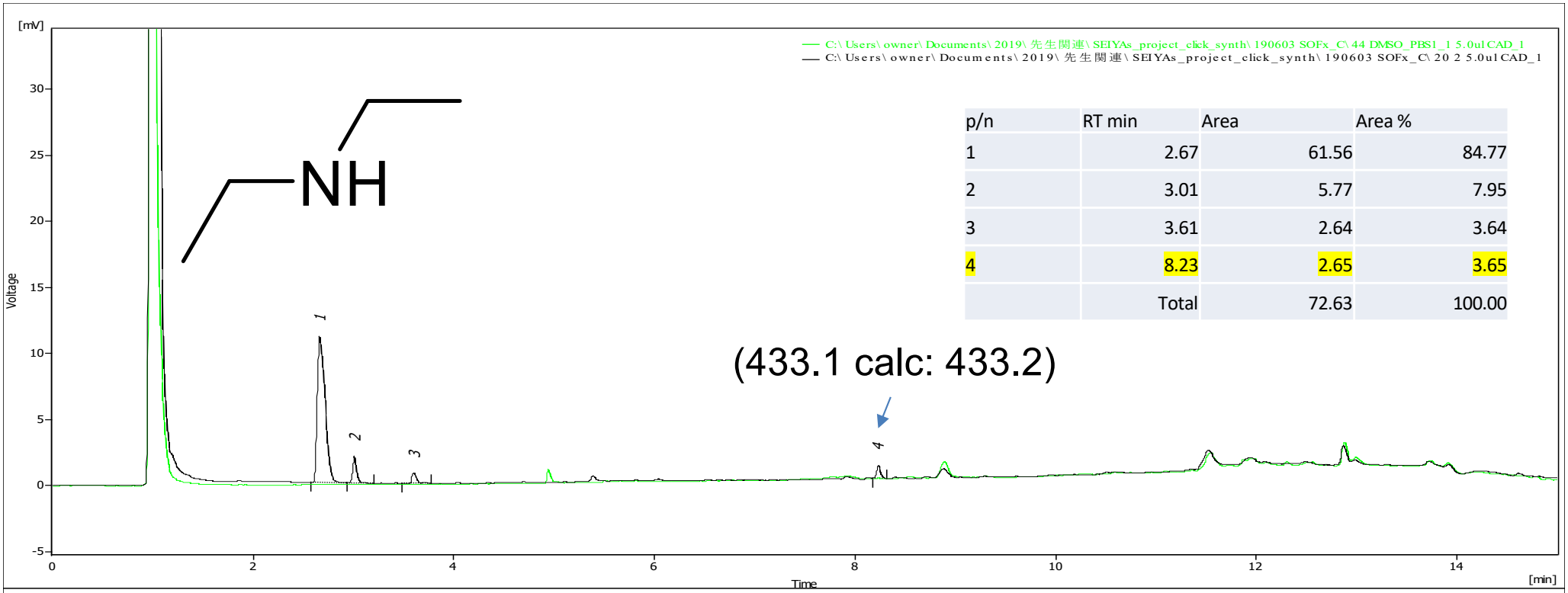

p/n	RT min	Area	Area %
1	2.67	61.56	84.77
2	3.01	5.77	7.95
3	3.61	2.64	3.64
4	8.23	2.65	3.65
	Total	72.63	100.00

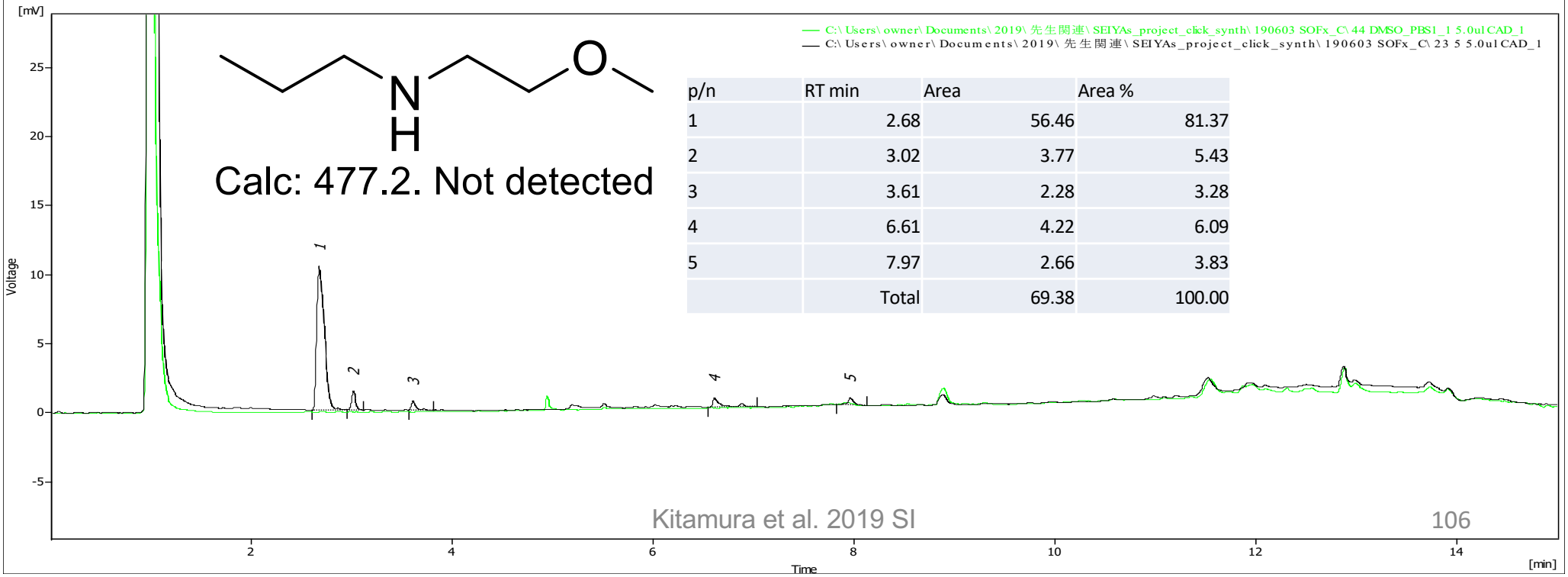

p/n	RT min	Area	Area %
1	2.68	56.46	81.37
2	3.02	3.77	5.43
3	3.61	2.28	3.28
4	6.61	4.22	6.09
5	7.97	2.66	3.83
	Total	69.38	100.00

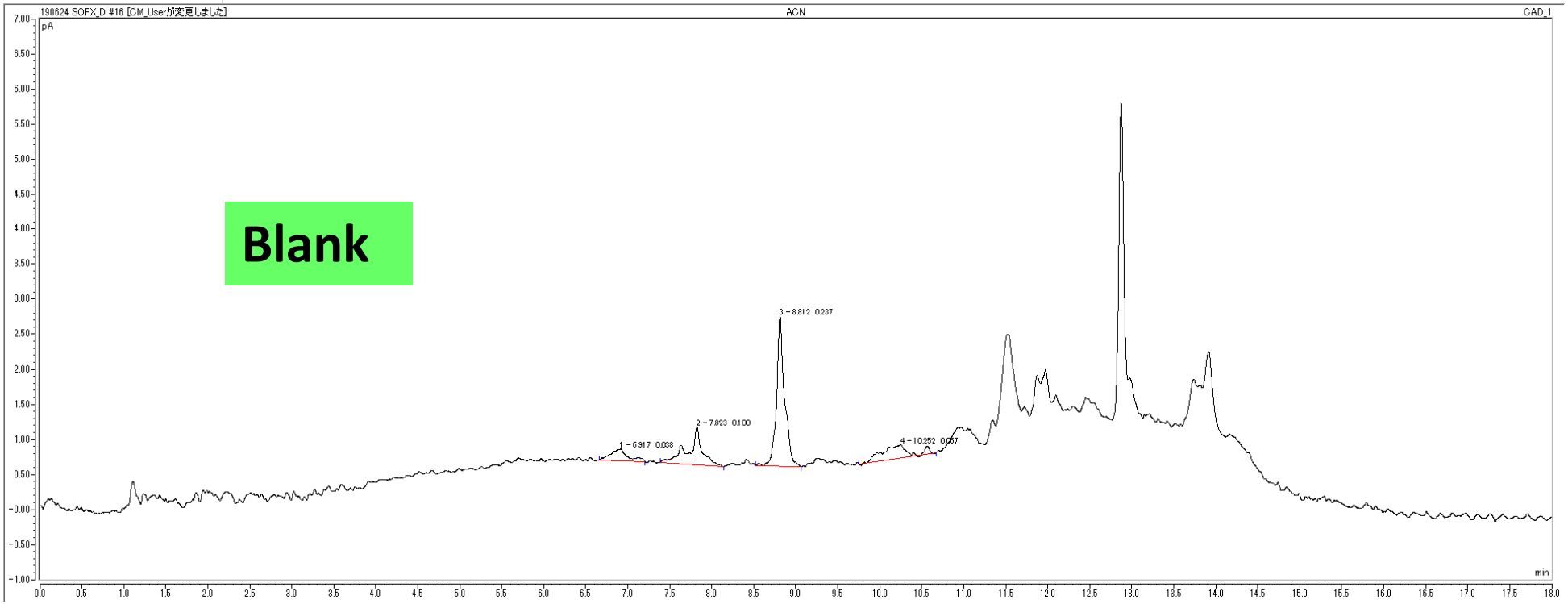

p/n	RT min	Area	Area %
1	2.68	55.46	76.99
2	3.01	7.39	10.26
3	3.62	2.08	2.89
4	5.29	7.10	9.86
	Total	72.03	100.00

Calibration curves of representative molecules